EUROPEAN COMMISSION

SCIENCE
RESEARCH
DEVELOPMENT

# THIRD EUROPEAN MARINE SCIENCE AND TECHNOLOGY CONFERENCE

**Lisbon, 23 to 27 May 1998**

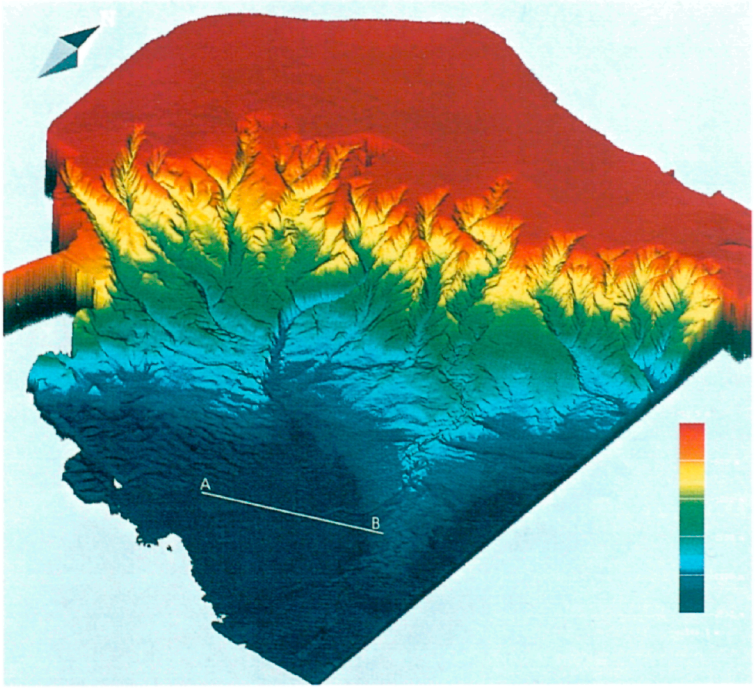


# SESSION REPORT

## Seafloor characterisation

European Commission

Edith Cresson, Member of the Commission
responsible for research, innovation, education, training and youth

DG XII/D.3 — Marine sciences and technologies

*Contact: Mr G. Ollier*
*Address: European Commission, rue de la Loi 200 (SDME 7/85)*
*B-1049 Brussels — Tel. (32-2) 29-56630; fax (32-2) 29-63024*

European Commission

# Third European marine science and technology conference

Lisbon, 23 to 27 May 1998

## Session report

### Seafloor characterisation/mapping including swath bathymetry, side-scan sonar and geophysical surveys

Edited by
Gilles Ollier, Pierre Cochonat, Luiz Mendes Victor

Directorate-General
Science, Research and Development

**Acknowledgements**
Cover page: 3D view of the Western Rhone Shelf, slope and rise (S. Berné et al., this volume).

*The editors wish to thank Christine Vaines, DG XII/D-3 of the European Commission,* for her helpful contribution in finalising the manuscript.



Cataloguing data can be found at the end of this publication.

Luxembourg: Office for Official Publications of the European Communities, 1999

ISBN 92-828-5060-9



*Printed in Belgium*

PRINTED ON WHITE CHLORINE-FREE PAPER

**TABLE OF CONTENTS**

# Sea floor characterisation/mapping including swath Bathymetry, side-scan sonar and geophysical surveys

## Introductory speech

Luiz MENDES VICTOR, Chairman

The challenge of the Earth Science System on the ability of researchers to solve key problems related to ocean floor phenomena, has produced many experiments in the domain of geophysics, geochemistry and biology.

It involves rather complex systems, requiring the deployment of specific sensors at the ocean floor. The efficiency of the observations which cover a wide range of phenomena depends very much on the design of instruments and structures, able to work under very aggressive environmental conditions.

The need for sensors and recording systems that can be used with special purpose manned submersibles or ROV systems, is increasing rapidly, particularly those equipped with robotic arms and/or deep-sea ocean capability.

The feasibility of ocean bottom exploration will be determined by the solutions to the engineering challenges. Data recovery, accurate timing and power sources, are key issues under discussion; modularity, standardised components and formats to guarantee lower costs and provide easy maintenance are not yet at the stage where the advantages of certain designs for common use can be stated.

Nevertheless, in this session the papers are reflecting: a) the efforts made by the scientific community to solve some of the above questions; b) the results of another step forward, taking advantage of the developed tools, presenting the methodological approach to allow adequate processing of data, mapping and interpretation of phenomena.

Selected case studies resume the achievements on ocean bottom sediment instabilities research, strongly correlated with sea floor dynamics expression and natural hazards concerns, using some advanced tools and methodologies.

# Seafloor characterization/mapping including swath bathymetry, sidescan sonar and geophysical surveys

## Summary of Session debate

Gilles OLLIER, Session convener

After approximately 10 years of work and investment achieved through the MAST programme together with the national agencies, the session aimed at assessing through selected presentations, the state-of-the-art and the progress made in the domain of seafloor characterisation and mapping in Europe. It was intended to initiate in Lisbon a debate in the very challenging area of seafloor exploration, in particular addressing deep-sea environmental research issues based on recent research development, and which could be preparatory for further research programmes.

The colloqium programme included 9 presentations organised according to the following three themes:

- 1) the new tools
- 2) the processing and interpretation means
- 3) case studies

The keynote speaker gave an overview on the spectacular evolution of the acoustic devices used for characterisation and mapping of the seafloor, which nowadays almost enable the seafloor to be seen.

It was quite clear from the various speakers' talks that in the future the technology developments required for seafloor exploration should preferably concentrate on two domains: 1) systems mounted on ships or satellites, enabling efficient and extensive survey and 2) near bottom deep-sea devices (*e.g.* new seismic sources) enabling image resolution to be increased. Although deep-water surveys are becoming more and more important, the continental shelf remains quite a challenging area in two respects: Firstly, there is a clear need for bathymetry and seafloor morphology assessment in shallow areas (coastal management) at low cost, that can be covered by promising new technology from remote sensing and air-borne technology. Secondly, full mapping coverage of the continental shelf remains relatively difficult to achieve through the standard swath bathymetry means, because of their low efficiency in shallow waters. Therefore implying more technological research to be conducted to develop efficient survey equipment for this physiographic area.

In the domain of processing, interpretation, and displaying of seafloor images, tremendous progress has already been achieved enabling now noise to be taken out in a very effective manner, to conduct interpretation with the assistance of interactive, intelligent information systems, and to produce very attractive, and more easily understandable representations of the seafloor. Although improvements are still needed in the processing domain, the expected progress will depend now more on the acquisition accuracy of the next generation of acoustic devices, the compatibility between systems, the rapidity of processing execution (real time),

the availability of user-friendly softwares, and the improvement of modelling in physics and geoacoustics, with the definition of inverse problem methodology.

The strategy for exploring the seafloor in the near future was also tackled by several speakers. It is now quite clear that large-scale studies, integrating surveys from the coastline to the deep-sea, are a priority, relying on thematic objectives rather than on purely geographic criteria, implying multidisciplinary approaches in key areas, and a co-ordinated methodology with studies in adjacent terrestrial areas. With regard to the European seas and oceans, much has already been achieved in terms of seafloor mapping. However more has to be done in order to integrate the data, to fill the gaps, and to publish cross-border thematic maps of the different regions. The mapping of the seafloor includes assessing and quantifying the benthic community, which implies specific approaches to be developed, and is a prerequisite in view of the sustainable management of marine ecosystems.

Characterising and assessing the seafloor and sub-seafloor on the European margin is becoming of strategic interest nowadays, and is of mutual interest to both industrialists and researchers. Improving the contribution of research to industry, and the collaboration with industry in this domain, implies for the funding agencies to support sound, and well-structured research projects, rather than projects intending to answer short-term problems raised by commercial activities. On the European margin the technologies and research for seafloor characterisation and mapping are of primary importance in order to study sedimentary processes and sequences, to assess potential geohazards, and to conduct new research in the domain of geosphere/biosphere coupling.

Finally, emphasis has been put by many speakers on the necessity of obtaining groundtruth data, which is allowing the validation of the seafloor and sub-seafloor images, in particular with clear reference to needs in the domain of scientific drilling type data.

# Seafloor mapping and imaging: Characterisation of seafloor spatiotemporal variability

Pierre COCHONAT, Keynote speaker

Abstract:
*The capabilities for exploration of the sea have undergone a revolution during the last 30 years and the knowledge of the seafloor has subsequently highly increased. After a period of important development of research in plate tectonics and global climate change, the key issues will probably be environmental studies and assessment of resources of the sea and their interaction. The future will allow addressing questions about the seafloor dynamics at different scales which means that the seafloor will be studied at different scales in terms of spatial variability but also in terms of temporal variability to observe active processes.*

---

Since the mid-19th, navies and oceanographers have constantly attempted to improve their knowledge of the morphology and the nature of the seafloor. From wide beam to narrow beam aperture echo sounders and more recently to multiple beam arrays, the techniques of seafloor mapping and characterisation have grown impressively. New acoustic mapping systems have undergone a revolution thanks to the development of modern multibeam echo sounders. Figure 1 shows the difference of time necessary to produce a bathymetric map for a given area : 1.5 months in 1974, involving numerous scientists working by hand, using data acquired with a monobeam system to be compared with 12 hours in 1990, using the multibeam echo sounder of the R/V L'Atalante. Figure 2 shows the bathymetric map of the Nice- Baie des Anges completed after the 1979 collapse of Nice airport, this map can be considered as the best bathymetric map possibly produced at that time using the SEABEAM system hull-mounted on the R/V Jean Charcot. Twenty years later, the SIMRAD EM 1000 system enables the production of a fully detailed bathymetric map which gives us a totally different view of the seafloor.

Nowadays, the spectacular development of sonar imagery and improvements in digital signal processing almost enable the seafloor to be "seen". Modern techniques have been further

developed in the framework of, and for the purposes of, international scientific programmes aiming at a better understanding of global seafloor processes as well as for industrial needs related to increasing use of the sea and the exploitation of its resources. Due to the broad range of submarine processes and seafloor morphology wavelengths, there are a large number of tools available. In terms of frequency, they vary from some Hz to some hundreds kHz enabling the recording of all the data required for ocean floor mapping and characterisation, from multichannel seismics to high-resolution side-scan sonar. It may also be worth remembering that the scale of investigations ranges from global scale (e.g. altimetry) to working site scale (e.g. station) (see the following table).

| | | *Range :* resolution: | Spatial |
|---|---|---|---|
| Scale 1 | Satellites, altimetry | *Global* | 2500 m |
| Scale 2 | Research vessel, Multibeam echo sounder, multichannel seismics | *regional survey* *($10^3$ km)* | 100 m |
| Scale 3 | High resolution seismics, Deep-tow | *local survey* *($10^1$-$10^2$ km)* | 10 m |
| Scale 4 | Very high resolution seismics, Deep-tow, Submersible | *site survey* *(1-10 km)* | 1 m |
| Scale 5 | R.O.V. / in situ experiment, sampling, monitoring | *working site* *(station)* | $10^{-1}$ m |

The papers assembled in this volume on "Seafloor characterisation/mapping including swath bathymetry, side-scan sonar survey and geophysical survey" exemplifies the research being conducted on European seas and the methodological and technical developments undertaken and in progress. It is clear that European research institutes play an important role in this domain through several international programmes such as MAST and by means of a large number of existing devices such as GLORIA, TOBI, SAR, different commercial multibeam systems hull-mounted on many European research vessels and other tools allowing in situ experiments.

## SCIENTIFIC OBJECTIVES

The seafloor can be considered as an active domain where many processes are still poorly understood. The processes can be grouped into three main fields according to both their scientific and technological aspects: coastal areas, margins and the oceanic crust.

### Coastal areas:

The coastal areas are, for example, typically affected by the action of currents and the erosion, transport and deposition of sediments interacting with man's activities (pollution, infrastructures). Specific problems arise for mapping the coastal area. If we consider the shallowest part of the sea (<20 m water depth), which is directly related to man's activities, it appears that mapping this zone is surprisingly not an easy task and therefore far from being achieved . This is due to several reasons including heavy traffic in this area (boats, tourism, fishing...), tidal movements and mainly narrow multibeam coverage in such shallow water. Therefore, the use of satellite data can be considered as a serious alternative (see paper from G.J. Wensink et al., in the present issue) when it is possible in very shallow water even if marine surveys are still essential.

Many studies which demand an accurate knowledge of the seafloor morphology propose models for currents and subsequent sediment transfer in coastal water. A significant effort remains however to be made to map coastal areas. Many local studies have already been indeed conducted for various purposes in several European countries. From these studies the specific acoustic responses of the seafloor provide spectacular example of seafloor characterisation such as mapping of benthic communities (see paper from P.S Soerensen et al., in the present issue). These different approaches probably call for a better intercalibration of the data and definition of good practices.

### Margin:

European margins, as any margins, have given rise to numerous investigations using all sort of tools to map and characterise the seafloor. Margins are considered as the place where many fundamental sedimentary processes, such as active sediment transfer to the deep ocean, take place and provide a record of climatic changes. Margins are also of major interest for the record of sea level change, earthquakes, gas hydrates, slope instability, cold seeps... (Fig. 3) This is also the area where human activity is increasing and moving towards deeper water (e.g.: deep offshore oil industry).

Among the various phenomena that can be mapped and characterised on the ocean margin, the slope failures and associated mass-movements are processes of utmost importance. Large sediment failures along the world's ocean margins have recently been recognized. Striking examples of major slides are given by two case studies presented in this volume. One of these examples concerns recent slope failures and associated mass-movements in the NW Mediterranean Sea representing huge sedimentary events characteristic of the post-glacial history in this area (see paper from S. Berné et al in this volume). The other example refers to the well known Storegga slide which is presented as a natural laboratory for the interaction between gas hydrates and slope instabilities (see paper from J. Mienert et al in this volume). Megaturbidite occurring during the last glacial Maximum are often reported and are tentatively associated to the presence, at the time of the failure, of gas hydrates such as, for example, the Balearic Basin of the Western Mediterranean (Rothwell et al 1998). These examples highlight the importance of gas hydrates, and their potential role in slide triggering. They demonstrate that there is huge interest in the scientific community for this topic including fluid migration processes, gas escape at the seafloor, colds seeps, associated specific biosphere (macro and micro-) and geochemical reactions and even interaction with climate change related to the hypothetical release of substantial amounts of greenhouse gas. Many processes have still actually to be understood which may explain how fluid migration interacts on the dynamics of the seafloor such as for example slope failures.

Several European research programmes such as MAST ENAM and STEAM and numerous industrial ventures and academic regional investigations have also demonstrated evidence of giant slope failure on the European continental margins. These events can obviously form major hazards to human settlements along European coasts such as tsunamis (e.g.: the well-known event which occurred in Lisbon in 1755). These geohazards can also directly impact human activity on margins where significant development in deeper water takes place: e.g. the deep offshore oil industry. These major processes are also mainly responsible for sediment transport from the slope to the deep sea. Their study can contribute to a better understanding of oil and gas reservoirs, as for example through the spectacular case study of the recently discovered deep sea fan in the Celtic Sea (fig 4; Auffret, pers. comm.). With the recent development of deep offshore exploration, the understanding of sequence architecture and depositional facies in turbiditic environment is becoming one of the main issues for sedimentology studies to be conducted on modern depositionnal systems. It implies integrated studies (from the alluvial plain to the deep sea) of sedimentation on European margins including Quaternary sea-level changes, sequence stratigraphy and gravity-laden processes.

The oil industry activities are concentrated in N.W Europe, Brazil, Golf of Mexico and West Africa where new resources are expected. European oil companies are involved in all these areas. This industrial development calls for new research in Earth Sciences and technology for deep-water investigation. Development of new methodologies implying efficient tools and software for mapping and characterising the seafloor at different scales are also required. All the objectives relating to geodynamics, thermicity, sedimentary basins, sequence stratigraphy, gas hydrates, gravity processes and deposits, slope instabilities, are in fact the basis for a new beginning for margin and sedimentary process studies for geoscientists through a genuine scientific approach. Several initiatives have therefore been proposed in different countries (European and North American) to launch MARGIN programmes.

**Oceanic crust** (D. Needham, pers. comm.).:
It is useful to remember that about less than 10 % of the deep ocean floor has been covered using modern surface ship mapping and imaging. Concerning crustal studies, the crest of the mid-oceanic ridge has attracted particular attention. The mapping had led to huge advances in knowledge of the details of segmentation and surface structure, in guiding the collection and interpretation of all sorts of geophysical and petrological data and in helping an understanding of active hydrothermal systems. Crustal studies require a global approach and it is important therefore that Europe has a global and not a provincial approach. There is also clearly a particular opportunity to develop research in the region of the Açores and surrounding area. Many problems, not only of local, but also of general interest are posed there.

The Açores represent a major mantle-melting anomaly (hot spot). The North American/African/Europe plate boundary triple junction is located there. Both normal and unusual deep and shallow crustal processes are expressed in the region. It is an area of important hydrothermal activity and associated biological communities and metallic sulphide deposits. It is a zone of volcanic and seismic activity which presents natural risks to the population. And it provides an exceptional opportunity (thematical and logistical) for developing submersible projects, for exploring the possibility of new R.O.V.s and for planning long-term seafloor observations. Future aims as different as assessing hydrothermal chemical and thermal budget and their impact on the oceans or understanding the distribution and modes of tectonic and submarine volcanic activity, can be addressed only in harmony with an intimate knowledge of bathymetry, morphology, slopes, sediment and bare-rock distribution and other properties of the sea-floor. This implies mapping and imaging at all scales, including the use of deep-towed devices. A start has been made, the axial area cutting through the Açores plateau and to the South and part of the plateau itself, for example have

been mapped and imaged with hull mounted EM 12 systems. But there are years of work, particularly fine-scale work still to be done in order to have a full picture of the area and to begin recording temporal variations in this active part of the ocean.

Characterisation of the mid-ocean is crucial for understanding accretionary processes and, for example, their consequences on biological populations associated with the creation of new crust. The study of the ridge gives us a good example of the necessary tools needed to map it by successively using a range from satellite altimetry, multibeam bathymetry, acoustic imagery and finally to optical imagery (Desbruyeres D. Michel J.L 1997).

## TOOLS, DATA PROCESSING AND METHODS

### Mapping:

More efficient and therefore cost-effective tools such as hull-mounted systems, which permit more efficient and extensive surveys, should be one of the major trends in future technology where it is possible and when appropriate resolution can be attained. The major development of these systems concerns the improvements of their performance, especially in terms of imagery and therefore data processing (see papers from G. Canepa et al. and X. Lurton et al. in this volume).

Moreover, the need for more accurate geophysical measurements, in response to the demand for high or very high-resolution deep-water studies, implies the development of new deep-towed multipurpose tools. In this volume, B.Savoye et al describe the recent development of the PASISAR system which is a first step to solve the problem of near bottom seismic profiling in deep water. The future tools which will follow the generation of SAR and TOBI sonars will obviously integrate several sensors such as mid-range side-scan sonar, multibeam system, deep-towed seismics and other geophysical and geochemical sensors. A significant breakthrough would be the development of deep towed seismic sources. The problem of positioning, although facilitated by using ultra short base line positioning system, still remains to be improved in order for such instruments to be routinely used by scientific teams.

### Seafloor characterisation:

New acoustic mapping systems have recently undergone a revolution; standard image processing algorithms such as contrast enhancement are an example, but data processing is definitively more than just image processing. If acoustic backscatter generally relates to sediment characteristics, some simple assumptions such as the hypothesis that coarser sediment always produces greater acoustic backscatter are wrong. An example is given by

figure 4 exhibiting sandy lobe deposited in Celtic fan (N-E Atlantic) which indeed produces a spectacular low reflectivity patch. We therefore need both ground truth and appropriate data processing system for characterising the seafloor. The aim of seafloor characterisation is to subdivide an entire image into classes that possess unique sets of image attributes (Pratson and Edwards, 1996). One of the most active areas of research is the development of automated techniques for classifying different seafloor sections in remotely sensed data. The new generation of swath system allows the simultaneous record of the bathymetry and the seafloor reflectivity. The calibration of the reflectivity by samples generates an acoustic characterisation. A new image is calculated and forms the base of the classification; the geologist teaches the software the different facies by locating them on the mosaic. The acoustic signatures of these facies are determined and stored if they are discriminating enough; the label of the most similar facies is assigned for each of the pixels. The result is the so-called "segmented image" (see X. Lurton et al., in this volume).

**Use of existing data:**

3-D seismic data, usually acquired for oil and gas exploration purposes, is now being used to supplement or in some cases, even replace conventional high resolution geohazard surveys (Gafford, 1996). Migrated 3-D seismic exploration data represents a significant contribution to the detection, interpretation, mapping of deep-water hazards, drilling operations and seafloor engineering. Thanks to the regular density of coverage and the ease of manipulation of data in a computer workstation environment, the ability to extract reflectors information and to produce comprehensive 3-D maps of subsurface stratigraphy and seafloor images is a valuable addition to offshore geohazard investigation.

**In situ experiments:**

In situ measurements of physical and geotechnical properties of marine sediments are a prerequisite to calibrate marine acoustic data. These properties cannot be accurately obtained with laboratory analyses because of the remoulding effect of core sampling. For example, in case of study devoted to slope stability assessment, some specific physical and geotechnical parameters are required to characterise the sedimentary layers involved - or potentially involved - in slope failures. Some static parameters such as density, shear strength etc... are first measured. For that purpose boreholes can be considered as the best, but more expensive, way to access to in situ measurements. For cheaper, and probably more efficient measurements, some equipment has been recently developed in European research institutes aimed at superficial in situ experiments such as SAPPA (see paper from A. Best et al in this volume). A few tools have also been developed for deeper penetration. These first

experiments are preparatory for deeper penetration tools enabling the study of mechanical behaviour of the seafloor through in situ measurements.

On the other hand, dynamic parameters are also ideally needed, for example seismic acceleration in case of earthquakes or excess pore pressure as a response to earthquakes or in case of fluid migration processes. For that purpose, long term monitoring would be necessary to study either sediment behaviour or any seafloor processes. Many tools exist in fact - or can be improved - to investigate the seafloor, but a key question nowadays is the temporal variability of seafloor processes at different scale (roughly 1 sec. to 10 years) (Desbruyeres and Michel, 1997). Important developments will take place, implying great technological progress for developing new sensors and solving problems of energy, high capacity data storage, specific communications systems between seafloor and laboratory on shore such as the research conducted in the MAST-GEOSTAR programme.

## CONCLUSION

Tremendous progress has been made mainly in the framework of plate tectonics and climate change research programmes; they have now created the scientific context for developing new challenges that will probably be increasingly focused on environmental studies and assessment of resources of the sea and their interaction. Therefore, an exceptional opportunity exists now to develop research on margins where there are clear present common interests of science and industry, especially for the deep offshore oil industry.

Hull-mounted systems such as multibeam echo sounders should still undergo an important development in terms of higher resolution for mapping and especially for imaging the seafloor. On the other hand, new deep-towed devices integrating several sensors are required for very high-resolution deep-water multipurpose studies. In any case, experience shows that a better use of highly sophisticated tools and methods requires the support of ground-truth. Ground-truth calls for specific technology such as sampling, in-situ measurements involving specific developments of instrumented platforms, the use of R.O.Vs and obviously the urgent need for boreholes. Many local studies have been conducted and have produced good geophysical data, but we greatly lack calibration. Drilling should be now considered as the ultimate test of all geological model, especially on continental margins where both scientific and industrial objectives are concentrated.

These objectives will demand the development of new technologies, and their intensive use. Discussions have been recently undertaken between several European marine research

agencies to take further steps towards the creation of a unified European fleet of research vessels with a common scientific programme (see Nature, 392, 637;1998). When taking into account the numerous existing data and national programmes in progress, we can at least hope that at the European level (1) a better coordination of research will be organized, especially for an efficient use of ship-time, which remains the most important means - and therefore difficult to obtain - for marine scientists and (2) an effort in standardization will be made to reach one of the ultimate objectives : to map all the European margins and ridges, because mapping is the first step of all oceanographic research programmes. Many areas are still to be systematically investigated to produce a map of the European seas, even if many initiatives have already been taken, especially in deep sea where some regions are almost totally covered.

REFERENCES:

Pratson L.F. and Edwards M.H. 1996. Advances in Seafloor Mapping Using Sidescan Sonar and Multibeam Bathymetry Data. Marine Geophysical Researches, Special Issue, Volume 18, Nø 6 December 1996.

Gafford W.T. 1996. The use of Exploration 3-D Seismic Data for Geohazards Assessment in the Gulf of Mexico. OTC paper 7987, 277-281

Rothwell R.G. , Thomson J. and Kahler G. 1998. Low-sea-level emplacement of a very large Late Pleistocene 'megaturbidite' in the western Mediterranean Sea. Nature, vol. 392, 26 March 1998.

Desbruyeres, D. et Michel J.L. 1997. Ecosytemes oceaniques profonds : les enjeux scientifiques et technologiques. In techniques Avancees, Nø40, Juin 1997, 26-33.

Marchand P. 1997. L'instrumentation oceanographique. In techniques Avancees, Nø40, Juin 1997, 34-41.

Auffret G., Berne S., Henriet J.P., Hovland M., Kudrass H., Labeyrie L., Lancelot Y., Le Moign Y., McKenzie J., Ludden J., Pezard P., parkes J., Skinner A., Sparks C. and Wefer G. 1997 . European initiatives in science and technology for deep-sea drilling coring and drilling. Editors L. d'Ouzouville, C. Jacobs. EMaPs Position Paper, June 1997

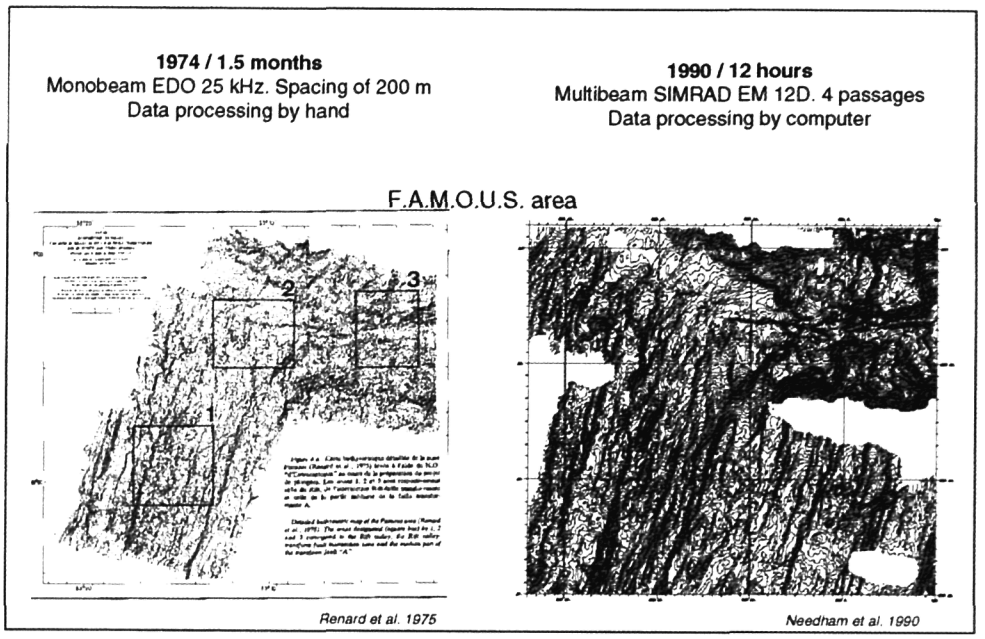


Fig. 1: Bathymetric map of the FAMOUS area. Comparaison of efficiency of different means between 1974 and 1990 for mapping the same area.

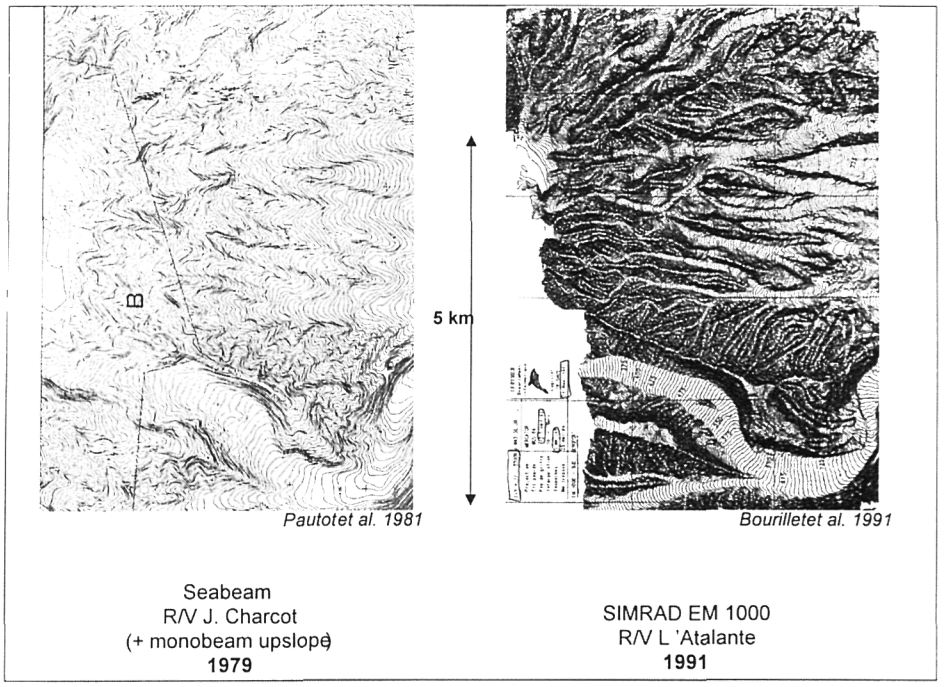


Fig. 2: Bathymetric map of the Nice-Baie des Anges. Different quality of maps acquired in the same area using different generations of multibeam echo sounders.

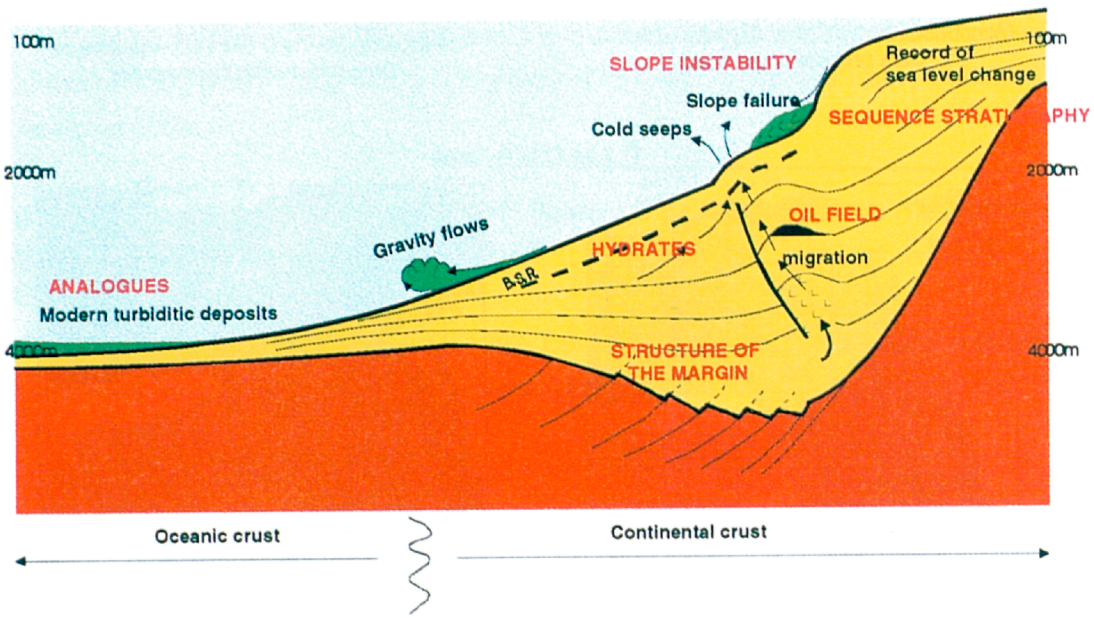


Fig. 3: Main scientific questions which can be adressed on margins in terms of sedimentary processes.

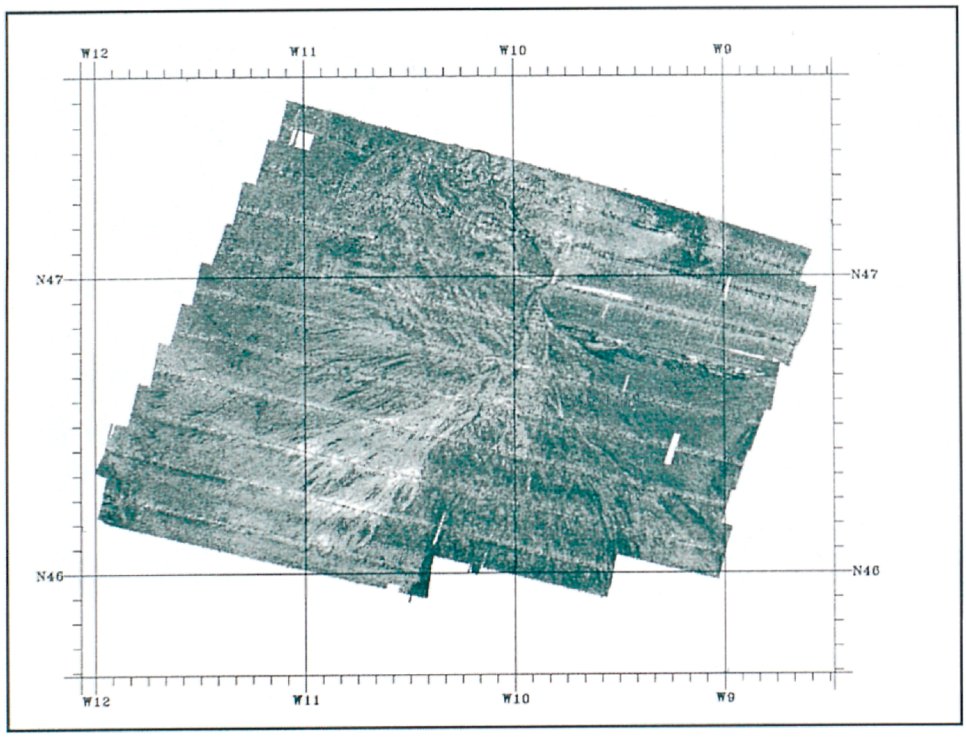


Fig. 4: Sonar imagery of the Celtic Fan exhibiting low reflectivity patches related to recent sandy lobe deposits (example showing that coarser sediments do not always produce greater acoustic backscatter). (by courtesy of G.A. Auffret, MAST Project/ENAM)

# SECTION I

# The New Tools

# *PASISAR: SEVERAL ASPECTS OF NEAR BOTTOM SEISMIC PROFILING IN DEEP WATER*

Bruno SAVOYE, Yannick THOMAS, Hervé NOUZE, Bruno MARSSET

IFREMER (Institut Français de Recherches pour l'Exploitation de la Mer), 29280-Plouzané, France

## ABSTRACT

*The PASISAR prototype enables the acquisition of near bottom seismic data in up to 6000 m water depth. It combines a surface conventional source with a single channel seismic streamer, towed at about 100 m above the sea bottom. This unconventional device geometry reduces the width of the first Fresnel zone and therefore increases the lateral resolution. The geometry of this hybrid system is such that the seismic resolution is largely better than the one obtained using conventional sea surface systems, but this geometry creates time arrival distortions and induces large incidence angles. A dedicated processing software package has been developed to deal with this specific system geometry and to obtain a readable seismic section. The PASISAR system is now operational and routinely used during SAR cruises. PASISAR and conventional seismic profiles being usually simultaneously recorded, we illustrate the interest of using a hybrid seismic device by comparing PASISAR data and conventional seismic data. The SAR added with PASISAR can be considered as the forerunner of near-bottom towed systems capable of integrated seabed studies in water depths up to 6000 m, useful for fundamental research studies as well as for industrials needs. Already used within the framework of EEC funded oceanographic projects, the PASISAR tool could be the start base of a new cooperative work between the main European oceanographic institutes, to develop a new generation of deep-tow multipurpose geophysical systems.*

## INTRODUCTION

After decades of large scale ocean exploration, one is witnessing the emergence of research projects increasingly targeted, both on thematic and geographical plans and this, even by great water-depth. Efficient seismic systems are available « off the shelf » for water-depth corresponding to the continental shelf (0-200 m), for greater depths, present conventional seismic systems, because they are towed at the sea-surface, present several disadvantages:

(1) due to the water-depth increase and in order to avoid seismic information overlapping several successive shots, the shooting rate has to be decreased and therefore the spatial resolution decreases.

(2) the seismic sources are rarely directive; the diameter of the shed zone, called the Fresnel zone, increases with the water-depth. And contrarily to what is most often observed on the continental shelf, the 200-3000 m deep sea-floor domain shows rugged relief and is often characterised by steep slopes; thus the average seismic response hardly reflects the geological reality (see Figure 1).

It is therefore illustratory to try to study at great water-depth, fine lateral geological variations or dense nets of small fractures or faults using conventional techniques. For long, it

has been known that such detailed investigation is only possible by using seismic devices towed near the sea-bottom.

The PASISAR tool is intended for such objectives. It has now entered in an operational phase, and we assess here its characteristics, performances and potential application.

## PAST WORKS

In the past, several attempts of near bottom seismic have been concluded, amongst which two projects had near bottom emission and reception:

(1) DTAGS (for Deep-Towed Array Geophysical System) was initiated by the NORDA (Naval Ocean Research and Development Activity, Mississippi) in the beginning of 80's (FAGOT, 1983). This project, that benefited from a very large military budget, was especially dedicated to the design of a deep-water source emitting a sweep of acoustic wave whose frequency was comprised between 260 and 650 Hz. This source had a volume of 2 $m^3$ and weighed more than a ton. It was composed of 5 ceramics and was omnidirectional. At full power, the source could emit during 250 ms every 12 sec. The 1000 m long seismic streamer consisted of 24 channels. The whole system source-streamer was towed near the bottom at an altitude comprised between 100 and 500 m and at a speed comprised between 0.5 and 1.5 knots. The primary objective was to achieve a better mapping of the geological basement and the depth of penetration was in the order of 500 to 1000 m. It was tested successfully in 1984 and in the following years up to a water-depth of about 4500 m. This system was heavy to handle and only enabled the collection of seismic profiles.

(2) A second project, named SEABED, with a total cost of 20 M French francs, has been developed by the HUNTEC private company on the request of the Bedford Institute of Oceanography (Halifax, Canada). The fish was equipped with an « off the shelf » side-scan sonar, a seismic source of boomer type including its capacitors, with attitude sensors, as well as with a short single channel seismic streamer (Dodds, 1983). Designed to work in water depths between 500 m and 2000 m, it was thought to be a first step before the realisation of a 6000 m water-depth tool. Only the 2000 m prototype has been built and tested at sea. It gave good results, but because it appeared to be very expensive, too heavy, bulky and difficult to maintain, this project was abandoned.

Bowen (1983) showed that, at great water-depth, a very large amount of the reduction of the Fresnel zone that one could expect by placing the source and the streamer near the bottom, could be obtained by placing only one of these elements near the sea-floor (hybrid systems). Based on this discovery, some experiments with streamers near the bottom have been conducted over the past 15 year. In the USA, the experiments have been through the DSDP 51, 52 and 53 legs (International Deep-Sea Drilling Project) led by the Lamont and Woods-Hole Institutes (Purdy and Gove, 1982). Also a team of the University of Washington has conducted experiments on the West coast. In Great Britain, the experiments have been carried out by the University of Cambridge (Bowen, 1983) and the University of Birmingham. Finally, in Japan recent development have been realised by the Geological Survey (Kisimoto and al., 1990). Most of these experiments only concerned prototypes. Most of them did not have any continuation. In most cases, the objective was to better characterise the geometry of the basement; better imagery of the sedimentary cover was not the goal.

## LATERAL RESOLUTION IMPROVEMENT

The lateral resolution refers to how close two reflecting points must be situated horizontally apart to be recognised as two separate points rather than a single one.

The first Fresnel zone is defined as the portion of the subsurface ensonified by two wave fronts separated by a quarter of the signal wavelength (l/4). Two reflecting points that fall within this zone are merged (Yilmaz, 1987). Hence, features with a lateral extent smaller than this zone will be hidden.

The width of the first Fresnel zone is related to the geometry of the acquisition device and the signal wavelength (or the signal frequency and the seismic velocity). As previously discussed and shown in Fig. 1), a large part of the improvement between a fully deep-towed device and a conventional device is achieved by using the hybrid system. For large water depth (5200 m) and a dominant frequency of 60 Hz, the first Fresnel zone is 510 m wide for the conventional device (without lateral offset), 70 m wide for the fully deep-towed system (100 m above the sea floor, no lateral offset) and 130 m wide for the hybrid system (with a lateral offset of 3450 m). With the hybrid system, the lateral resolution theoretically increases by a factor of 3.9 compared with the conventional system. The fully deep-towed device only improves the resolution by a factor of 1.85 compared with the hybrid system.

## REMINDERS ON THE PASISAR PROJECT

Even if the technical aspects of the project have already been largely described (Savoye and al., 1994; 1995, Sibuet and al., 1996) it is worth reiterating some essential points of the project.

Technical solutions enabling the development of a THR seismic source able to work down to 6000 m water depths being either confidential, or very heavy to implement and costly, it is the hybrid solution, that consists in placing solely the streamer near the bottom, that IFREMER decided to retain for the PASISAR project (Savoye and al., 1995). This project received, from its beginning, the support of the Ecole Normale Supérieure (Paris, France), user of the SAR system.

The SAR (working since 1984) is usually towed near the sea-floor. It is equipped with a high-resolution side-scan sonar, able to work until 6000 m of water-depth. The sea trials have shown that the analysis of sonar data (view in plan) is indispensible for the analysis of "seismic" data (view in 3D cross-section). Also users of the SAR have become used to acquiring seismic profiles using conventional surface systems simultaneously with the acquisition of SAR profile. This is why, both for scientific and technical reasons, the SAR tool has been retained to conduct this project of near bottom seismic.

The SAR is composed of an armed coaxial cable, a depressor and a hydrodynamically profiled vehicle. The vehicle is towed at an average altitude of approximately 100 m above the sea-floor down to 6000 m of water-depth and at an average speed of 2 knots. Multiple sensor data, as well as attitude and navigation data are numerically transmitted through the cable to the ship at the sea-surface every 1.5 second.

The PASISAR (SeIsmic PAssenger for the SAR) has been added to the SAR without rebuilding the system (Fig.2). The SAR electronics and the SAR management and acquisition programs have therefore not been modified. The PASISAR Seismic data are analogically transmitted via the cable, by using a pre-existent transmission channel unused in routine.

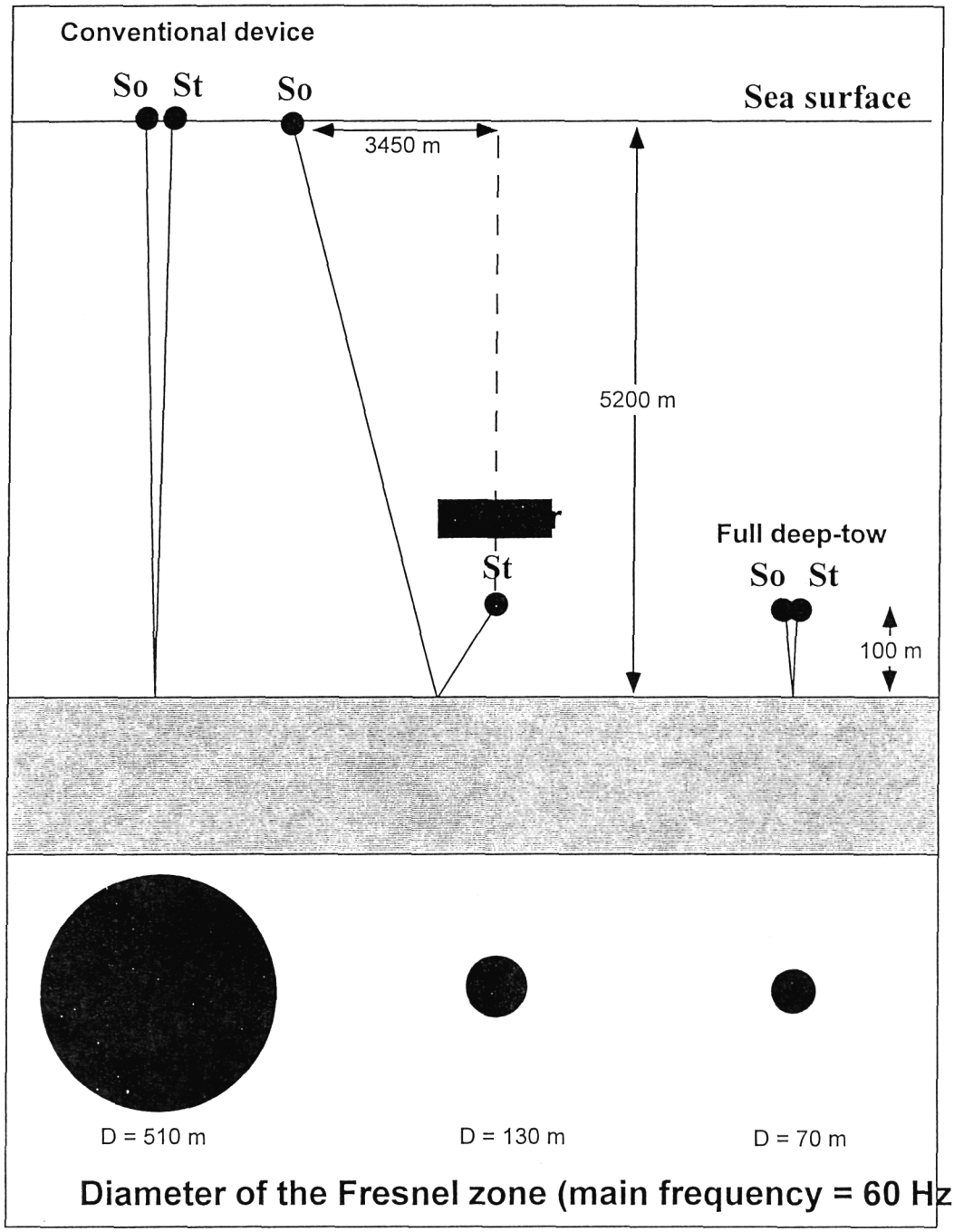


Figure 1 - values of the width of the first Fresnel zone for geometries corresponding to the three main acquisition devices (surface, hybrid and deep-towed), in the case of a 2D problem with an air gun source type..

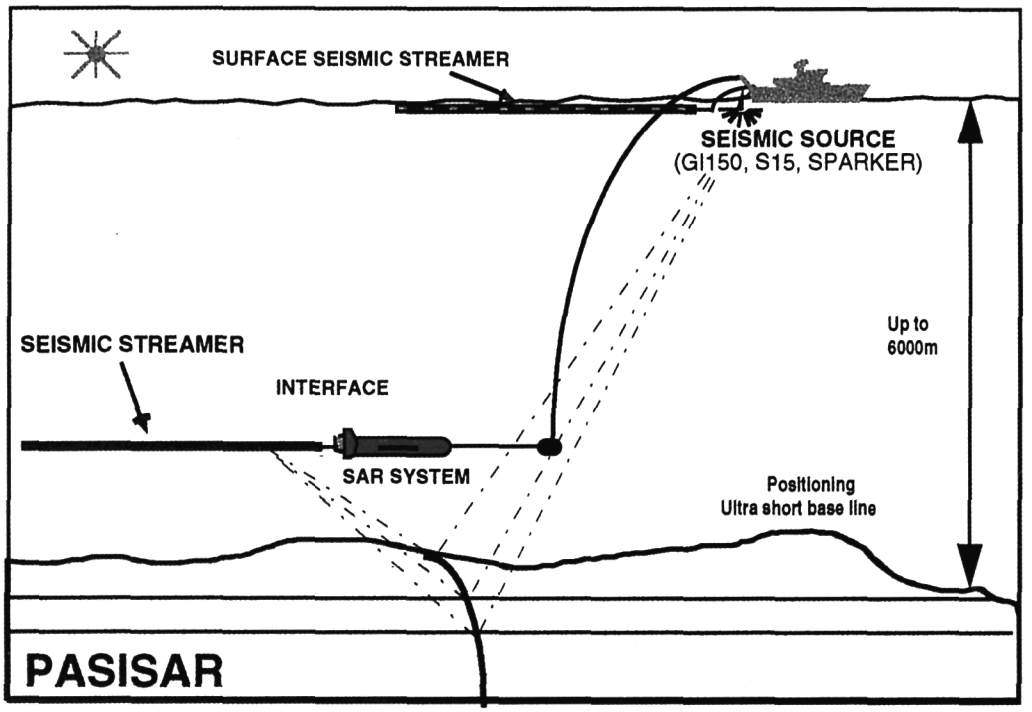


Figure 2 : Schematic drawing of the PASISAR concept. Note that the dissymetrical acquisition device implies the skewness of the rays and therefore the positioning of the reflecting points along a hyperbola.

The seismic source towed near the sea-surface is conventional (air guns or water guns, sparker,...). As in the case of conventional seismic surveys, the choice of the source depends on the requested penetration and resolution.

The streamer has been specially designed for PASISAR. It is 20-m long and towed just behind the SAR vehicle. It comprises a 11 m long active section of 21 hydrophones of similar type to those used by Avedik (1986) for its vertical streamer. The hydrophones are mounted into a special polyester sleeve armoured with four towing Kevlar cables. The special polyester sleeve, more rigid than a traditional one, reduces the effects of variable towing speeds, and better protects the hydrophones during launching and recovery operations.

Due to the seismic ray obliquity, signals received on the streamer are relatively weak in amplitude. Before transmission through the cable, they are amplified in an interface tank located in the SAR vehicle. The gain level can be remotely controlled from the vessel, to best manage observed signal amplitudes variations. The systematic tracking of all polluting noises, either of electrical or acoustic nature, allowed to improve significantly the performances of the system. In routine mode, the acquisition of PASISAR data is undertaken on board the ship simultaneously with the surface seismic data acquisition. The recording of data is performed using a conventional PC based system, typically a Delph2 (manufactured by ELICS). It has been adapted to the management of PASISAR data; it allows to manage the two types of data (surface and near-bottom) independently and to acquire on the same recording device the navigation parameters of the SAR (especially, source-streamer offset, immersion and altitude of the vehicle).

The project began at the end of 1992 and the first tests at sea were undertaken in February 1993. Since this date, two other testing cruises as well as seven research cruises (Fluigal, Guiness2, Nicasar, Jason, Tokai, Sarridge, Sedifan) have been achieved. These are therefore several thousands of PASISAR profile kilometres that have been collected in water-depths ranging between 200 m and 5200 m.

## LIMITS OF THE PASISAR CONCEPT

The PASISAR solution, i.e. the hybrid geometry does not present only advantages. The pilot of the SAR tries to keep the fish at a relatively constant altitude (100 meters) above the sea-floor in order to obtain the best side-scan sonar images. To perform this, he can only vary the length of the towing cable. The variations of the length of the cable produce a non linear variation of the oblique offset, of the horizontal offset, of the immersion and of the altitude. The oblique offset is the direct distance between the source and the streamer, its value is close to the length of the cable. However, there exists a difference due to the curve of the cable, which is linked to the speed of the ship and the resistance of the water mass. One has therefore to take into account at least 4 drawbacks: 1) the PASISAR streamer is towed neither at a constant altitude above the bottom, nor at a constant immersion; 2) one does not work at a vertical angle; 3)the geometry of the device varies all along the profile; 4) the source-streamer offset is not negligible.

*The PASISAR streamer is towed neither at a constant altitude above the bottom, nor at a constant immersion*

Even if the pilot of the SAR tries to keep the fish at a relatively constant altitude (100 meters) above the sea-floor, the altitude of the SAR above the bottom varies continuously in the range 50-200 m. The variations of the sea-floor-streamer distance induce variations of the reflection point-hydrophones travel time, that create artefacts, a flat bottom being able to appear undulated as shown in Fig. 3.

Similarly, to follow a regularly descending slope, the pilot can run in or to run out cable all along a profile. This produces a continuous increase or decrease of the source-streamer distance and therefore a vertical distortion of the profile.

*One does not work at vertical angle*

In a conventional seismic device, the source and the streamer are almost at the same immersion level. For each shot, the reflective points of the different geological interfaces are located on a same vertical. In PASISAR, the source and the streamer are not at the same immersion level. The reflective points of the different interfaces are no longer located on the same vertical, since their position depend on the source-reflector and reflector-streamer offsets. For each shot, the reflective points of the different interfaces are aligned along a hyperbole in the subsurface. Thus each trace of a rough PASISAR seismic section corresponds to information which are not corresponding to a vertical cross section, even if the trace is vertically printed (Fig. 2).

A seismic trace does not represent a vertical cross section of the subsurface, as in the case of a conventional surface profile, but a cross section according to a hyperbole whose form is function of the propagation velocity of seismic wave and the obliquity of rays, therefore of the geometry of the device (Fig. 2).

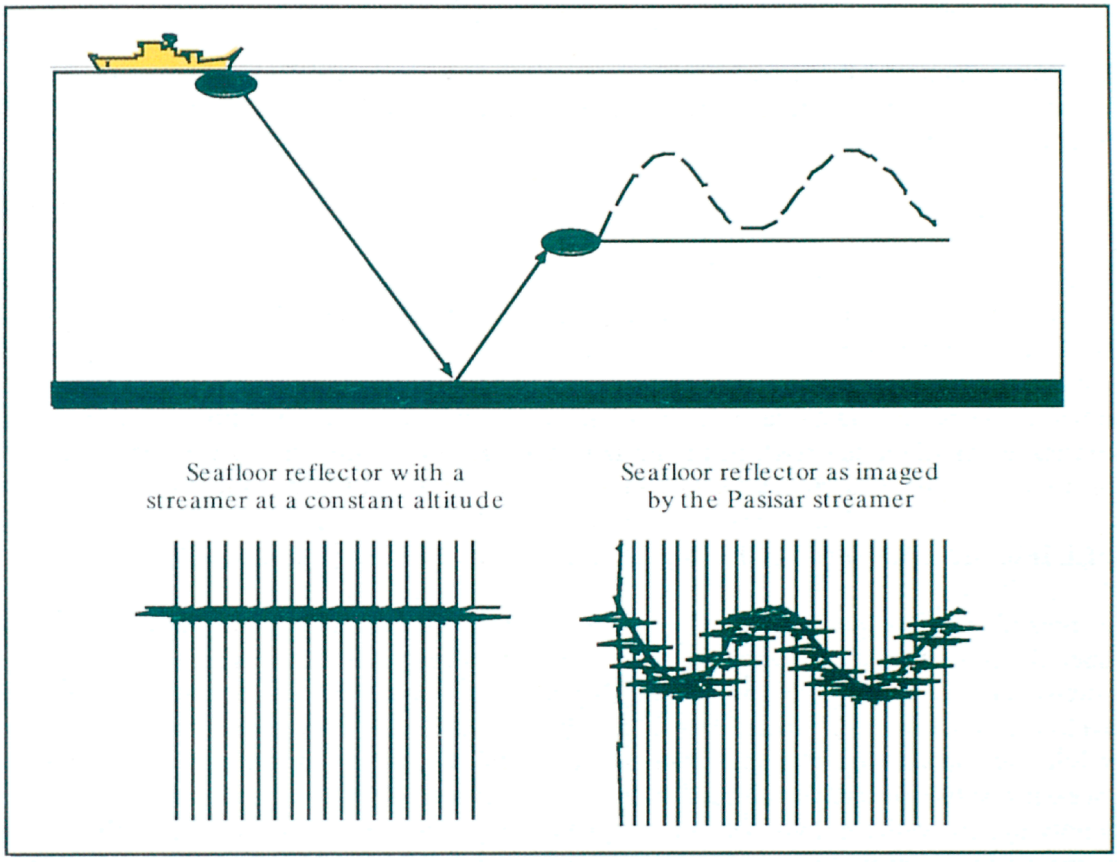


Figure 3 - Artefacts due to the motions of the SAR vehicle above the sea-floor

*The distance source-streamer is not negligible*

At great water-depth and due to the cable drag, the SAR is located far behind the ship. When the source-streamer distance is great, the ray angle of impact can reach 50°. One risks then to have refracted waves that interfere with reflected waves. Mazé (1991) showed that, in conditions of utilisation of the SAR, one approaches the critical zone for water depths exceeding 4000 m and only if superficial velocities are high enough (outcrops of basement for example). In fact, refracted waves have been rarely observed on PASISAR profiles and it was always at great water-depth and in extreme limit conditions.

*The geometry of the device varies during the profile*

The geometry of the device (immersion, altitude, offset) is susceptible to vary for each shot and in order to correct the artefacts previously described, one has imperatively to know the exact geometry of the device for each shot.

*The seismic information positioning*

By admitting that one could correct seismic sections for the artefacts previously described, it is important to know precisely the geographical position of each seismic trace. This is not a trivial problem, assuming that the position of the first reflection on the bottom is offset as compared to the position of the SAR (Fig. 2) and that the value of offset varies for each shot. Moreover, each traces of a raw profile corresponds to a hyperbolic section of the subsurface, for which the position of the first reflection on the bottom is not representative.

## SPECIFIC DATA PROCESSING

Seismic sections obtained in real time with PASISAR can not be interpreted directly and a specific processing module has been developed to correct distortions inherent to the hybrid systems. During three years, various algorithms and procedures of processing have been developed and tested (Thomas, 1995). By the end of 1995, a satisfactory data-processing module was available. The last step consisted of its integration in an already existing processing software usable onboard a ship. The software is now operational. It is a user-friendly system which minimises and simplifies the actions of the operator, it facilitates the on-line quality control of the processing and makes use of the modules of the Sithère software (Lericolais and al., 1990).

The first step of the PASISAR data processing consists of elaborating, by sifting, filtering and smoothing a clean file, including for each shot the following parameters: immersion of the streamer and streamer-source offset (Thomas, 1995). Depending on the quality of data acquisition, this step requires a greater or lesser intervention by the operator. If the knowledge of the former affects directly the end result, experience has shown that, with a minimum of training, a non warned operator could obtain good results with the dedicated developed software. The position of each source point is known thanks to the ship navigation data. The offset between the source and the receivers is computed using two positioning parameters: the depth of the streamer (immersion) and the oblique distance between the source and the receivers (fig. 2). The immersion is recorded using a depth gauge placed on the SAR vehicle. The oblique distance is calculated by automatically picking the first arrivals (water travel times between source and receivers) on the raw seismic sections.

The second step is more rapid although more sophisticated. It concerns the seismic data correction itself. Several algorithms have been envisaged, developed and evaluated. It is possible to obtain, rapidly, a seismic section more readable than the raw one, by a rapid processing:known as the « static » correction. This correction allows the correction of the artefacts only due to the variations of altitude. Doing that, one corrects the immersion of the fish and therefore of the seismic streamer for each shot fixing it at a constant immersion level, which is the reference immersion (Fig.4). This level of reference is, in the case of PASISAR, the minimal immersion level of the fish all along the profile.

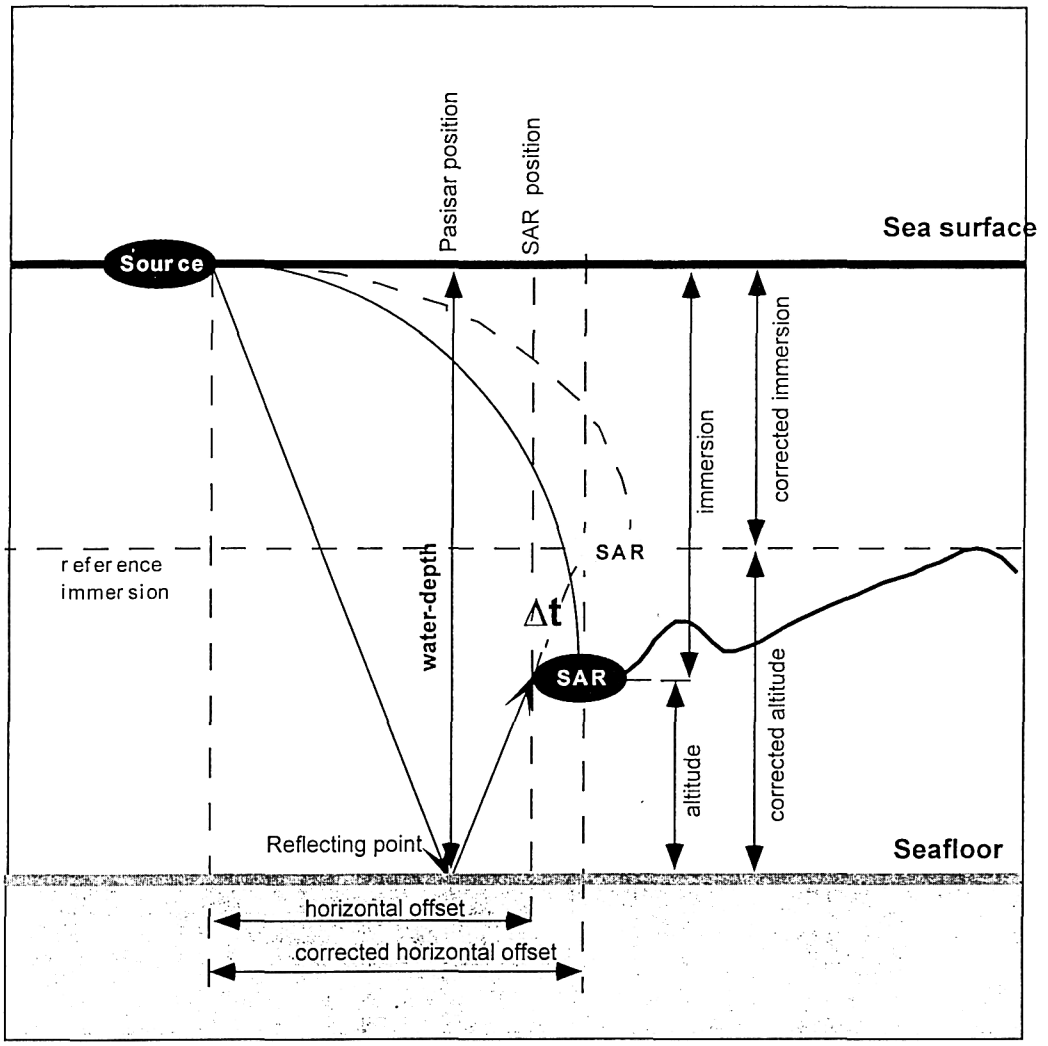


Figure 4. Principle and parameters of the static correction

Given that the level of immersion of the SAR is not constant, the source-streamer offset varies according to the variation of the bottom depth and the immersion of the fish. To obtain the information on the sea-floor geometry, it is necessary to know the gap in time $\Delta\tau$ between the streamer and the level of the reference immersion, for each shot. This gap in time $\Delta\tau$. represents the travel time of the wave, from the true position of the fish to its imaginary position at the level of immersion 0. To perform the geometrical correction, it is necessary therefore to calculate, for each shot, the gap in time $\Delta\tau$. The thoretical position from the reflective point is calculated for a locally flat bottom model. This is achieved by iteration from the parameters of immersion, altitude and horizontal offset. During this process, a verification of the position is made by comparing the calculated depth of the reflective point with the value of the true water-depth at this position, obtained from the navigation file. If the reflective point depth is identical to that of the navigation file, then the position from the reflective point is correct. Knowing the positions of the source, of the Reflective Point, of the

streamer and the level of the reference immersion, one calculates the difference $\Delta\tau$ between the travel time Source-Streamer and the travel time of Source-reference immersion. Then one corrects the seismic record of each shot by using this difference $\Delta\tau$.

However this simple correction algorithm, called " static correction ", which consists in reconstructing a profile at a virtual constant immersion in recalculating solely the first arrival time of the bottom, has been abandoned, because it did not give good results at great water-depths or when the motions of the SAR above the bottom are too great.

In fact, as in a homogenous medium, the device asymmetry is responsible for a lateral drift of the reflection point along a hyperbola (fig. 1) and the poor results of the static correction algorithm are not surprising; A new seismic trace, representative of a vertical section, must be recalculated for each shot. In more complex environments resulting from the seafloor topography and from the velocity field and because of the generally large source to receivers offsets especially in deep waters, the actual reflection point positions can be difficult to determine. Consequently, in addition to conventional processing (filtering, amplitude recovery), the PASISAR data have to be migrated in order to produce a readable image of the subsurface.

As the migration efficiency is very sensitive to the accuracy of the source to receiver offset, the immersion and the oblique distance are carefully edited to correct for any aberrant values.

For each shot, the source and the receiver are positioned on an equally spaced grid in the depth domain (the travel time grid). Note that the source and receiver positions do not have to fall on grid nodes. The arrival travel times between each point of the travel time grid and both the source and the receiver are computed using a finite difference algorithm solving the Eikonal equation (Podevin et Lecomte, 1991) and a user defined velocity model in depth. The finite difference algorithm can handle rather strong lateral and vertical velocity variations, as long as two important conditions (Hernandez et al., 1994) are fulfilled:

a/ the velocity field should be known and accurate along the profile;

b/ the first arrivals computed from the Eikonal equation, should be valid all over the section. By summing the two travel time grids (source to nodes and receiver to nodes), we obtain the source to receiver travel time grid.

According to the Fermat principle, the actual reflection points are minima of the travel time field. In the case of a simple slow varying velocity model, the nodes corresponding to these stationarities are defined, and the contribution of the current shot to the signal on these grid nodes and the close neighbours is obtained from the seismic trace. The resulting shot depth sections are stacked to produce the final section.

In the case of a highly contrasted velocity model, for each shot, the whole shot travel time grid is filled with the amplitudes of the seismic trace corresponding to the arrival times on each node. The reflectors appear thanks to the constructive interference generated when stacking the shot depth sections. This second migration method produces noisier depth sections, but takes into account all the reflection paths in complex velocity models.

In practice, because the geometry of the reflectors on raw sections are distorted and because a velocity model in depth is required, the processing has to be iterative. A first migration with constant water velocity is performed to define the actual geometry of the seafloor. Thanks to this information, a two half-spaces velocity model can be built, and the migration process repeated. The number of iterations (a migration followed by velocity model updating) will then be equal to the number of interfaces in the final velocity model.

This correction, called the « PASISAR »correction, gives the best results and is now used in routine on board the vessel with a SUN workstation (Spark 10).

## EXAMPLES OF PASISAR DATA

A hybrid seismic device such as PASISAR allows to use any kind of seismic source, either a high frequency source to conduct very high resolution surveys, or a more powerful but lower frequency source for deeper studies.

The profile of the figure 5 has been collected by 700 m of water-depth with a sparker emitting in the frequency range of 200-1000 Hz. The upper image corresponds to the profile realised with the conventional surface streamer. The PASISAR profile (middle image) has undergone the specific processing explained within the preceding paragraph. The comparison of the two profiles shows, without equivocal, the improvement of the quality of the seismic image with PASISAR. The signal / noise ratio, as well as the vertical and spatial resolutions are highly improved. The penetration obtained with the near-bottom streamer is even greater than those obtained with the conventional surface streamer.

Despite the complexity and the extent of processing undertaken on PASISAR data, the after processing profile shows no lost in quality as compared to the raw profile; the morphology of the seafloor and of the superficial reflectors are perfectly superposable with those of the 3.5 kHz subbottom SAR profile (lower part of the figure 5).

The profile of the figure 6 has been recorded at 5300 m of water-depth (Sibuet and al., 1996). The source was a G.I air gun of 150 c.i. emitting in the range of frequency 10-200 Hz. It illustrates the capacities of the PASISAR system in great water-depth.

Figure 5 : Example of conventional and PASISAR seismic profiles that have been collected simultaneously. The seismic source was a 700 J SIG sparker and the water depth was about 700 m.

A- Conventional surface data (migration using a 1500 $m.s^{-1}$ velocity).

B - PASISAR streamer data, with geometrical correction and processing sequence as in A. Note the increased signal/noise ratio, penetration and resolution compared to the conventional data in A.

C - corresponding 3.5 kHz SAR profile. Note that the detailed morphology is exactly the same as displayed by PASISAR data. The PASISAR profile usefully complements the 3.5 kHz data.

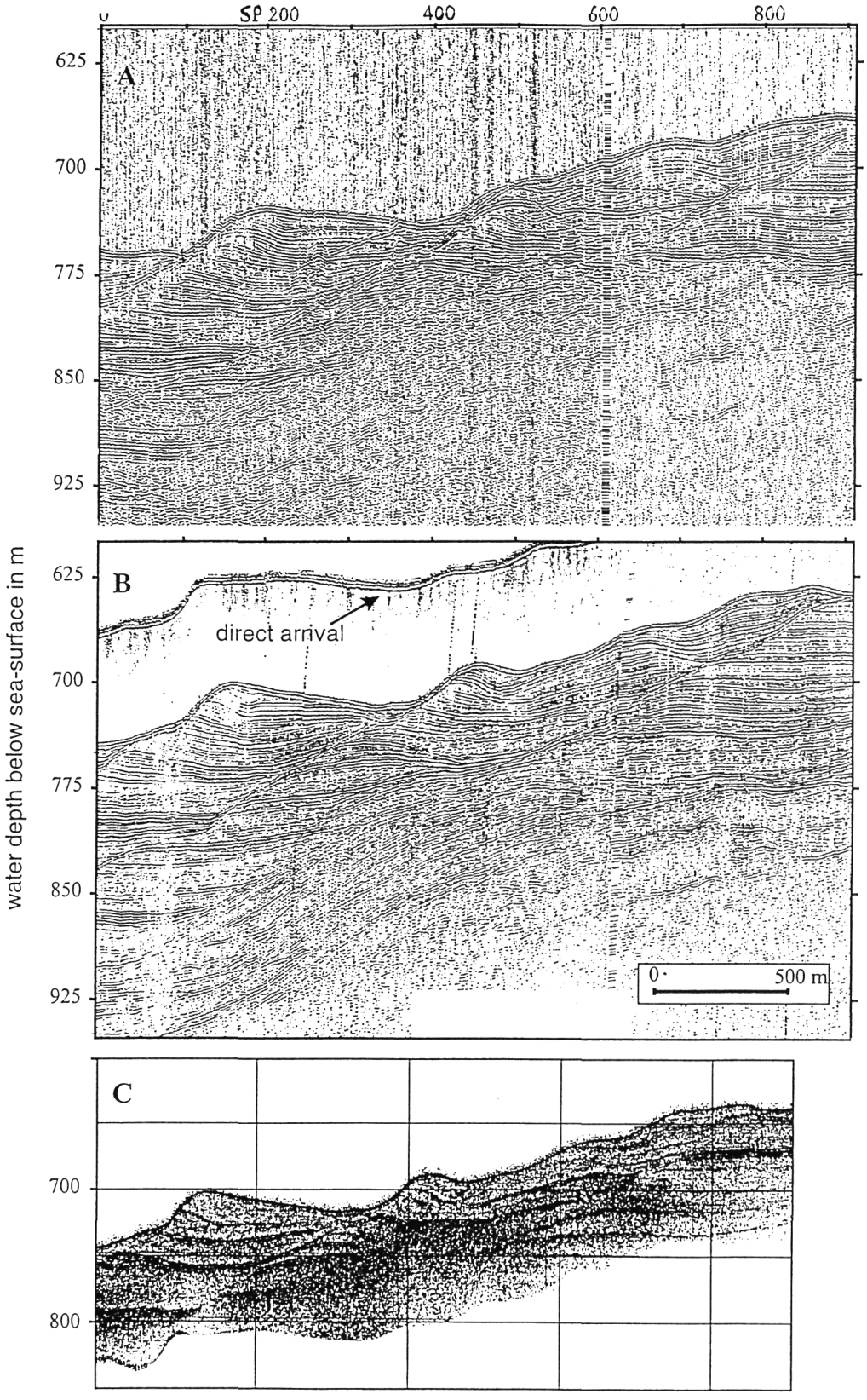
0
SP 200
400
600
800
625
700
775
850
925
A
B
direct arrival
0
500 m
C
water depth below sea-surface in m

Figure 6 : Example of conventional and PASISAR seismic profiles that has been collected simultaneously in the Iberia Abyssal Plain. The source was a 150 ci GI air-gun and the water depth was about 5300 m.

A- Conventional surface data (migration using a 1500 $m.s^{-1}$ velocity).

B - PASISAR seismic data, with geometrical correction. and processing sequence as in A. Note the increased signal/noise ratio, penetration and resolution within the sedimentary column compared to the conventional data in A.

## CONCLUSIONS

The PASISAR system is capable of acquiring high-resolution seismic data with significantly greater detail than conventional surface seismic, especially in areas of steep seabed slopes. Although the in-line offset between the source and the streamer is not negligible, the development of a specific processing package enables the production of a seismic section which can be used by geologists.

The PASISAR streamer generates a very detailed seismic profile, which can usefully complement other data from the SAR (very high- resolution side-scan sonar imagery, near-bottom bathymetry, near-bottom 3.5 kHz profiling, 3-component magnetometer data) and geophysical data collected from the vessel, namely conventional (surface) seismic and 3.5 kHz profiling. It gives good results even in very great water-depth (> 5000 m) using a GI gun. With a 750 J sparker, the results are satisfactory to a water-depth of 1500 to 1900 m (function of the state of the sea and the ambient noise level).

Thus, the SAR augmented with PASISAR is a high performance tool for detailed studies of stratigraphy, site surveys and deep-water mapping, particularly in areas of steep slope. It can be considered as a forerunner of near-bottom towed systems capable of integrated seabed studies in water depths of up to 6000 m

The recent expansion of offshore industry to deeper water has lead to the emergence of a new interest for detailed investigations at great water-depths (> 200 m), especially before setting up ...../exploration .....at the sea-floor. Industrial applications of PASISAR will be born soon. Already THOMSON MARCONI SONAR envisages to integrate PASISAR into a new tool in development. In the area of basic research, the existence of a tool such as PASISAR also opens up new prospects in geology as well as in geophysics (wide angle seismic, estimation of velocity models,....). PASISAR and in general the near-bottom geophysical tools could be the area of new intense cooperative work between the main European oceanographic institutions in the near future.

## AKNOWLEDGMENTS

We thank the commanders and the crews of the N/ O Le Suroit and N/O Le Nadir for the handling of the PASISAR system, sometimes in difficult conditions, and also P. Léon, J. Hervéou, P. Cochonat, J.-P. Chopin, G. Lebeuz, P. Pierre for their active contribution to the project.

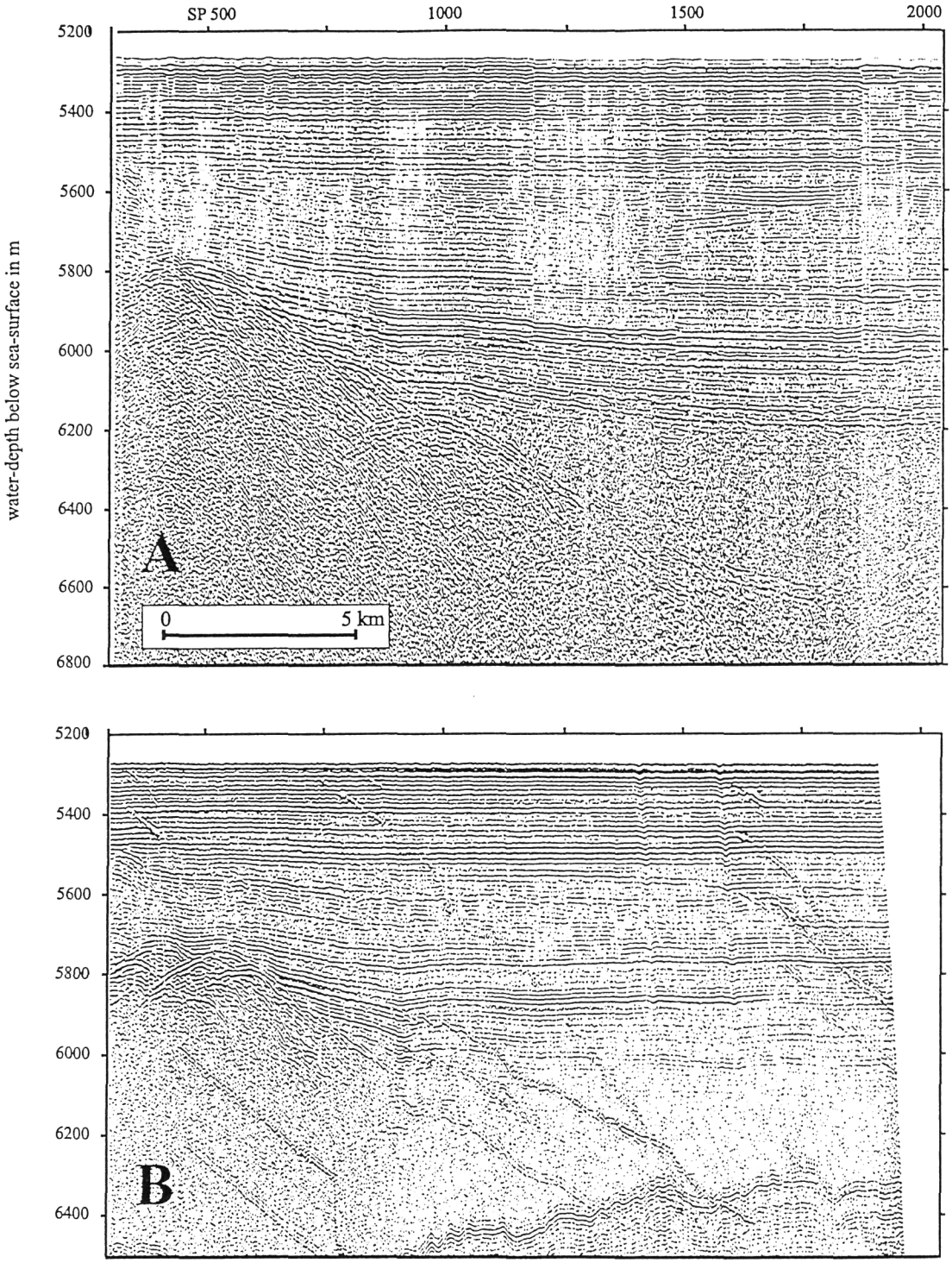
SP 500
1000
1500
2000
5200
5400
5600
5800
6000
6200
6400
6600
6800
water-depth below sea-surface in m
A
0
5 km
B

## REFERENCES


AVEDIK F., 1986. Sea-floor seismology : mobile Ocean Bottom Vertical Seismic Array (OBSVA) for controlled source experiments. In : T. Akal et J.M. Berkson (Editors), Ocean Seismo acoustics. Plenum Press, New-York.

BOWEN A.N., 1983. A high-resolution seismic profiling system using a deep-towed horizontal hydrophone streamer. *Marine Geophysical Researches,* 6, 275-293.

DODDS J., 1983. Seabed 2 program. *HUNTEC review* , 5(1), 1-3.

FAGOT M.G., 1983. A deep-towed sound source and hydrophone array system: performance, prediction analysis and hardware description. *Acoustics and the seabed.* Pace M. (ed.) Bath Univ. Press., New-York, 369-377.

HERNANDEZ F., MARSSET B., SAVOYE B., DE ROECK Y.H., MEUNIER J. and LOPES L., 1994b. PASISAR: Processing of very high-resolution near-bottom seismic data. *Proceedings Oceans 94, 13-16 Sept. 1994, Brest, France,* 2, 665-670.

KISIMOTO K., McKAY A. G. and NISHIMURA K., 1990. Data processing of deep-tow seismic data: Reflectivity modelling applied to the data from Oki Trough, Japan Sea. *Proc. SEGJ Annual Meeting, Tokyo,* 7 p.

LERICOLAIS G., ALLENOU J.P., BERNE S. and MORVAN P., 1990. A new system for acquisition and processing of very high-resolution seismic reflection data. *Geophysics,* 55 (8), 1036-1046.

MAZÉ J.P.,1991. Faisabilité méthodologique du système sismique source au bateau / récepteur sur le SAR. *Rapp. DEA, Univ. d'Aix-Marseille,* 40 p.

PODVIN P. and LECOMTE I., 1991. Finite difference computation of travel times in very contrasted velocity models: a massively parallel approach and its associated tools. *Geophysical Journal International,* 105, 271-284.

PURDY G.M. and GOVE L.A., 1982. Reflection profiling in the deep ocean using a near-bottom hydrophone. *Marine Geophys. Res.*, 5, 301-314.

SAVOYE B., MARSSET B., DE ROECK Y.H., LÉON P., LOPES L. and HERVÉOU J., 1994. PASISAR: A new tool for near-bottom seismic profiling in deep water. *OCEANS 94, 13-16 septembre, Brest, France. Proceedings,* I, 652-657.

SAVOYE B., LÉON P., DE ROECK Y.H., MARSSET B., LOPES L. and HERVÉOU J., 1995. PASISAR: a new tool for near-bottom very high-resolution profiling in deep water. *First Break,* 13, 6, 253-258.

SIBUET J.-C., THOMAS Y., MARSSET B., NOUZÉ H., LOUVEL V., SAVOYE B. and LE FORMAL J.-P. , 1996. Detailed relationship between tectonics and sedimentation from PASISAR deep-tow seismic data acquired in the Iberia Abyssal Plain. *Proc. ODP, Sci. Results, 149, College Station, TX (Ocean Drilling Program),* 649-657.

THOMAS Y., 1995. Le système d'acquisition sismique près du fond PASISAR : mise au point de la chaine de traitement. Diplôme d'ingénieur EOPG Strasbourg, Rapport IFREMER DRO/GM 95-22, Brest, 120 p.

# SAPPA: A NEW INSTRUMENT FOR SEAFLOOR SEISMO-ACOUSTIC MEASUREMENTS

ANGUS I. BEST

Southampton Oceanography Centre, European Way, Southampton, SO14 3ZH, UK.

## SUMMARY

The SAPPA is a new instrument designed for the rapid acquisition of seafloor geophysical and geotechnical data. It will enable detailed studies of acoustic wave propagation in marine sediments ranging from gravels to muds, and has direct application to pipeline and cable route surveying. The present system can penetrate two 1 m long probes into a sand or gravel seafloor and measure P-wave velocity and attenuation with depth up to a frequency of about 8 kHz. It can also measure the velocities of horizontally and vertically polarised shear waves at the surface at a frequency of about 200 Hz. Shallow water sea trials and beach trials show that SH-waves can be easily identified on the records, even in the presence of noise, thanks to the dual polarity source. Future developments will include the addition of a piezocone penetrometer for detailed stratigraphic information and shear strength measurements.

## INTRODUCTION

Remote acoustic methods are widely used by the offshore industry for seafloor assessment. High resolution sidescan sonar images and acoustic profiles combine to provide a detailed picture of the seafloor and the upper 100 m of sub-bottom sediment that is vital for choosing stable sites for large seafloor structures (e.g., Pelletier et al., 1997; Power et al., 1997). Cable and pipeline route assessments, on the other hand, require very detailed information in the upper 2 m sub-seafloor for predicting the ploughability of the sediment. In both cases, while recognising and tracing the extent of geological strata is helpful, the engineering geologist requires quantitative data, such as sediment strength, that will enable soil behaviour to be predicted under various scenarios. Only by understanding the relationships among the acoustic and geotechnical properties of marine sediments will it be possible to extract quantitative information using remote acoustic methods.

Most of what we know about marine sediment acoustic properties has come from laboratory measurements on cores or other sample types. The unconsolidated nature of marine sediments and the sampling methods themselves can often lead to sample disturbance that is difficult to quantify (Weaver and Schultheiss, 1990), which in turn leads to doubts over the validity of laboratory measurements. The alternative is to carry out careful measurements on the seafloor itself, which raised some significant, but not insurmountable, technological challenges. Indeed, the technology for in-situ acoustic measurements has been around for some time, but has not been used widely. On the other hand, the offshore industry uses seafloor instruments to measure geotechnical parameters as a matter of routine.

## THE SAPPA CONCEPT

There are several seafloor systems already in existence for measuring acoustic and geotechnical properties (Power and Eastland, 1986; Rodger, 1986; Barbagelata et al., 1991; de Lange, 1991; Theilen et al., 1992; Power and Geise, 1995). These are mostly shallow

water systems, although seafloor acoustic measurements have been made in deep water using, for example, a submersible (Hamilton et al., 1970), or a modified piston corer (Fu et al., 1996); IFREMER in France have developed an instrument for deep water geotechnical measurements in soft sediments (Damy, 1989). Despite these efforts, there is no single system that can work in all water depths and can offer a flexible approach to sensor configuration according to sediment type.

The concept of the SAPPA (Sediment Acoustic and Physical Properties Apparatus) is that it should enable both geophysical and geotechnical measurements to be made on the same volume of seafloor sediment at the same time. This is the only way to reliably investigate the fine-scale inter-relationships among sediment properties. It should also operate in water depths up to 2,000 m, which marks the approximate limit of offshore activities in the foreseeable future, and preferably to full ocean depth (6,000 m). It should also enable a fairly rapid and expansive coverage of a designated study area, given the financial constraints on ship time, and real-time data acquisition, if possible. Most importantly, it should be able to deal with a range of sediment types, from sands and gravels to silts and clays, that exhibit a wide range of geophysical and geotechnical properties. By using a single, well calibrated instrument such as this, it will be possible to make valid comparisons of sediment physical properties between seafloor stations only a few metres apart, or located in different ocean basins. The accuracy of the measurements is most important if subtle relationships are to be investigated, such as the effect of low-concentration, biogenic gas production on sediment strength.

**Figure 1. The SAPPA being assembled at sea during shallow water trials (CD104).**

## SAPPA FOR COARSE SEDIMENTS

The SAPPA development is ongoing, but the initial work was carried out during the POSEIDON Project (MAS3-CT95-0038) alongside several other instrument developments for detailed seafloor and sub-bottom studies in deep water (see Best et al., 1996). The first operational requirement of the SAPPA was to obtain seismo-acoustic data on coarse grained

sediments during a multi-disciplinary environmental survey in the Arabian Gulf (see Kenyon, 1997).

The main purpose of the SAPPA is to deploy instrumented, sediment probes. It is well known from marine sediment coring operations that probes (or core barrels) are difficult to penetrate into coarse sand and gravel under their own weight. Hence, a "pile-driver" system was designed where each probe is pre-loaded with a mass appropriate to the sediment resistance, and is struck repeatedly with a driver mass (or hammer). A basic system worked well during initial tests on a sandy beach. The SAPPA frame and probes are described below.

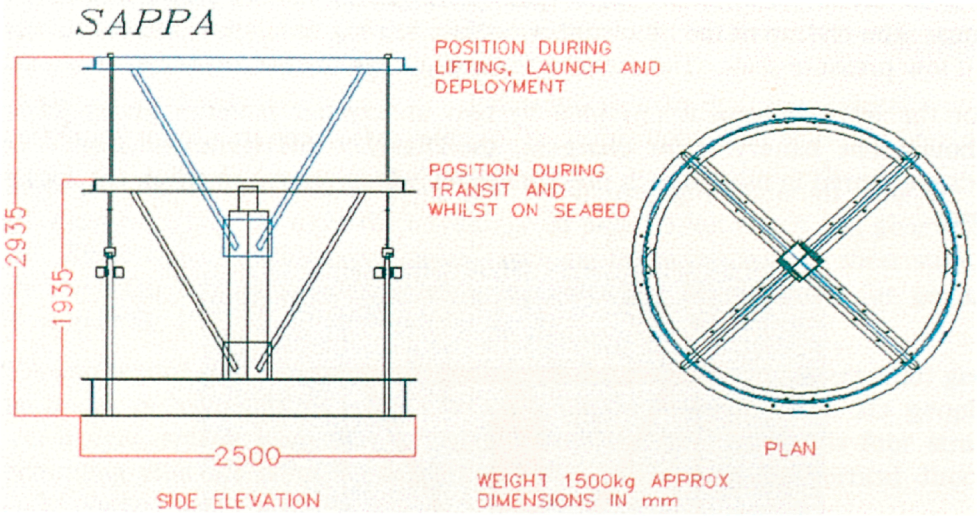


**Figure 2. The SAPPA frame showing its position during deployment and while on the seafloor.**

## FRAME AND PROBES

The SAPPA frame is made from steel and is divided into a lower and an upper part (Figures 1 and 2). The lower part comprises a circular space frame with a sturdy base supported by four cross members and has a central, vertical pillar for guiding the upper frame during lifting and lowering. The upper frame is also circular with four supports attached to the guide on the central pillar. The whole frame is lifted using a strop attached to the centre of the upper frame; the upper frame rises until it comes against end stops on the central pillar which then take the full weight of the lower and upper frames. The purpose of this design is to enable the two probes to be fully retracted inside the frame before it is lifted off the seafloor, and to achieve this without putting lateral stresses on the probes that could bend them during their extraction.

The frame has a versatile arrangement of attachment points for electronics tubes and ancillary equipment, and will allow new sensor systems to be mounted. It is 2.5 m in diameter and weighs approximately 1.5 tonnes in air when the electronics tubes and probes are attached.

The two steel probes are 38 mm in diameter, approximately 1.3 m long and give a sediment penetration of 1 m. A spring loaded hammer mechanism is used to drive the probes into the sediment under a pre-load that can be varied according to the sediment type. At present it is set up for coarse grained sediments and has a pre-load of 16 kg; the spring loaded hammer

delivers an impulse of approximately 1 N.s, releasing a stored energy of about 2.5 Joules. The hammer is raised and dropped using a cam driven by an electric motor via a sealed flexible drive shaft. The vertical probe displacement is measured by a taut wire wound onto a grooved drum that is coupled to a rotary spring and a multi-turn potentiometer.

Three motor units are used to drive the two probe hammers and the SH-wave generator (see below). Each unit comprises a Maxon motor and gearbox attached to a shaft via a flexible coupling housed within a modified 12-inch pressure tube. The shaft exits the pressure tube through two bearings and a high pressure seal into a pressurised oil chamber; the outer bearing takes the inward thrust resulting from the hydrostatic load on the shaft. The oil chamber is covered by a rubber boot to pressurise the oil and to take account of volume fluctuations. The endcap of the oil chamber holds a bearing to support the shaft and contains a series of low pressure seals. The motor units are attached to the lower frame assembly.

Power for the whole system is provided by two underwater batteries giving 24 volts, 38 ampere hours; one battery is for charging, the other is for operational use. The main electronics are stored in two 30-inch pressure tubes which are mounted on the spokes of the lower frame.

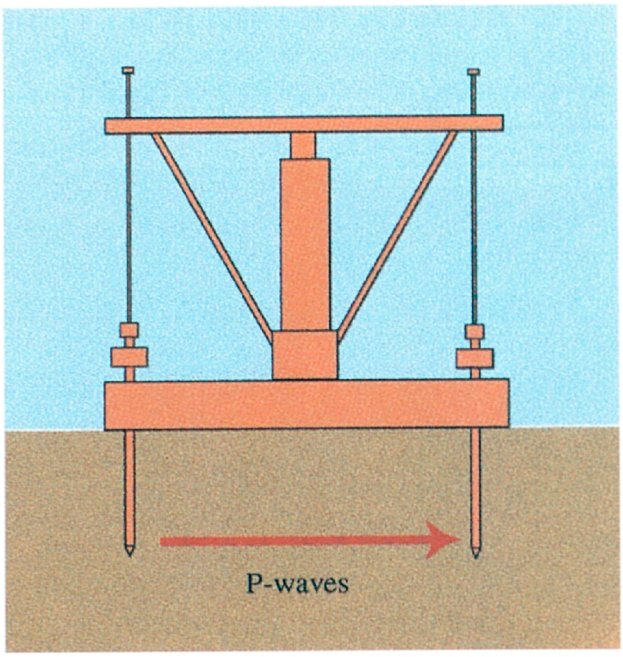


**Figure 3. SAPPA showing P-wave profile method.**

## P-WAVE MEASUREMENTS

A P-wave source is housed in the tip of one of the probes and transmits signals that are detected by two hydrophone receivers. One hydrophone is housed in the second probe tip, the other is mounted on the frame near the top of the source probe. High resolution profiles can be acquired by driving the probes into the sediment in tandem and recording a shot at each depth (see Figure 3). Alternatively, the probes can be driven into the sediment independently to obtain different source-receiver geometries and, hence, propagation directions through the

sediment column; the surface hydrophone gives the vertical direction. Being able to record waves in the vertical and horizontal directions can potentially give sediment anisotropy information.

The P-wave source uses a spring loaded axial hammer to strike a conical steel washer braced against the internal wall of the probe. Water tank tests were carried out to determine the source power, directivity and frequency content. The P-wave source was found to give useable energy up to a frequency of about 8 kHz making it possible to compare the results directly with most high resolution profiling systems. A source power of 152 dB re: 1 µPa @ 1 m was recorded using a calibrated reference hydrophone. Inspection with the reference hydrophone at different positions in the water tank suggested a spherical radiation pattern. The source produces repeatable signals that can be used for attenuation measurements, knowing the source power given above.

## SHEAR WAVE MEASUREMENTS

Shear waves are difficult to generate in low shear strength materials and are rapidly attenuated. However, they do have the advantage of polarisation which can give anisotropy information. Shear wave velocity is particularly relevant for estimating soil shear strength and is probably the most important seismic parameter that can be measured for geotechnical studies (Hovem et al., 1991).

The SAPPA can record shear waves of any polarity using a three-component (3D) geophone comprising three, orthogonally aligned, OYO GS-20DM elements. The 3D geophone is mounted on a light, spiked plate that is isolated from the steel frame via four struts with special decoupling joints; it is spring-loaded and free to move in the vertical direction to ensure a good contact with the seafloor.

Horizontally polarised shear waves (SH-waves) are generated using a ridged footplate that is impacted by two sprung, cam operated hammers driven by the motor/shaft arrangement described above (see Figure 4). The footplate is isolated from the steel frame and is free to move in the vertical direction in a similar manner to the 3D geophone.

The advantage of the SH-wave generator is that is generates opposite polarity waves that can help identify shear waves in the presence of noise. Vertically polarised shear waves (SV-waves) are generated by the probes as they are hammered into the sediment.

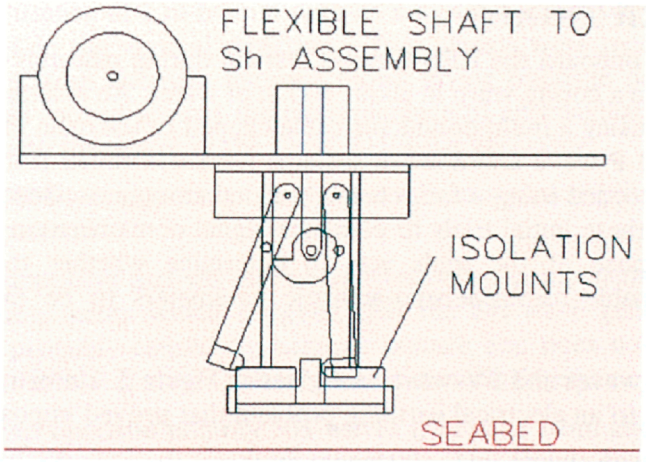


**Figure 4. SH-wave generator.**

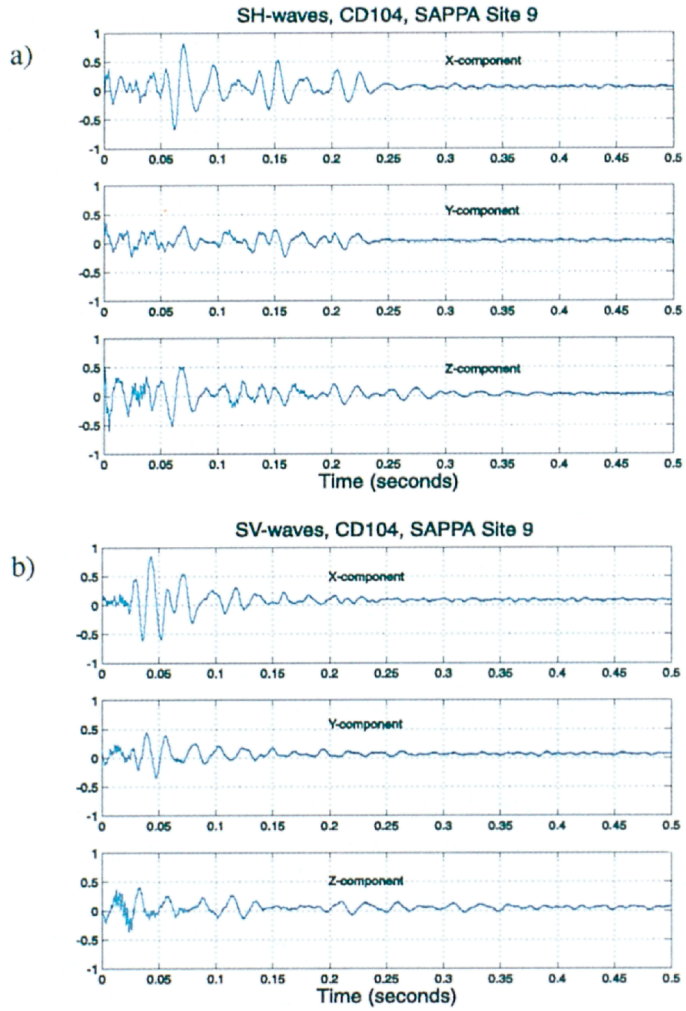


**Figure 5. Example three-component data recorded during shallow water trials: a) SH-waves; b) SV-waves.**

## SHALLOW WATER TRIALS

The SAPPA was taken onboard the RRS Charles Darwin during research cruise CD104 and deployed amidships from a coring warp in about 100 m of water. An analogue signal path was provided to the surface using a multi-conductor cable clipped to the main lifting warp. Hence, the SAPPA probes, and P-wave and S-wave systems were controlled from the surface; full waveform data were recorded using a four channel, digital storage oscilloscope. An analogue system was chosen for these initial trials to eliminate signal contamination by digital aliasing effects. The main purpose of the trials was to determine whether the SAPPA sensor configuration would enable useful seismo-acoustic parameters to be extracted from the recorded signals.

Example results for SH-waves and SV-waves are given in Figure 5. Unfortunately, no P-wave data were collected due to an electrical earthing problem that proved impossible to correct at sea.

The results show what look to be impulsive SH-waves on the transverse (x-) component in Figure 5a , including two similar, later arrivals; the first arrival gives a SH velocity of about 20 m/s. There is very little energy on the other two components. In Figure 5b, most of the energy is on the two horizontal components and there is a fair amount of noise, although there is a small amount of energy on the vertical (z-) component (SV-wave?). To assess the results, it is first necessary to determine the source signatures in the absence of the steel frame that may cause spurious "frame wave" arrivals.

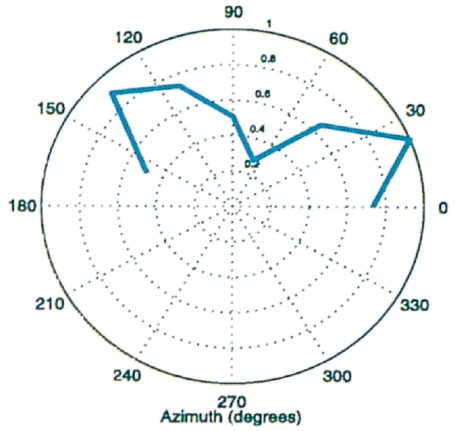


**Figure 6. Normalised amplitude versus radiation direction for the SH-wave generator. The particle motion is along the axis 0 - 180 degrees.**

## BEACH TRIALS

Trials were conducted on a sandy beach using the SH-wave generator, a probe (for producing SV-waves) and the 3D geophone detached from the frame.

The SH-wave generator was pushed firmly (about 1 cm) into wet sand and the 3D geophone was planted at a distance of 1 m from it with its x-axis in the transverse direction, its y-axis in line, and its z-axis in the vertical direction. Two signals were recorded at each geophone location, each one from alternate hammer blows giving opposite polarity signals. The 3D geophone was then moved around the circumference of an imaginary circle, always keeping the y-axis in line with the centre of the fixed, SH-wave generator.

The polar plot of SH-wave (x-component), normalised signal amplitude in Figure 6 shows a dipolar radiation pattern.

Figure 7a shows impulsive arrivals on the transverse (x-) component, and almost nothing on the other two components which suggests that the SH-wave generator works well. The second arrival is probably caused by hammer bounce and does not affect the results. The velocity of the first arrival is about 100 m/s with a dominant frequency of about 200 Hz.

Figure 8 shows two opposite polarity SH-waves generated from alternate hammer blows of the SH-wave source; the signals are quite repeatable. This facility enables several signals to be

stacked to suppress compressional waves such as frame waves, hence increasing the likelihood of detecting shear waves in the presence of noise.

One of the probes was hammered into the sand to a depth of about 50 cm at distances of 1 m, 2 m and then 3 metres from the 3D geophone. An example three component record is shown in Figure 7b. A similar pattern emerges to that observed during the sea trials in Figure 6b; large amplitude arrivals are seen on the horizontal components and a relatively small amplitude arrival on the vertical component. The dominant frequency of the first arrival on the vertical component is about 200 Hz. SV-wave velocities of 110 m/s, 181 m/s and 217 m/s at 1 m, 2 m and 3 m, respectively, were measured. This implies that lower velocity surface waves are measured at close source-receiver separations, while faster, refracted body waves are recorded at larger separations. When mounted on the SAPPA frame, the increasing depth of penetration of the SV-probe may produce a variable source signature that could cause problems for attenuation measurements. This is still under investigation.

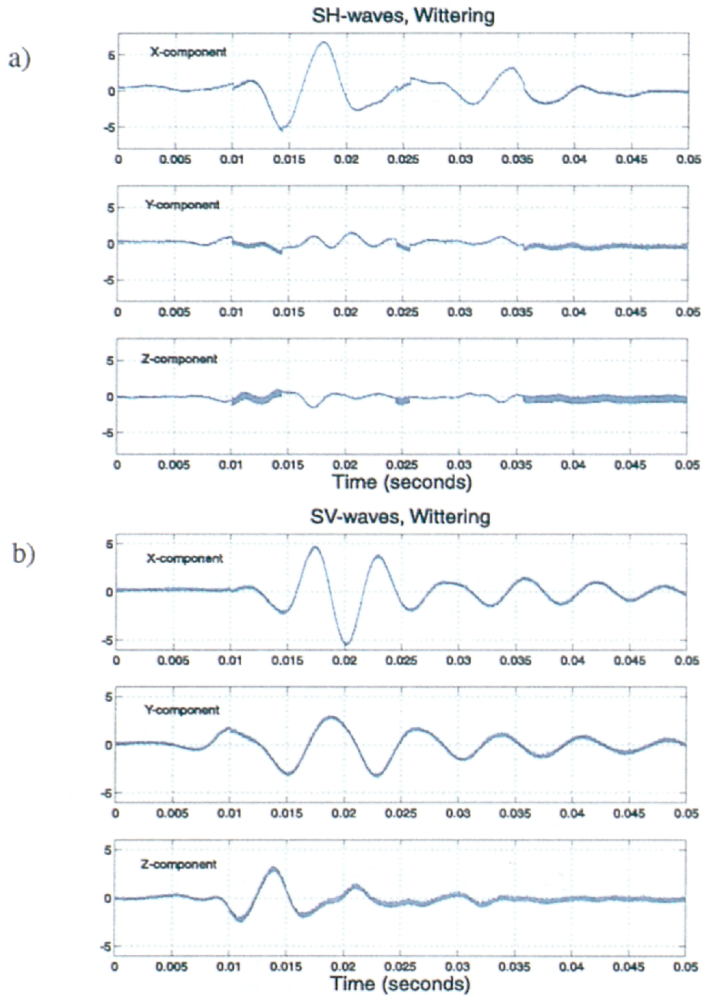


**Figure 7. Example three component data from Wittering beach trials: a) SH-waves; b) SV-waves.**

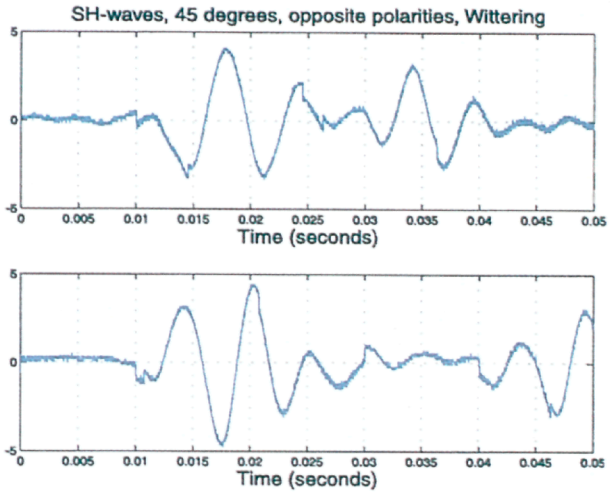


**Figure 8. Opposite polarity SH-waves (x-components) recorded during the beach trials.**

## CONCLUSIONS

In its present configuration the SAPPA comprises a steel frame with two probes capable of penetrating 1 m into coarse sand or gravel. It is possible to measure P-wave velocity and attenuation as a function of depth with a vertical spatial resolution of a few centimetres in vertical, horizontal and oblique wave propagation directions. S-waves are recorded at the sediment-water interface using a three component geophone. SH-waves are generated using a novel system positioned on the seafloor, while SV-waves are generated through the impacting of one of the probes as it is driven into the sediment. The P-waves have a broad frequency content up to 8 kHz in water, the SH- and SV-waves have frequencies of about 200 Hz in sediment. The P-wave system is still to be tested in sediment, but the SH-wave system in particular gives very good results. All systems generate sufficiently strong signals for measuring velocity and attenuation in coarse sands and gravels over distances of a few metres.

The SAPPA must be deployed on a load-bearing, conducting cable at present which restricts it to certain vessels. Acoustic telemetry and an onboard data logger would enable it to operate from a wider range of ships.

The aim is for SAPPA to provide a flexible and robust platform for sensor deployment according to the specific seafloor under investigation. Plans for the immediate future include the addition of a cone penetrometer for detailed stratigraphic information and shear strength. This will involve some modifications to the probe penetration system as a constant penetration rate is required. Other improvements could include the addition of a second 3D geophone so that S-wave attenuation can be measured. The ability to measure S-wave properties versus depth in a similar manner to the P-wave system would also be desirable.

## ACKNOWLEDGEMENTS

The SAPPA work was funded by the United Kingdom (UK) Natural Environment Research Council, and by the European Commission's Marine Science and Technology programme under contract MAS3-CT95-0038 (POSEIDON). Thanks goes to Geotek Limited (UK) for their involvement.

## REFERENCES

Barbagelata, A., Richardson, M. D., Miaschi, B., Muzi, E., Guerrini, P., Troiano, L. and Akal, T., 1991, ISSAMS: an in situ sediment acoustic measurement system. Shear waves in marine sediments, J. M. Hovem, M. D. Richardson and R. D. Stoll. Dordrecht, Kluwer Academic, 305-312.

Best, A. I., Bjørnø, L., Bourillet, J. F., Bruun, S. G., Mienert, J., Peirlinckx, L., Sessarego, J. P., Van Biesen, L. and Zakharia, M. E., 1996, The remote detection of sediment stability on the European continental margin and slope. Marine Science and Technology (MAST III) 1994-98 Project Synopses, M. Weydert. Luxembourg, European Commission, DG XII, Science, Research and Development. **1**, 80-81.

Damy, G., 1989, Module Géotechnique. Etude de la mise en oeuvre, Brest, IFREMER, 23.

de Lange, G., 1991, Experience with the seismic cone penetrometer in offshore site investigations. Shear waves in marine sediments, J. M. Hovem, M. D. Richardson and R. D. Stoll. Dordrecht, Kluwer Academic, 275-282.

Fu, S. S., Wilkens, R. H. and Frazer, L. N., 1996, Acoustic lance: new in situ seafloor velocity profiles. *Journal of the Acoustical Society of America*, **99**(1), 234-242.

Hamilton, E. L., Bucker, H. P., Keir, D. L. and Whitney, J. A., 1970, Velocities of compressional and shear waves in marine sediments determined in situ from a research submersible. *Journal of Geophysical Research*, **75**, 4039-4049.

Hovem, J. M., Richardson, M. D. and Stoll, R. D., 1991, Shear waves in marine sediments.Dordrecht, Kluwer Academic.

Kenyon, N. H. et al., 1997, RRS Charles Darwin Cruise 104 Leg 2, 21 March - 19 April 1997. Geological processes in the Strait of Hormuz, Arabian Gulf: a contribution to the Scheherezade Programme, Southampton Oceanography Centre, 61.

Pelletier, J. H., Doyle, E. H. and Dutt, R. N., 1997, Deepwater geotechnical investigations in the Gulf of Mexico. *Journal of the Society for Underwater Technology*, **22**(2), 63-73.

Power, P. T. and Eastland, D., 1986, Seasprite - a new seabed soil testing system. *Underwater Systems Design*, **8**(2), 32-35.

Power, P. T. and Geise, J. M., 1995, Seascout mini-CPT system, Proceedings of the International Symposium on cone penetration testing, Linköping, Sweden.

Power, P. T., Orren, R. J. and Stephens, R. V., 1997, Integrated site and route assessments in deepwater, Worldwide deepwater technologies, Institute of Marine Engineers, London.

Rodger, A. A., 1986, New seabed sampling and testing system. *Offshore Research Focus*, **51**, 9.

Theilen, F., Kogler, F. C., Van Bocxlaer, K., de Batist, M., Missiaen, T., Ori, G. G., Ollier, G., McGee, T. M. and Brussard, P., 1992, GISP - geophysical in-situ probe, European Conference on Underwater Acoustics, London, Elsevier Applied Science.

Weaver, P. P. E. and Schultheiss, P. J., 1990, Current methods for obtaining, logging and splitting marine sediment cores. *Marine Geophysical Researches*, **12**, 85-100.

# THE BATHYMETRY ASSESSMENT SYSTEM

G.J. WENSINK, G.H.F.M. HESSELMANS, C.J. CALKOEN

ARGOSS
P.O. Box 61, 8325 ZH Vollenhove, the Netherlands

## SUMMARY

In the presence of current and wind, submerged topographic features of the sea bed produce contrasts in radar images. These contrasts can be quantitatively understood and modeled, based on hydrodynamics and electromagnetic scattering theory. A suite of models has been developed based on the generally accepted imaging mechanism, which consists of three steps: (1) surface current modulation by the bathymetry, (2) modulation of the (small) wave spectrum by wave-current interaction, and (3) radar backscattering by the sea surface. In order to invert this depth-radar backscatter relation, a data assimilation scheme has been developed. These numerical models have implemented, leading to the Bathymetry Assessment System (BAS). An example of an application in the Dutch coastal waters is presented.

## 1. INTRODUCTION

Bathymetric data of shallow seas are of vital importance for shipping, fishery and all kinds of offshore activities as well as coastal management. Traditionally, depth information is collected from ships using (single or multi beam) echo sounders. Bathymetric surveys are therefore time and cost consuming. Remote Sensing methods may improve the efficiency of bathymetric surveys, since they give an instantaneous overview over large area's at relatively low costs.

In 1969 de Loor c.s. discovered that under suitable conditions (moderate wind and strong tidal current) bottom topography is visible in radar images [De Loor and Brunsveld van Hulten, 1978; De Loor, 1981]. This was a great surprise: the sea surface is an almost perfect conductor at radar frequencies and, as a consequence, the microwave radiation does not penetrate into the water column, but reflects from the surface only. In 1978 the SEASAT satellite was launched, carrying for the first time an imaging radar in space. The nice images of bottom structures in the Southern Bight of the North Sea and in the Nantucket Shoals at the eastern coast of America further demonstrated the potential of microwave techniques.

The results of SEASAT aroused much interest in the phenomenon, both from the experimental and from the theoretical side. Alpers and Hennings [1984] came with the first model of the imaging mechanism. This model proved to be essentially correct, not only for bottom topography but also for other phenomena causing surface current variations like internal waves, fronts and ship wakes. It could also be applied to the optical window, especially when looking into the reflection of the sun on the sea surface. Surface expression of bathymetry can, under suitable conditions, even be observed with the naked eye, a fact known for centuries by sailors and fishermen.

The ERS-1, carrying a C-band Synthetic Aperture Radar (SAR), was launched succesfully in 1991. It was followed by ERS-2 in 1995. Now radar images became available at a regular base. This motivated a number of studies, supported by the Netherlands Remote Sensing Board (BCRS) and the European Commission (EC), in which the various submodels in the imaging mechanism were improved and practical applications were considered. Given the depth of an area, the wind speed and its direction, and the tidal phase, it is now possible to predict quantitatively, with reasonable accuracy, how a radar image will look like. This is nice from a scientific point of view, but for practical use one would like to go the other way round: predict the depth given the radar image. This is not feasible by analytical inversion of the imaging model, due to its complexity. Therefore numerical techniques were developed to achieve this, leading to the Bathymetry Assessment System (BAS). BAS constructs a depth map from one or more radar images (and a reduced number of traditional echo soundings. The soundings are needed to adjust some model parameters which are not well known. They are also used as constraints to the depth map. One may view the BAS as an "intelligent interpolator" which interpolates between transects of echo soundings using the depth information in radar images. The accuracy of the resulting depth map depends, of course, on the distance between the transects.

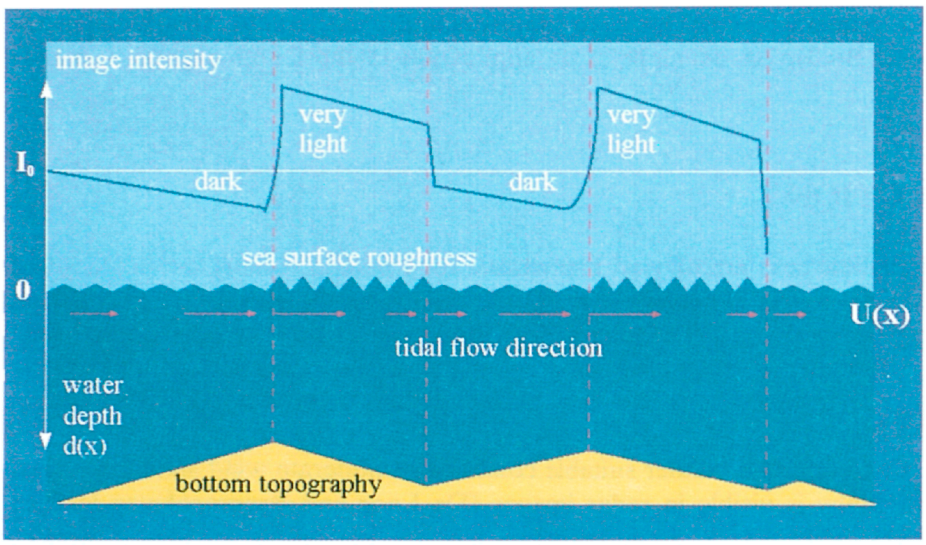


Figure 1 Bathymetry by imaging radar

## 2. BATHYMETRY ASSESSMENT SYSTEM

Under favourable meteorological and hydrodynamic conditions (moderate winds of 3 to 9 m/s and significant tidal currents of 0.5 m/s or more), air- or space borne Synthetic Aperture Radar (SAR) imagery shows features of the bottom topography of shallow seas (Alpers and Hennings 1984, Vogelzang et al., 1989).

The imaging mechanism of mapping sea bottom topography by imaging radar consists of three stages (a more detailed mathematical formulation is given in Calkoen et al., 1993):

(1) Interaction between (tidal) flow and bottom topography results in modulations in the (surface) flow velocity. This relation can be described by several models with an increasing level of complexity: continuity equation, shallow water equations, and the Navier Stokes equations.
(2) Modulations in surface flow velocity cause variations in the surface wave spectrum. This is modelled with the help of the action balance equation, using a relaxation source term to simulate the restoring forces of wind input and wave breaking.
(3) Variations in the surface wave spectrum cause modulations in the level of radar backscatter. To compute the backscatter variations a simple Bragg model can be used, but also available are two-scale and first iteration Kirchoff (Holliday) models.

Based on the above three stage mechanisms, a suite of computer models has been developed and operationalized at ARGOSS. Models with different levels of complexity and physical detail are available for each step. These models describe the flows, waves and electromagnetic scatter and can be used for a quantitative analysis of radar imagery.

This suite of computer models generate the radar backscatter given the bathymetry and the wind. In order to invert this depth-radar backscatter relation, a data assimilation scheme has been developed, minimizing the difference between the calculated and the measured radar backscatter by adjusting the bottom topography.

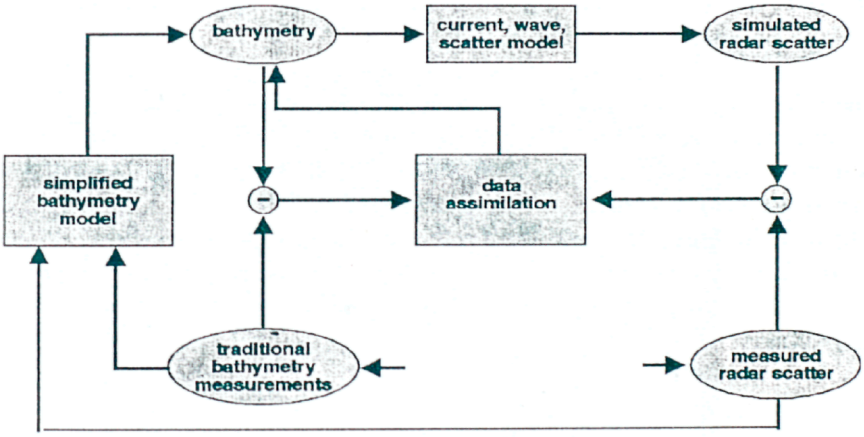


Figure 2 Bathymetry Assessment System

The imaging model in BAS contains two-dimensional models. This means that the flow and the wave field need not be schematised as one-dimensional, in the same direction as the radar look direction. However, a fully two-dimensional data assimilation scheme for BAS is presently not yet available. At the moment two one-dimensional limits of BAS are available: one in which the main depth variations are supposed to lie perpendicular to the flow direction and one in which the depth variations are mainly parallel to the flow. These two limiting cases are called the sand wave system and the channel system, after their main application. The structure of this modular system is shown in figure 2.

# 3. ZEEGAT VAN AMELAND

The Bathymetry Assessment System has been applied in the "Zeegat van Ameland" area, which is shown in figure 3. The purpose of the project is to assess the applicability of (the current version of) the BAS and assess its accuracy as a function of the distance between section lines.

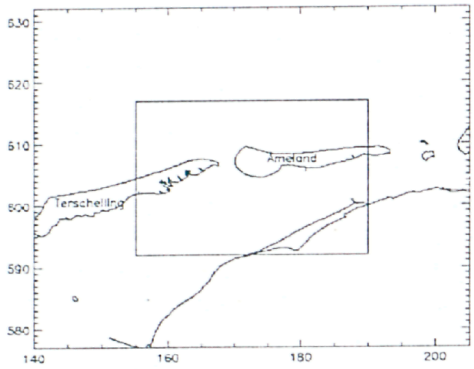


Figure 3 Map of the northern part of th e Netherlands showing the project area.
The axes show the location in the "Rijksdriehoek" coordinate system.

The area of interest, is a tidal inlet in between the Dutch islets Terschelling and Ameland in the Waddenzee, north of the Netherlands. The area measures 35 km by 25 km. The project area lies approximately between 5° 23' and 5° 55' E, and 53° 19' and 53° 33' N.

The Bathymetry Assessment System requires, amongst others, SAR data and a limited number of sounding data. Most important are the SAR images from which the depth maps are constructed. The limited number of ship's soundings are needed to calibrate model parameters in BAS. Other required *in situ* measurements are: the wind speed and direction, and the tidal phase from which the flow field and the water elevation is computed. In this study the following data sets were obtained: ERS-1 images, hydro-meteorological conditions, sounding data, positioning data.

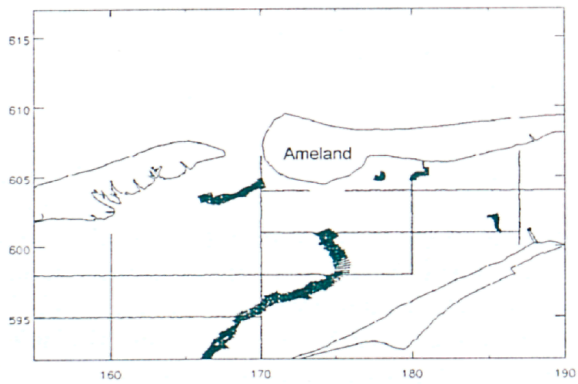


Figure 4 Sounding data of 1996.

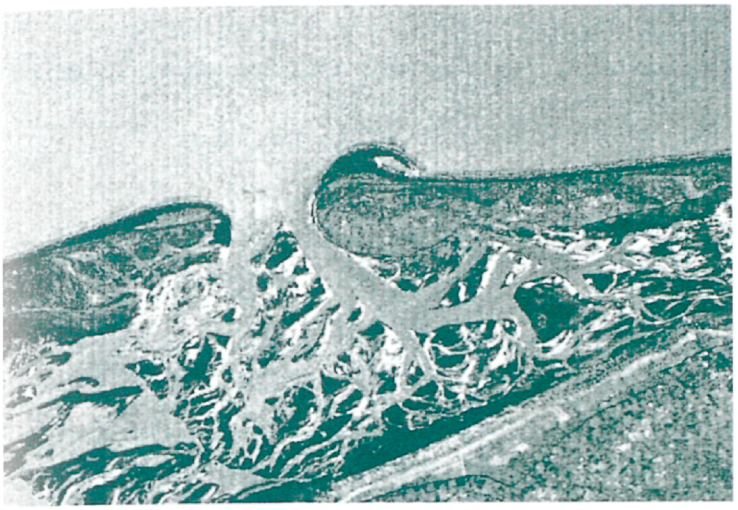

Figure 5 ERS-1 SAR image of Zeegat van Ameland acquired at April 12, 1996.

The Bathymetry Assessment System uses an imaging model, which contains a flow, a wave and a radar backscatter model, to simulate a SAR image for a given first depth assessment. The simulated SAR image is compared with the measured images and the ship's measurements and observed differences are used to adjust the first assessed depth map with the help of data assimilation techniques. Figure 6 shows the depth map of the test site produced with BAS.

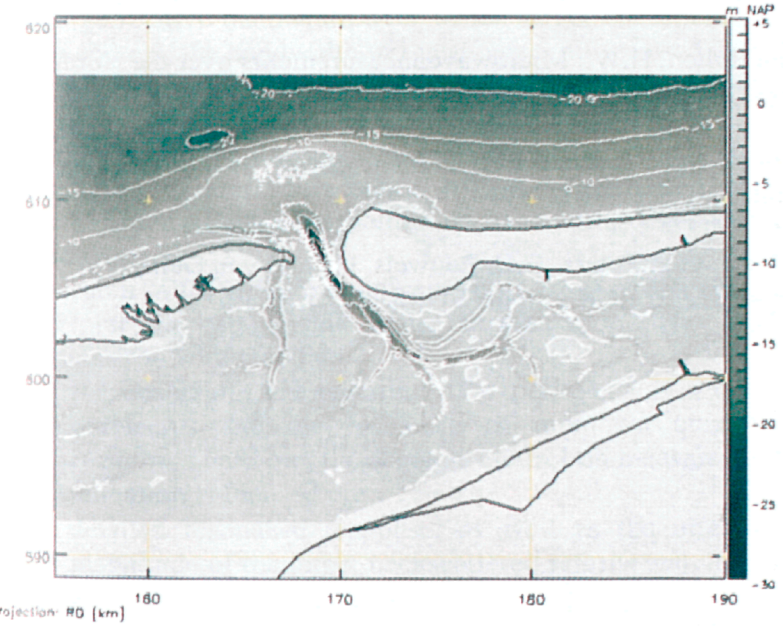


Figure 6 Bathymetric map of the project area based on ERS SAR imagery and all soundings. The depth range is between -30 m and +5 m. Contour levels are drawn at 10 m interval. Depth is shown on a grey scale.

# 4. CONCLUSIONS

- Results show that BAS constructs accurate depth maps from SAR imagery and a limited number of calibration tracks.
- The system at the moment can only be operated successfully by specialists.
- Survey efforts can be reduced with a factor 5.

## REFERENCES


Alpers, W., and Hennings, I., A theory of the imaging mechanism of underwater bottom topography by real and synthetic aperture radar. *Journal of Geophysical Research*, **C89**, 10529-10546, 1984.

Calkoen, C.J., Wensink, G.J. and Hesselmans, G.H.F.M., *ERS-1 SAR imagery to optimize the NOURTEC ship-based bathymetric survey: feasibility study*, Delft Hydraulics report H1875, November 1993.

Calkoen, C.J., and Wensink, G.J., Use of ERS-1 SAR imagery to optimize ship-based bathymetric surveys in theWaddenzee: feasibility study. Delft Hydraulics report H1985, December 1993.

Hesselmans, G.H.F.M., SAR surveyZeegat van Ameland, ARGOSS, November 1996.
Hesselmans, G.H.F.M., Update SAR surveyZeegat van Ameland, ARGOSS, December 1997.

De Loor, G.P., and Brunsveld vanHulten, H.W., Microwave measurements over the North Sea. *Boundary Layer Meteorology*, **13**, 113-131, 1978.

De Loor, G.P., The observation of tidal patterns, currents and bathymetry with SLAR imagery of the sea. IEEE Journal of Oceanic Engineering, **6**, 124-129, 1981.

Vogelzang, J., Wensink, G.J. de Loor, G.P.,Peters, H.C. Pouwels, H., and van Gein, W.A., *Sea bottom topography with X-band SLAR*, BCRS report BCRS-89-25, 1989.

# UNDERWATER RAIL FACILITY FOR HIGHLY CONTROLLED EXPERIMENTS AT SEA

S. FIORAVANTI, A. MAGUER, W.L.J. FOX,
L. GUALDESI, AND A. TESEI

SACLANT (NATO) Undersea Research Centre
Viale San Bartolomeo 400
19138 La Spezia, Italy

## SUMMARY

A description of an experimental facility designed to measure bottom reverberation and scattering from buried objects insonified by low-frequency broadband acoustic pulses, at various aspects and grazing angles.

## 1. INTRODUCTION

The high levels of acoustic attenuation characteristic of some ocean sediments complicate detection and classification of buried objects at conventional sonar frequencies. Recent research has focused on experimental broadband sonar, utilizing frequency bands that extend down to the order of 1 kHz. As acoustic attenuation is generally less at lower frequencies, acoustic detection of buried objects may be feasible. The broadband nature of the sonar gives a large relative bandwidth over which target classification information may be extracted. In this context, the bandwidth of the acoustic pulses used is in the *ka* range [1-15].
In this frequency range, one characteristic of target echoes which may provide classification clues is the so-called resonance scattering response, the characteristics of which are attributable to the target elastic properties.
Furthermore, the physics of sub-critical sound bottom penetration (Maguer *et al*, 1998) and methods for reducing the bottom backscattering level (Fioravanti *et al*, 1996) are subjects for further study.
Research in these fields involves a high level of modeling to develop data simulators and to interpret the phenomena under investigation. The models must also be validated by comparison with real data.
As the designing and planning of experiments is a critical and complex task, inaccurate measurements and the influence of unknown quantities can invalidate the proposed conclusions. Therefore, the accurate control on measurement is required.
The attention is focused on:

- detailed resonance response, as well as the effect of full and partial burial on the magnitude of the target backscattered returns and, hence, on the target *detectability* as the grazing angle and the target aspect angle vary
- acquisition of backscattering data under known and controlled geometry in order to allow *reproducibility*
- synthetic aperture experiments
- comparison of resonance scattering of the same target in free field, proud, or buried in sediment; features from resonance phenomena may be extracted as classification clues

## 2. EQUIPMENT DESCRIPTION

Fig. 2.1 shows the underwater rail. The SIMRAD Topographic Sonar Parametric Array (TOPAS) is used as transmitter. The rail is equipped with a motor which allows accurate and reproducible displacement of the chassis along the rail. The TOPAS transmitter is mounted in a pan-and-tilt assembly with a MRU (Motion Reference Unit) so that arbitrary transmission directions can be accurately measured.
As a receiver, a 1.4 m, 16-element array can be deployed either vertically, as in the picture, or horizontally close to the transducer.

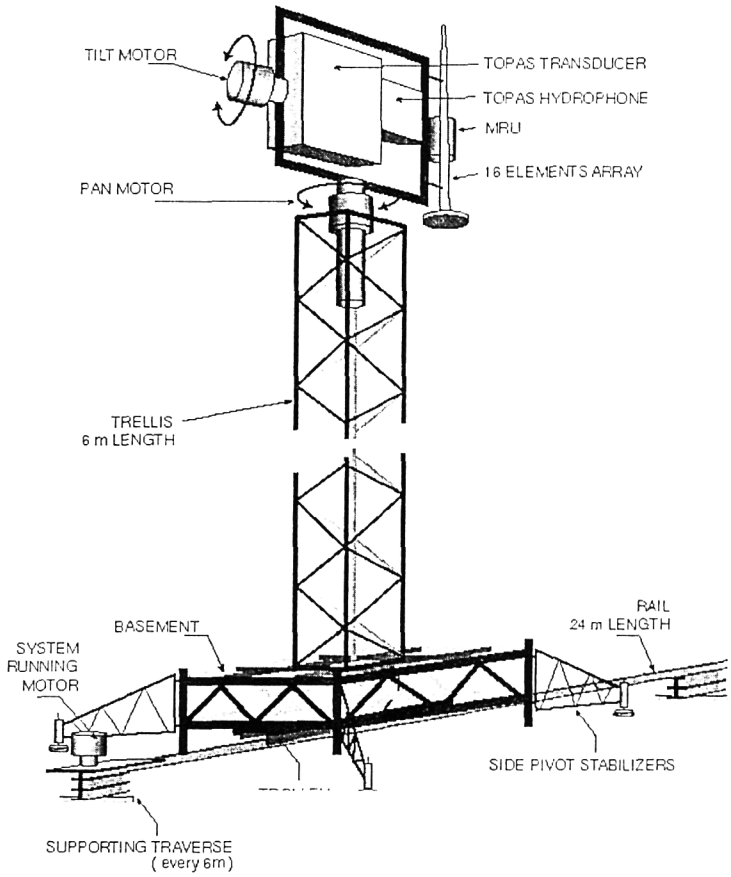


TOPAS RAIL

Fig. 2.1 The underwater rail structure

THE UNDERWATER RAIL

The rail system shown in Fig. 2.2 allows stable and repeatable acquisition of multiple aspect data of both proud and buried targets. The 24 m steel rail on the bottom and a mobile structure which traverses the rail supporting a tower (Fig. 2.2(b)) on which the sonar transmitter and receiver were mounted (Fig. 2.2(a)).
The structure is lifted by air tanks attached to the tower, and moved along the rail using pneumatic motors and a chain drive.

The structure could move along the central 20 m of the rail's length. For the experiment the sonar was mounted 8 m from the sea bottom.

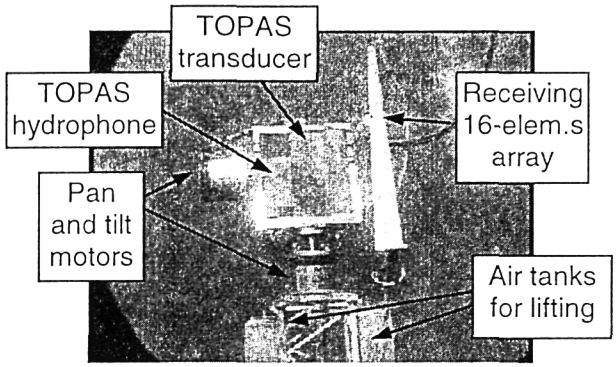


(a)

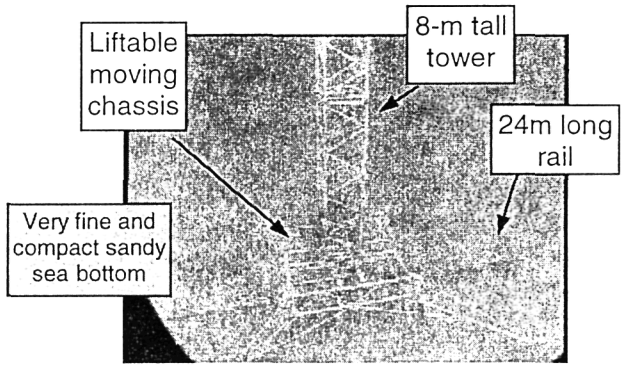


(b)

Fig. 2.2 (a) The tower top with transmitter and receiver;
(b) the rail, the liftable and moving trolley and the tower.

THE SONAR

The TOPAS generates a short single pulse by transmitting a weighted HF-burst at the primary frequency. The TOPAS transducer consists of 24 electronically controlled staves forming a beam in a chosen direction (~ 40°). The primary frequency is 40 kHz, while the difference frequency goes from 1 kHz to 10 kHz. The transmitting source is of the order of 243 dB for the primary frequency. The source levels (Tesei *et al*, 1996) obtained at different frequencies varies from approximately 190 to 213 dB/1μ*Pa* ref. 1 m (Table 2.1) using frequency from 1 to 10 kHz.

| Pulse | Beam Width HP/LF (-3 dB) | band Width LF (-3 dB) | LF SL (dB/1μ*Pa*) | HF SL (dB/1μ*Pa*) |
|---|---|---|---|---|
| Ricker 10 kHz | 2.1°/5.5° | 6 kHz | 208.6 | 241.5 |
| Ricker 8 kHz | 2.2°/5.5° | 7 kHz | 209.9 | 242.3 |
| Ricker 5 kHz | 2.2°/5.5° | 6 kHz | 212.4 | 244.9 |

Table 2.1 Source level measurements

The beam pattern of the difference frequency has good directivity (almost the same as for the primary frequency conventional sonar) with extremely low side-lobes (Fig. 2.3)

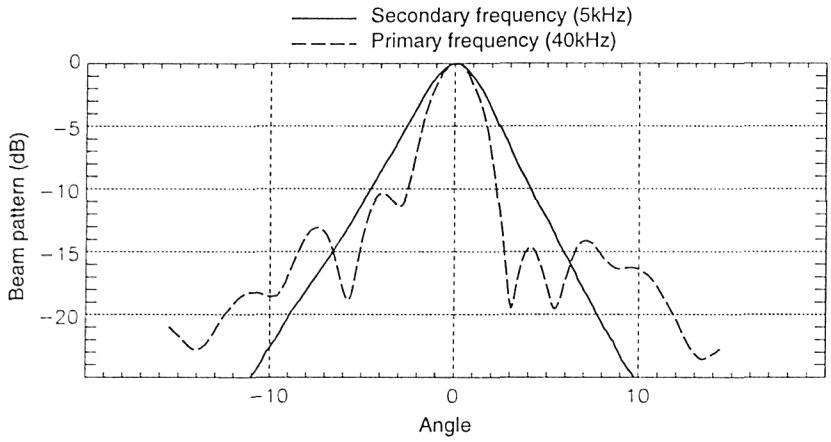


Fig. 2.3 Beam pattern for primary and secondary frequency

The receiving system of the parametric sonar consists of 3 receiving hydrophones: primary frequency (40 kHz), difference frequency (called low frequency), harmonic frequencies (80 kHz).

## THE RECEIVING ARRAY AND THE ACQUISITION SYSTEM

The array consists of 16 spherical hydrophones spaced at 94 mm (corresponding to $\lambda/2$ at 8 kHz). Each hydrophone consists of two hemispherical parts $1''\phi$.

A pre-amplifier was designed and associated with each hydrophone in order to reduce the intermodulation effect to the minimum. Phase response of this pre-amplifier is linear over the bandwidth of interest i.e., for 1 to 50 kHz. Fig. 2.4 shows how each hydrophone/pre-amplifier pair is configured in the array.

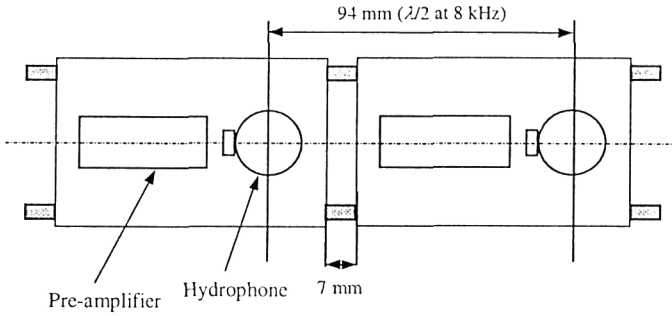


Fig. 2.4 Scheme of a segment (two elements) of the receiving array.

The receiving system scheme for the array is shown in Fig. 2.5. The 16 hydrophones are set with variable gain (0, 20 and 40 dB) in order to adjust the dynamic range of the signal.

All the hydrophones and associated pre-amplifiers are moulded into a polyurethane cylinder attached to the TOPAS tower close to the transmitter in a monostatic configuration.

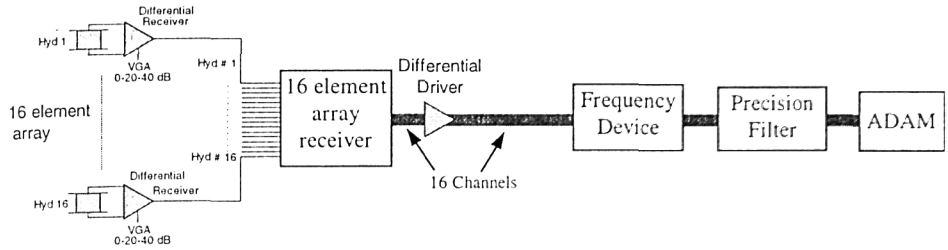


Fig. 2.5 Diagram of the receiving system

## 3. EXPERIMENTAL CONFIGURATIONS

The experiments address the following topics:

- multiple aspect target detection and classification
- sea bottom sound penetration at very low grazing angles
- synthetic aperture sonar

### MULTIPLE ASPECT TARGET DETECTION AND CLASSIFICATION

Detection and classification of objects lying proud on the sea bottom by sonar imaging systems are severely limited in effectively detecting buried targets due to absorption of high-frequency sound by bottom sediment.

The Centre has investigated a number of alternative approaches including the use of parametric sonar in the frequency range [2,12 kHz]. In this frequency range, one characteristic of target echoes which may provide classification clues is the so-called resonance scattering response, the characteristics of which are caused by the target elastic properties. This response is strongly aspect dependent. Therefore, a precise control and reproducibility is necessary to validate theoretical achievements with experimental data.

An experiment in which the targets were suspended in mid water (i.e., under approximately free field conditions) was performed in 1996(Fox *et al*, 1996). In this case, the objects were rotating on their axes of symmetry to obtain multiple aspect data. However, when dealing with proud or buried targets this is no longer possible.

The rail offers a solution to these requirements.

### SEA BOTTOM SOUND PENETRATION AT VERY LOW GRAZING ANGLES

A severe limitation of sonar systems for buried object detection and classification, especially in shallow water, is the coverage rate. This is limited by the fact that such systems must operate with grazing angles above the critical, after which, theoretically, no penetration occurs.

The centre is designing a sonar system able to work at very low grazing angles (well beyond the critical angle). This system will allow larger areas of coverage than traditional systems using normal incidence or swath survey approaches.

Three mechanisms have been identified which contribute to an explanation of sub-critical sound penetration into sediment and quantification of the results for sonar detection performance prediction:

(a) a Biot slow wave in the sediment (Chotiros, 1995);

(b) surface roughness (Thorsos *et al*, 1997);

(c) scattering of the evanescent wave by volume inhomogeneities within the sediment (Schmidt *et al*, 1997);

*In situ* acoustic measurements were performed on a sandy bottom the geoacoustic properties of which were carefully identified. A parametric array mounted on a tower traversing a rail was used to insonify hydrophones located above and below the sediment interface. An extensive data set covering most grazing angles (including both above and below critical angles) and frequencies (2-50 kHz) was acquired.

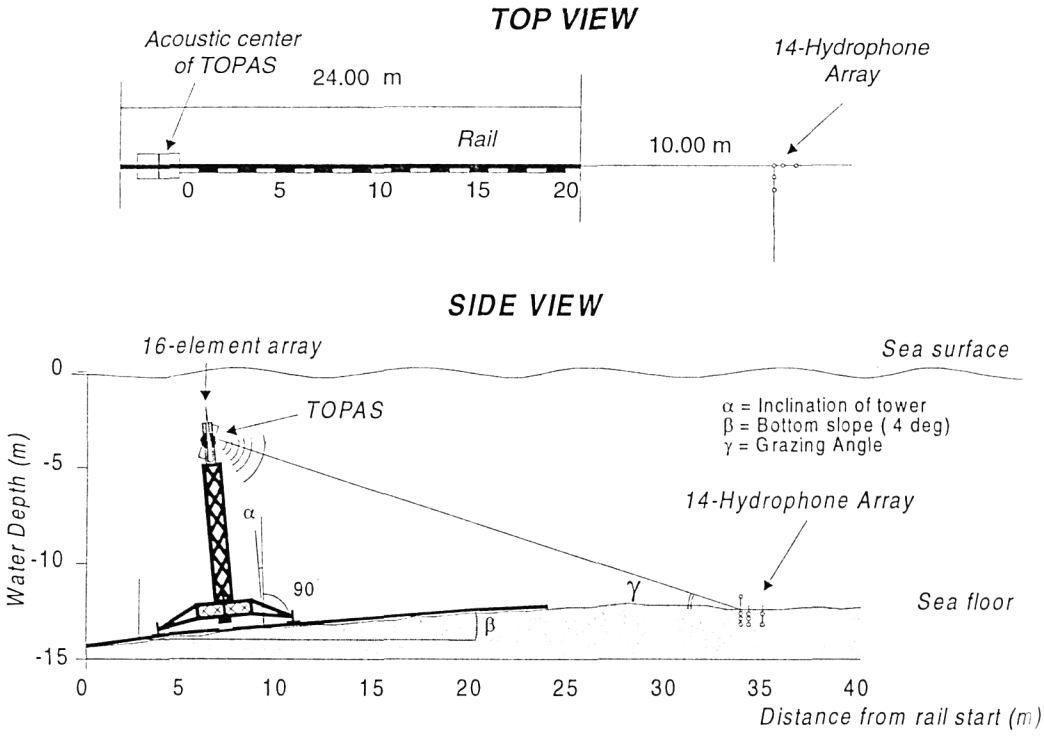


Fig. 3.1 Multiple grazing angle configuration

Fig. 3.1 shows the experimental configuration. A 3D array of 14 hydrophones was buried into the sediment. The two and three hydrophone arrays were insonified as the tower traversed the rail. The array allows the identification of the different waves travelling into the seabed.

## SIDE-SCAN SYNTHETIC APERTURE SONAR

The interest in resolution to reduce the reverberation level in low frequency systems and to increase classification performance of imaging sonar has focused attention on research into synthetic aperture techniques.

The underwater rail offers a unique opportunity to obtain experimental data for comparison with models. In side-scan mode, the sonar, mounted on the tower can ping on the target field while the rail is moving to obtain a data set for synthetic aperture processing.

The tower traverses the rail at constant speed. The stability of the system is sufficiently accurate for low frequency sonar (less than 10kHz). At higher frequencies, the tower may be used to test autofocusing algorithms against ground truth.

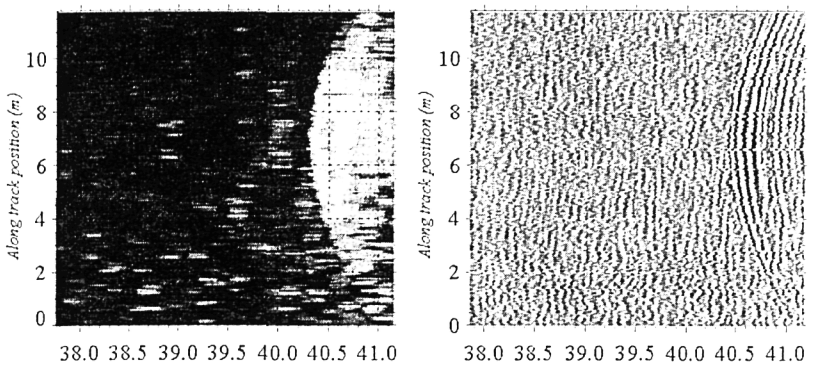


Fig. 3.2 Example of synthetic aperture data (envelope and time series)

Fig. 3.2 shows an example of synthetic aperture data acquired with a different rail structure (Fioravanti *et al*, 1996). The insonified object was a proud 1 m-diameter sphere at a range of 40 m. The synthetic array can be directly beamformed to give the image in Fig. 3.3.

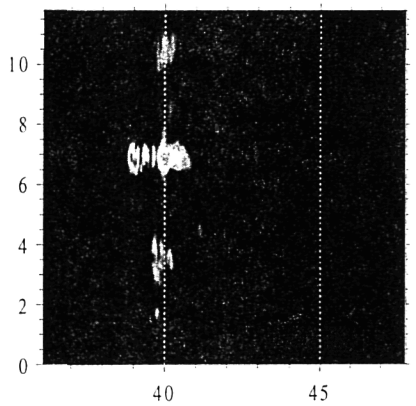


Fig. 3.3 Beamformed image

The result shows a significant improvement in the resolution and in the signal to reverberation ratio, as theoretically predicted.

## 4. THE ELBA EXPERIMENT

The experiments occurred over two periods in mid-1997 (Fox *et al*, 1998): Phase I took place between 14 and 30 April, and Phase II took place between 11 and 24 June.

EXPERIMENT SET-UP

Fig. 4.1 and

Fig. 4.2 show the trial geometry. The rail was located at around 40 m 18 m and from the target. As the target position was at one extreme of the rail, the maximum variability of aspect angles was 53.0° when the rail was 40 m from the cylinder; 48.0° at most if the rail was 18 from the target.

The grazing angle of transmission direction with the sea bed was 12° if the rail was at 40 m, 22° at 18 m. In both cases it was lower than the fine sand critical angle (~26÷28°).

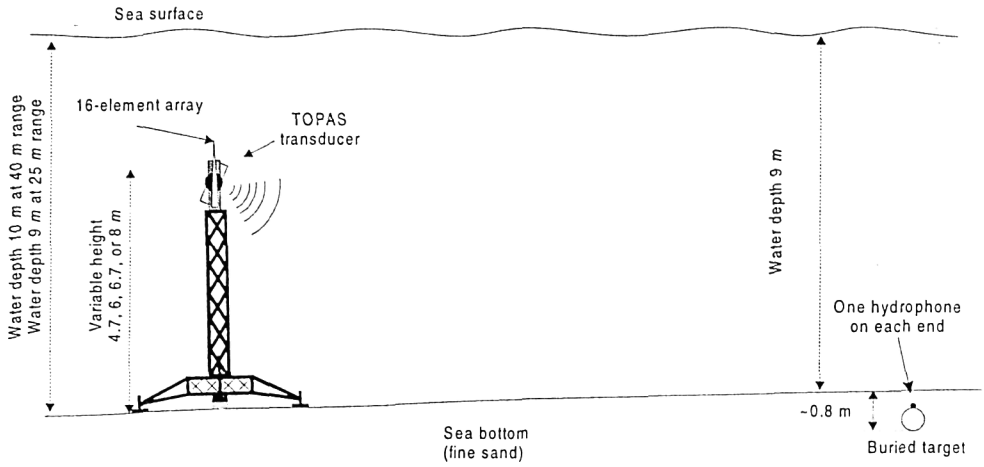


Fig. 4.1 The trial geometry section.

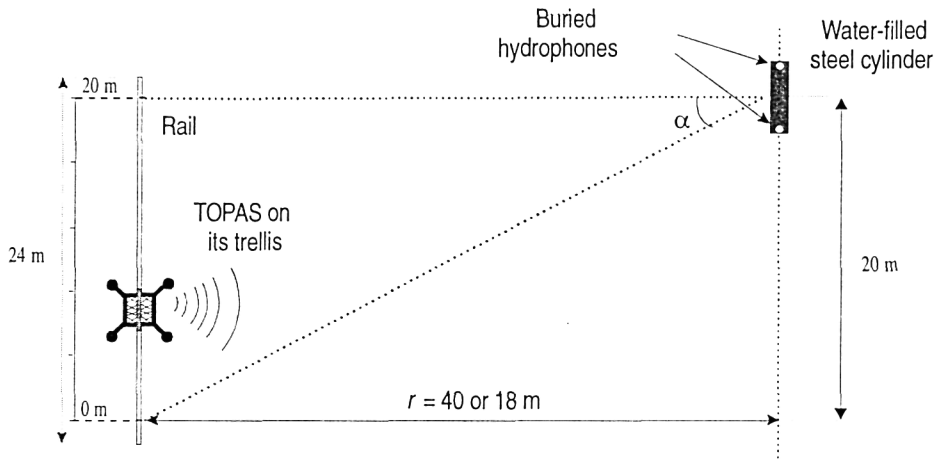


Fig. 4.2 The trial geometry plan.

From the on-line displaying and pre-processing of data, the first measurements with the rail at 40 m from the target appeared to have very low Signal to Reverberation Ratio. For this reason, the rail was moved to a distance of 18 m from the target. In such a configuration the sonar worked under limited conditions as the parametric effect of generation of a low-frequency narrow beam could not be ensured at lower ranges, as the maximum tower height was 8 m.

The array was oriented vertically in order to be able to cancel the return from the surface through beamforming.

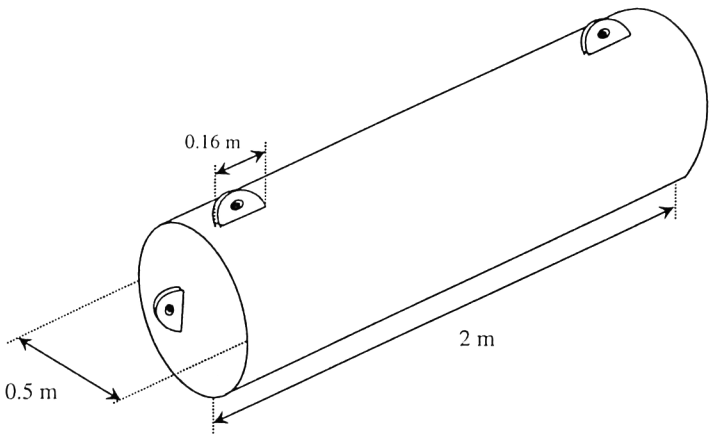


Fig. 4.3 The cylindrical target

The sea-water-filled, thin-walled cylinder with flat end-caps (Fig. 4.4(a)) used in the first SACLANTCEN trial in the free field was employed as a buried target by divers, with a vacuum-maker during the trial Phase I (Fig. 4.4(b).
The cylinder was left on the site from the end of April to the middle of June in order to allow sediments moved during burial to recover to a natural state.
When the site was visited in June, the sea bottom was vitually indistringuishable from the surrounding area, with sand ripple peaks 2-3 cm high.

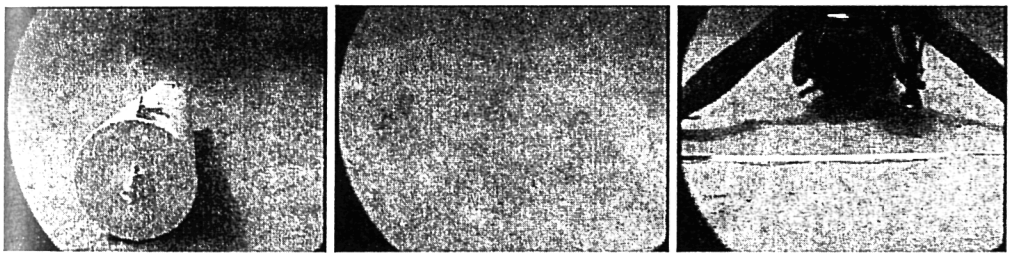

(a) (b) (c)

Fig. 4.4 (a) The water-filled cylindrical target proud on the sea bottom;
(b) the sea bed over the target as left by divers after burying;
(c) the same bottom area two months later.

## ENVIRONMENTAL MEASURES

The trial location was in the Golfo della Biodola off the Island of Elba, approximately (Fox *et al*, 1998), 42° 48'N and approximately 10° 15'E. The water depth was approximately 10 m 400 m from the beach, with a 2.5% slope toward the beach.
Sound speed measurements of the water column showed nearly uniform conditions. As an example, Fig. 4.5 plots the measurements of sound speed on June 21 during the experiments.

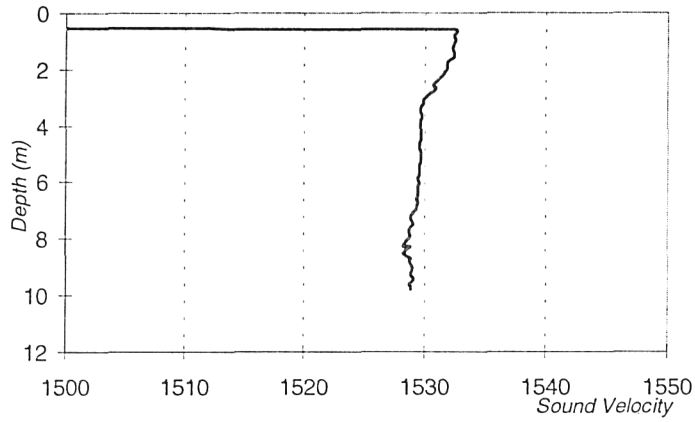


Fig. 4.5 Water sound speed profile - CTD measurements.

A geophysical analysis of the sea bottom at the experimental site showed a mostly homogeneous layer of fine sand 1.8~m thick overlying stratified, mixed layers of sand, silt, and gravel, giving way to bedrock.
Sediment core properties of the upper 30~cm of sand are summarized in Table 4.1. Note that the mean grain size is reported in $\varphi$ units, where $\varphi=-\log_2 d$
and $d$ is the mean grain size in mm.

| Property | Core 1 | Core 2 |
|---|---|---|
| Mean Grain Size $\varphi$ | 2.3 | 2.4 |
| Porosity (%) | 44.6 | 43.6 |
| Density [g/cm$^3$] | 1.92 | 1.94 |
| Compressional sound speed (m/s) | 1723 | 1734 |

Table 4.1 Mean measured values for sediment cores taken in experimental area.

Although the site was selected for the experiment with regard to optimum the water depth, bottom and weather conditions, winds to 30~knots and high incoming swell created dangerous conditions for deployment and recovery of the experimental equipment and therefore the available time for data collection was significantly reduced.

## 5. PRELIMINARY RESULTS

### MULTIPLE ASPECT TARGET DETECTION AND CLASSIFICATION

Multiple aspect data were recorded for proud and buried cylinders. In the former case, we were able to acquire back-scattering signals with a high signal to reverberation ratio (SRR).
Fig. 5.1 shows that the backscattered response varies with the aspect angle of the cylindrical target. The signals exhibits changes in the specular part of the echo and in the resonant area.

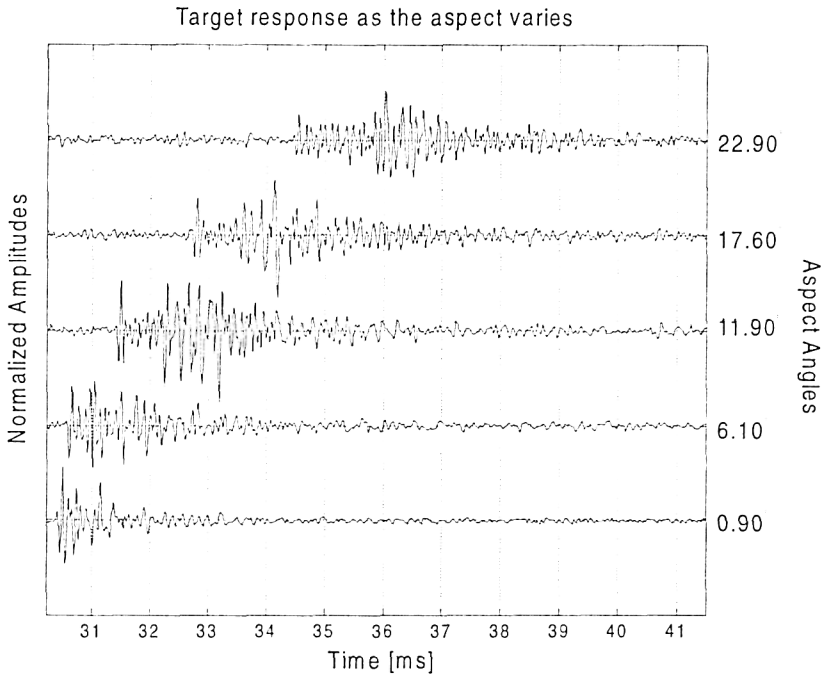


Fig. 5.1 multiple aspect back-scattered data from a cylindrical target

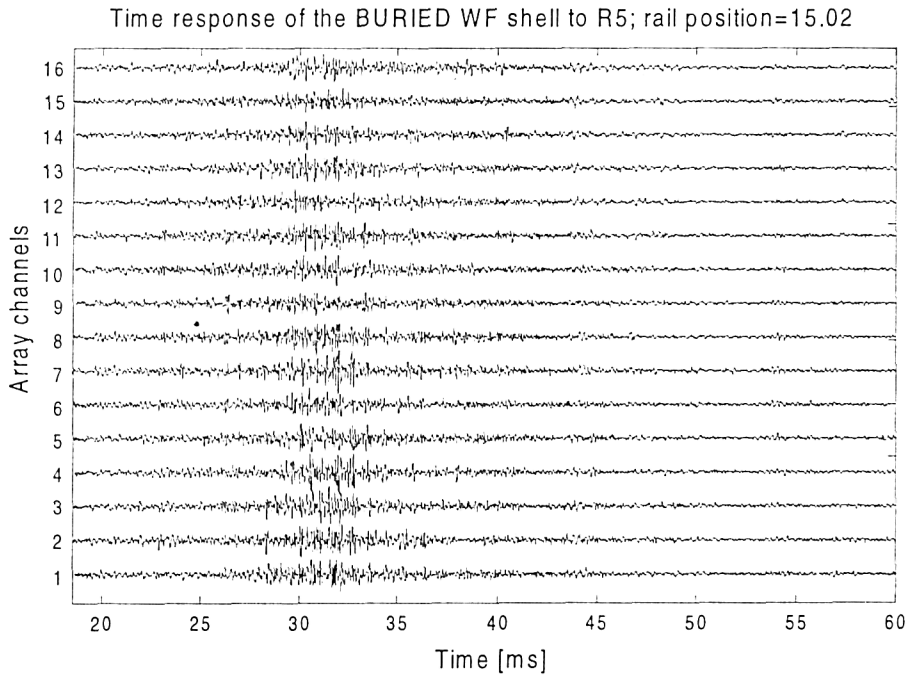


Fig. 5.2 Temporal target response to a Ricker-5kHz pulse.

With buried targets, due to the bottom absorption and to the low grazing angle, the SRR was significantly reduced. As an example, the response of the buried water-filled cylindrical shell to a 5 kHz Ricker pulse is shown when the sonar was at the rail position 15.02 m and the rail

was at a range of 18 m. It is clear from the trial geometry that the selected position corresponds to a target aspect angle of 14.93°. Fig. 5.2 shows an overview of the response as acquired separately by each array element.

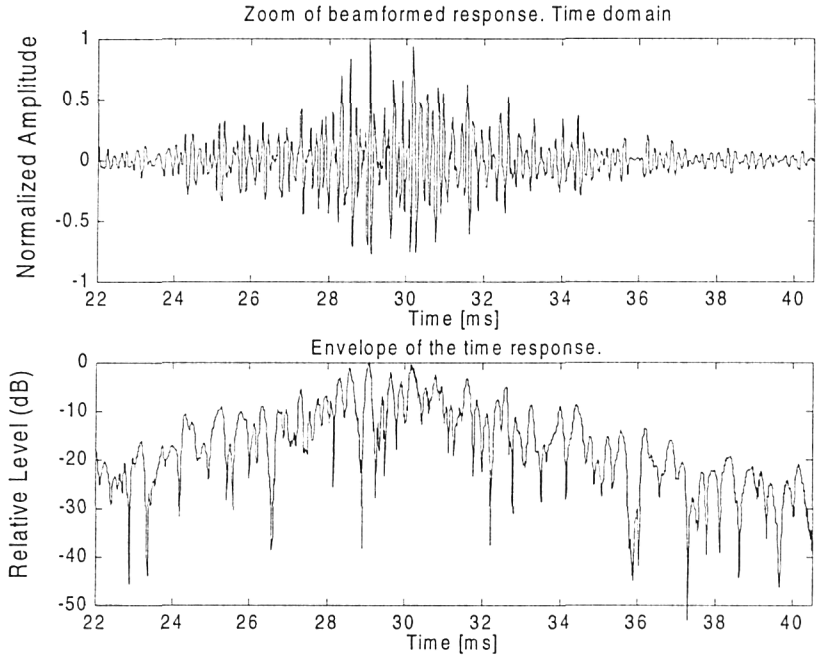


Fig. 5.3 Beamformed average response zoomed around the expected time of arrival of the first target echo.

In order to improve data quality and cancel reflections from the sea surface, beamforming is applied to data received by the linear array.

The time series of the averaged beamformed target response on 52 pings is presented in Fig. 5.3. The maximum peak of the response is measured around 29 ms, which we can assume is scattered by the target.

Preliminary analysis of the beamformed data presented in Fig. 5.3, gives the computed Signal to Reverberation Ratio (SRR) as approximately 2 dB. Hence, not only the extraction of features suitable for classification purposes but also the target detection may be difficult to achieve.

The poor signal to reverberation signals recorded may be attributed to:

- target burial depth
- grazing angle
- sediment type

## DETECTION OF BURIED TARGETS WITH DIFFERENT GRAZING ANGLES

In this configuration, the rail was perpendicular to the cylinder. The cylinder was flush buried. Different grazing angles were obtained by moving the tower along the rail: around 20 degrees when the tower was furthest from the target; up to 30.5 when close.

The data obtained above the critical angle may also provide data with high enough SRR for validation of buried object scattering models.

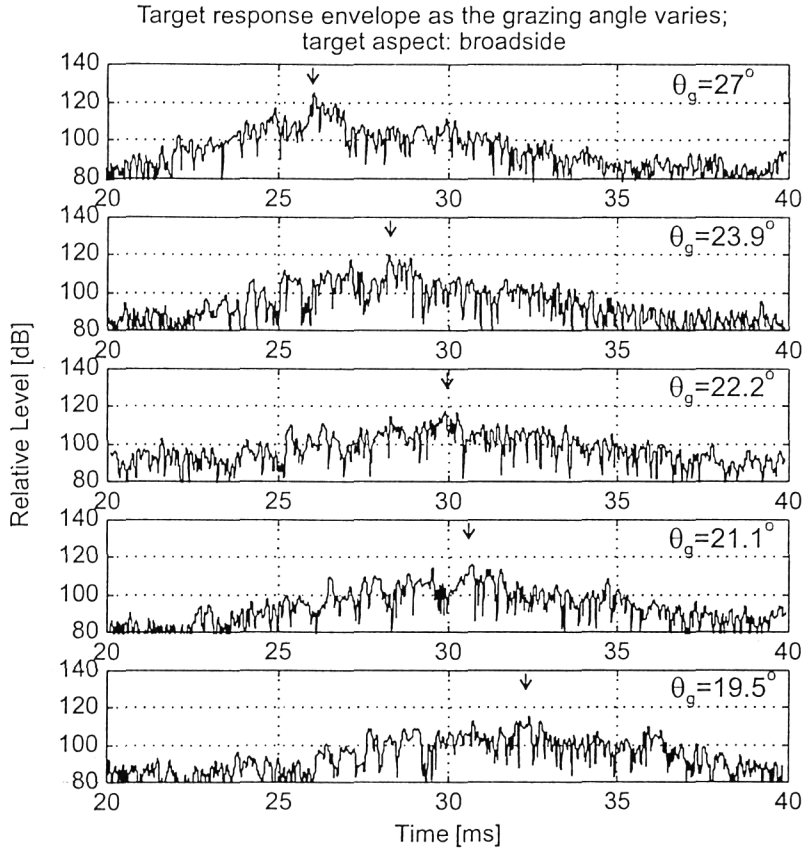


Fig. 5.4 Variation of target backscattering as a function of grazing angle

Fig. 5.4 shows the variation of the target backscattering signals as a function of the grazing angle. The arrows indicate the estimated time of arrival of the cylinder echo computed using the one way signal received on the buried hydrophones.

## 6. CONCLUSIONS AND FUTURE WORKS

A new system, using an underwater rail with a mobile, variable-height tower supporting the sonar was tested successfully during the sea trials described in this paper. The main advantages are accurate control of the trial geometry, trial reconfiguration and repeatability, and measurement stability. Measurements of bottom reverberation and target scattering could be obtained at multiple target aspects and various grazing angles even when the objects are embedded into the bottom sediments.

## REFERENCES

Tesei, A., Fioravanti, S., Maguer, A., Bergem, O., Pace, N., "Description and calibration of the TOPAS PS 040", SACLANTCEN contribution to DEO Deliverable D1, July 1996.

Fox, W.L.J., Fioravanti, S., Maguer, A., Tesei, A., Løvik, A., "First trials report", MAST-III DEO Project deliverable, SACLANTCEN, November 1996.

Fox, W.L.J., Fioravanti, S., Maguer, A., Tesei, A., Løvik, A. "Second trials report", MAST-III DEO Project deliverable, SACLANTCEN, January 1998.

Fioravanti, S., Maguer, A., Løvik, A., Brussieux, M. A parametric synthetic aperture sonar. Proceedings of the third European conference on underwater acoustics, *In*: Papaadakis, J.S., *ed.* Crete, FORTH-IACM, 1996: pp.1085-1090. [ISBN 960-85709-3-X].

Chotiros, N.P. Biot model of sound penetration in water saturated sand. *Journal of Acoustical Society of America*, **97**. 1995:199-214.

Thorsos, E.I., Jackson, D.R., Moe, J.E., Williams, K.L. Modeling of subcritical penetration into sediments due to interface roughness. *In*: Pace, N.G., Pouliquen, E., Bergem, O., Lyons, A.P., *editors*. Proceedings of High Frequency Acoustics in shallow water. La Spezia, Italy, NATO SACLANT Undersea Research Centre, 1997: pp.563-569. [ISBN 88-900194-1-7]

Schmidt, H., Lee, J., Fan, H., Le Page, K. Multistatic bottom reverberation in shallow water. *In*: Pace, N.G., Pouliquen, E., Bergem, O., Lyons, A.P., *editors*. Proceedings of High Frequency Acoustics in shallow water. La Spezia, Italy, NATO SACLANT Undersea Research Centre, 1997: pp.475-482. [ISBN 88-900194-1-7]

Fioravanti, S., Maguer, A., Løvik, A., Brussieux, M. A parametric synthetic aperture sonar. Proceedings of the third European conference on underwater acoustics, *In*: Papaadakis, J.S., *ed.* Crete, FORTH-IACM, 1996: pp.1085-1090. [ISBN 960-85709-3-X].

Maguer, A., Bovio, E., Fox, W.L.J., Pouliquen, E., and Schmidt, H., Comparison between subcritical penetration models and in situ data, Proceeding of the 135$^{th}$ ICA/ASA 98' Meeting, Seattle (WA), USA, 20-26 June 1998 (accepted).

**Acknowledgement**

This work was partially funded by EU in the context of MAST-III DEO (Detection of Embedded Objects) Project.

# SECTION II

# Processing and Interpretation

# SEAFLOOR CHARACTERIZATION USING MULTIBEAM ECHO SOUNDERS: METHODOLOGY AND FIRST RESULTS

*J-M. AUGUSTIN, L.GUILLON, L.HELLEQUIN, X.LURTON, S.UNTERSEH & M.VOISSET*
*IFREMER - Centre de Brest*
*BP70 - 29280 PLOUZANE, France*

*Abstract - Modern multibeam echosounders (MBES in the following) provide high precision bathymetry data, together with sonar images representing the seafloor fine structure. Due to their capability of quick surveying and mapping of large areas, they provide a unique tool for the surficial seafloor characterization, since various acoustical features may then be associated with extended areas. We present here a methodology derived from our recent works in the field of multibeam data processing for seafloor characterization. Three major steps are to be considered. A preliminary data checking and preprocessing is intended to eliminate as far as possible all the MBES artefacts. Then the sonar image of the studied zone can be segmented into homogeneous regions according to acoustical criteria. Finally the characteristic features of the seafloor are to be used for a characterisation, or at least a classification of the seafloor geological features. These various points are presented together with application results and discussions.*

## 1. INTRODUCTION

Geologists use a large range of acoustical tools to investigate the sea floor nature from oceanographic vessels. Low-frequency devices (from seismic to subbottom profilers) provide seabottom cross sections with a vertical resolution ranging from 3 m to 50 cm. In a higher frequency range, imaging systems provide acoustical images of the sea floor. Classical side scan sonars only give high-resolution reflectivity information whereas data from the more recent multibeam echo sounders contain both bathymetry and reflectivity. The various MBES available nowadays have the great advantage of providing very quickly a coverage of large areas. Moreover, in the case of the deep water MBES, due to their relatively large wavelength, the observed backscattering strength (BS in the following) features volumic effects and, consequently, the image contains some information about the vertical structure of the surficial seafloor layers.

The classical geological means of investigations (cores or *in-situ* measurements) are nevertheless always of paramount importance in the process of seafloor characterization; these measurements and samples are finally the only way to have access to geoacoustical parameters such as sound speed, porosity etc... This is a point one should always keep in mind. Consequently, comparisons between acoustical levels and ground-truth results have to be systematically conducted , together with adequate modeling.

The segmentation of sonar images into homogeneous zones is very helpful in the process of seafloor characterization on an extended region. Once segmented, the acoustic imagery appears to be more readable, with smoothing effects and connections between homogeneous acoustical areas; moreover, this procedure produces a mosaic whose parameters are objective because having been rid, as far as possible, of artefacts brought by bathymetry and sensor imperfections. So, it makes the comparison between different zones or different tools (geophysical data or ground truth data) easier for the geologist. However, a lot of precautions must be taken to avoid an oversimplification of the so-obtained areas : the learning zones must be drawn accurately, relying on an expert geological advice, and taken numerous enough to be representative of the geological variety, even if some of them may be merged during the segmentation process.

Seafloor characterization can be led following two major approaches: quantitative estimation of objective parameters, or direct global comparison. The first one aims at extracting some discriminating features, for a given sea floor type, from the acoustical signal. Once validated for one type of MBES, this method can be applied everywhere and it might allow an inversion of the acoustical data back to geophysical parameters, provided that relations are available from modeling or laboratory experiments; this last point requires one-to-one relations between acoustical and geophysical properties. In the case of low-frequency MBES because of the volumic effects, the geoacoustical modeling includes too many parameters to use this kind of process. In that case, the characterization can be achieved by direct comparison between ground-truth results and features extracted from acoustical measurements. This approach has to rely upon training phases on selected zones, which inevitably limit the generality of its application; on the other hand, it may allow to deal with more global physical descriptors, which facilitate the geologist's interpretation.

The works presented here deal with three aspects of multibeam echosounder data processing. One has to make sure that the data quality is sufficient for their correct exploitation in a process of seafloor characterization ; this check concerns the imagery data, which is associated with the finest details. A preliminary data cleaning and preprocessing is then to be applied, intended to eliminate as far as possible all the MBES artefacts. This constitutes the first part of the paper. Then the image segmentation principle is exposed; its particularity is that it relies on a sufficient knowledge of the involved physics. It is shown that high frequency sonars provide a high-fidelity representation of the sea-floor interface roughness which may be used to complement the set of usable physical features. Finally a geologist interpretation of one MBES image is presented, with emphasis on the ambiguities arising between acoustical level and physical ground-truth, and the answers that can be brought by an adequate modeling.

These various aspects will be illustrated by actual experimental results, mainly coming from the raw data set presented in fig.1; this sonar image was recorded by a low-frequency MBES on a deep-sea zone [1].

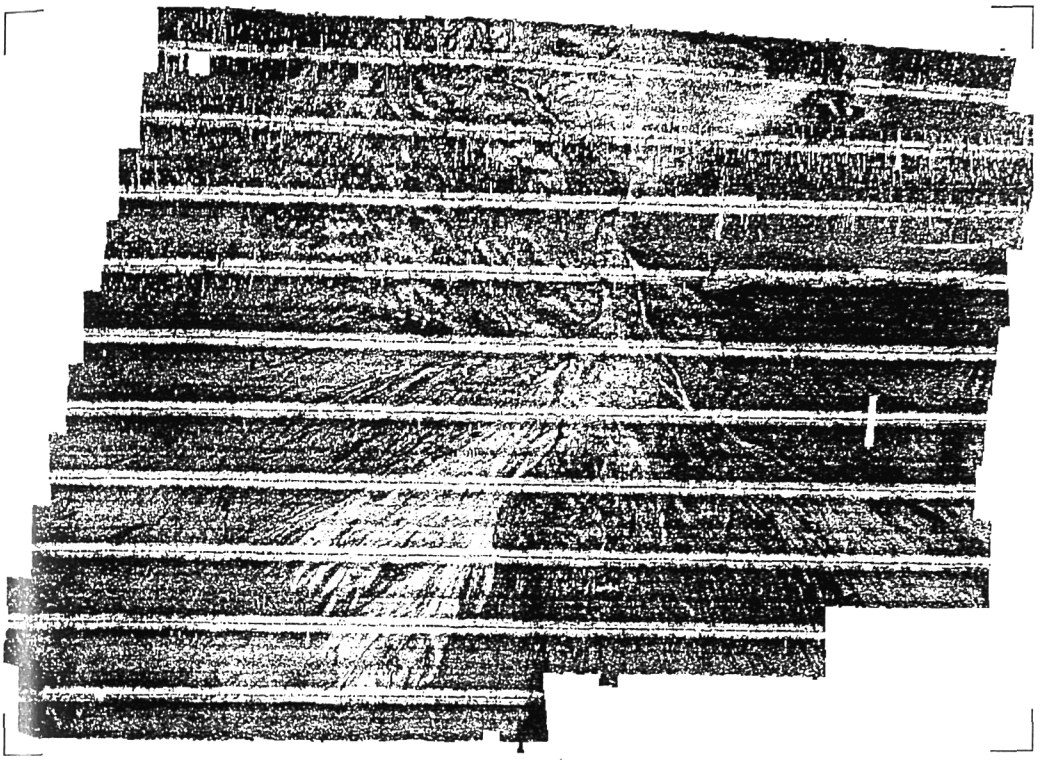

*Fig.1. Low frequency (13 kHz) sonar image of the Celtic Fan: raw data presented here are affected with physical effects (specular reflection insufficiently compensated) and echosounder artefacts (gain control, array directivity)*

## 2. PRELIMINARY DATA PROCESSING

Due to the fact that acoustical analysis of the seafloor essentially relies upon signal amplitude exploitation (average levels and fluctuation statistics), one has in any case to make sure of the validity of the levels provided by the echosounder and to eliminate artefacts, in order to go securely upstream back to the original physical data. The actual precise characteristics (level, sensitivity, directivity patterns) of a MBES installed aboard a vessel are practically impossible to obtain ; hence a partial sonar image, recorded on a flat homogeneous zone, and the corresponding average amplitude versus the emission angle, may be used to identify the main artefacts. Consider the example presented in Fig.2, obtained with a high-frequency MBES (95 kHz) on a shallow-water zone. First of all, grey tone contrasts appear for shallow grazing angles, presumably deriving from uneven electronic gains and array sensitivity at the signal emission and reception. Secondly, strong fluctuations appear with amplitudes increasing as the angle tends to zero, creating alongtrack artificial lines in the sonar image. These stable oscillations correspond to uncompensated directivity diagrams of the reception beams. Finally the low backscattered level measured in the specular region (dash curve on fig.3) is suspicious, since the physics predict an energy peak. To understand this last phenomenon one has to detail the normalisation procedure (the Time Varying Gain law) implemented in the echosounder, especially the footprint area compensation.

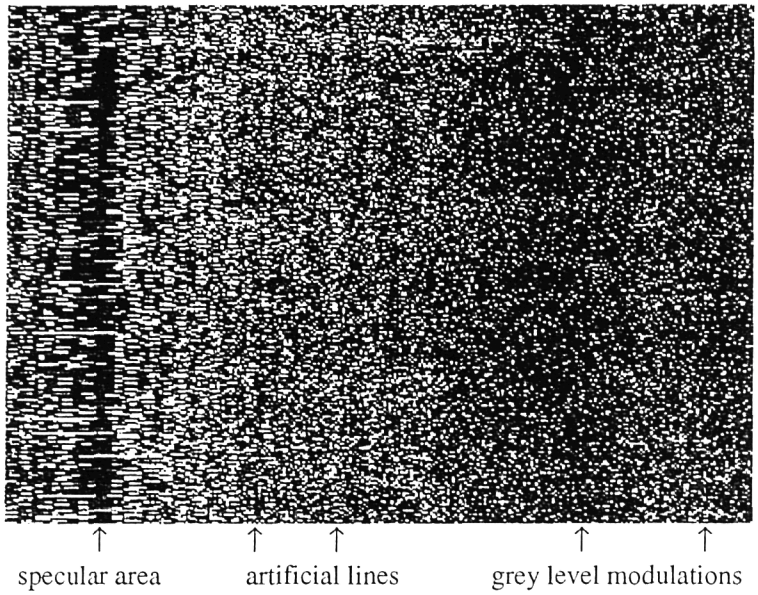


*Fig. 2 : Partial sonar image recorded on a flat homogeneous seabed with a high-frequency MBES, highlighting the array directivity pattern effects*

Confronting [2] the theoretical and the sounder-implemented "sonar equation" (linking the measured echo amplitude, the emitted level, the transmission losses, the various array and processing gains, and the target size and backscattering strength), a bias between the estimated BS and its actual physical value is searched for. Here this bias is expected to depend mainly upon the array directivity diagram. Since the antenna directivity measurement may be not available, this directivity effect is identified from training on one (and preferably several) flat and homogeneous zone, and compare the obtained response with a reference backscattering model. Also the footprint size and propagation losses may be not precisely computed and compensated by the sounder; the next step of the correction procedure is to account for the insonified area difference in order to retrieve bettered actual backscattered levels, especially around the vertical in the specular zone where the physics become quite complex. The Lambert's law correction classically applied in the receiver has also to be restored if one wishes to obtain a physical evolution of BS for shallow grazing angles.

Results of such a correction procedure are depicted on Fig.3. The level oscillations with angle have nearly disappeared at oblique incidences and have been quite smoothed in the vertical zone. In addition, the backscattering strength became symmetrical and closer to its expected theoretical evolution.

The processing steps described above have two major applications. At first, they are an obligation for anyone wanting to exploit quantitatively the backscattered levels, whatever the approach. But they can also be used, more readily, to correct the original sonar image, and hence to propose to the user a classical sonar image completely rid of the various artefacts. Such an example is presented on fig.4: the raw data have been corrected for the MBES directivity effect, and the specular effect has been compensated.

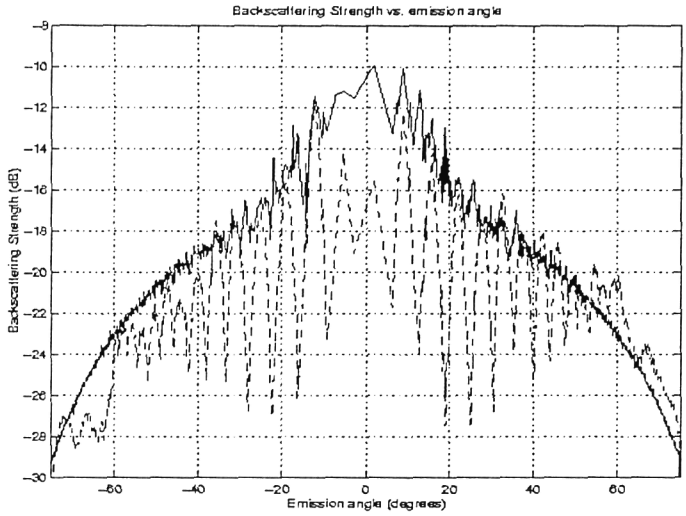


*Fig. 3 : Backscattering level vs. emission angle before (dash) and after (full) artefact compensation.*

## 3. SONAR IMAGE SEGMENTATION

The purpose of the method (presented in details in recent publications, see e.g. [3]), is to provide automatically a partition of a sonar image into homogeneous zones according to acoustical (and hopefully geological) descriptors. As a first step, this partition is realized according to the backscattering strength as a function of incident angle, since this physical feature (dependent on sediment roughness, impedance and inhomogeneity) is expected to be a good classifier of the sea-floor type. Also it was found from studies [4] on signal amplitude statistics from a low-frequency (13 kHz) system that the mean backscattered intensity was the only practically usable feature. It was also verified *a posteriori* that the averaged BS as a function of angle is really characteristical of the seafloor type, and that effective classifying potentialities are to be expected from such an approach despite ambiguities raising from intricate physical configurations. The problem is that the backscattering strength is not directly exploitable from the raw sonar image, since a number of undesirable effects perturb its estimation.

First BS considerably varies with incident angle, in particular near normal incidence (refered to as specular effect in the following), and at shallow grazing angles. These variations, clearly apparent on raw sonar images, preclude a direct segmentation, and have to be accounted for in the image processing. Their precise estimation implies to be able to first estimate the actual incident raypath angle on the seafloor, acounting for its refraction down the water column, and the local seafloor slope; this can be done only after a full processing of the bathymetry data. Also, the BS estimation may be biased by the echosounder characteristics such as processing gains and array directivity patterns. These have to be carefully checked and calibrated in order to be fully compensated, as explained above.

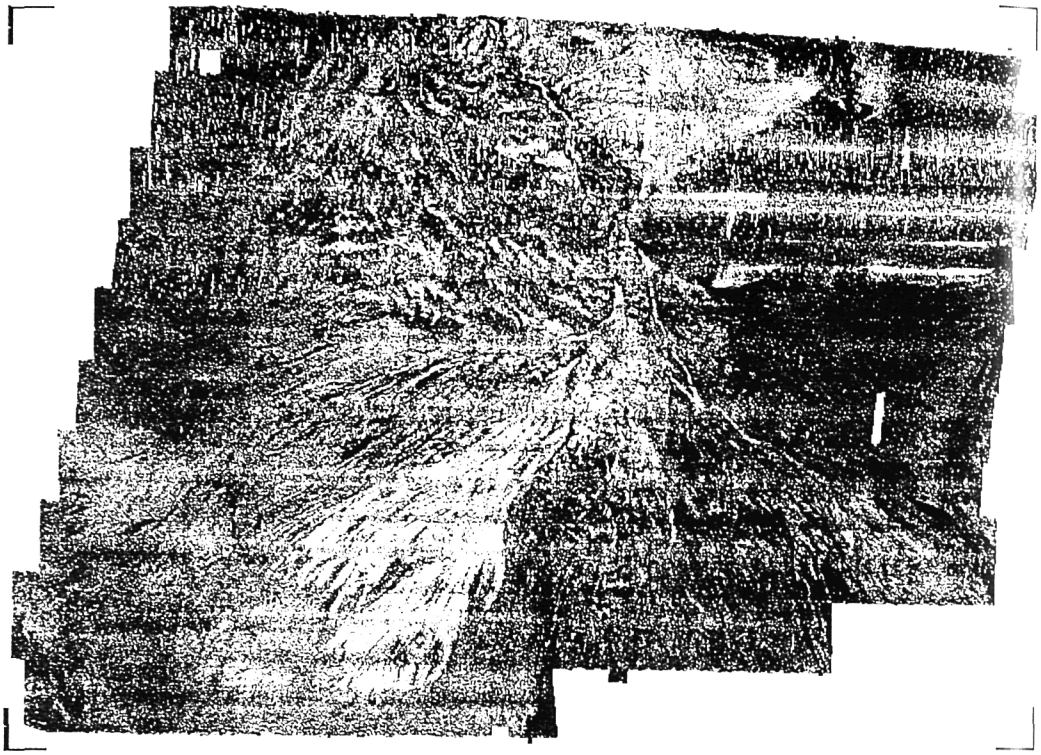

*Fig.4 - Sonar image of Fig.1 corrected of echosounder array directivity and specular effect*

Once the tools for a correct BS estimation have been precised and developed, the objective is then to segment the sonar image according to a small number of representative angular BS variation laws. This is obtained by first delimiting, inside the sonar image, a small number of homogeneous zones expected to be representative of the geological variety over the studied zone. This task is performed by an experienced geologist, from the sonar image cleaned as far as possible from various artefacts such as directivity diagram modulations.

The segmentation process may then begin. At first, for every pixel in the image, the BS value together with the corresponding incident angle is compared to the whole set of reference BS laws; the shortest statistical distance is searched for, accounting for the mathematical modeling, namely the amplitude statistical distribution. This first result is then submitted to successive iterations of a regularisation function whose purpose is to enhance the influence of the neighbours on the affectation decision for every pixel. This processing is rigorously controled by a strict application of Markov's field theory, which is considered as a convenient theoretical frame for such a problem [4]. After a few iterations, the process converges towards a stable segmented representation: the obtained zones then correspond to acoustically homogeneous areas, compensating the angle effects due to sea floor slopes and BS.

When high resolution MBES are involved, the statistical and spectral features of the echo signals should be considered in order to improve image segmentation algorithms and to provide new useful criteria for seafloor characterization. The classical reverberation theory,

associated with Rayleigh statistics and untextured sonar images, has to be adapted to account for smaller insonified areas which succeed in describing small scale seafloor roughness.

If high resolution MBES operate on rocky or geologically disturbed zones, the seafloor microstuctures induce textural patterns on the corresponding sonar image. Then, the single point statistics exhibit a strong distribution tail on the received energy histogram as depicted on Figure 5. The Rayleigh law fails in describing this spiky distribution and should be generalized by the use of a *K*-law distribution [5]. In addition to a good experimental data fitting, the *K*-law distribution is advantageously linked to a non-Gaussian reverberation theory. This theoretical background allows to predict the statistics evolution with the sounder characteristics (insonified area) on one hand, and, on the other hand, the processing particularities (sampling level, data averaging,...) could then be more efficiently designed.

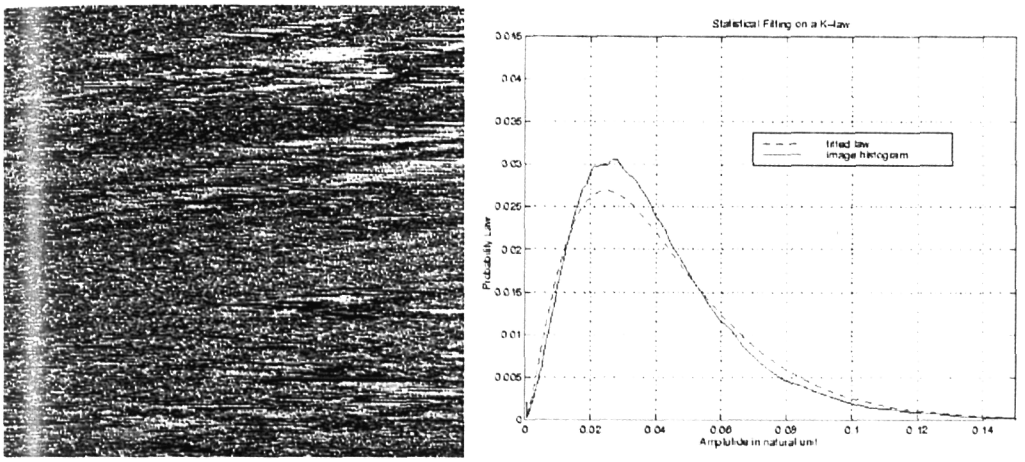


*Fig. 5 : Statistical law fitting of the backscattered amplitude from a rocky seabed area (image left) with a K-law distribution (right)*

In the same way as the classical backscattered level descriptor, the amplitude distribution shape could, firstly, offer a new powerful feature to discriminate seafloor acoustical behaviours. Nevertheless, such statistical features should not be exploited without involving the sounder geometry influence. In a second step, this statistical behavior could also be used in order to improve the segmentation algorithm efficiency, by changing the classical Rayleigh law into a *K*-law description.

## 4. SEAFLOOR CHARACTERISATION

### 4.1. A case study of image interpretation

The sonar image presented in Fig.1 was acquired during the SEDIFAN 1 cruise (ENAM II project) aboard *RV L'Atalante* in June 1997, using a low-frequency EM 12 echosounder. A very important deep sea fan (more than 17000 km²) can be observed, named the *Celtic Fan* in [1]. Situated down the continental marge at the western end of the English Channel, this fan begins by a channel in continuity with the Whittard Canyon, boarded South by a huge sediment wave field, and North by a small sediment wave field and by the distal part of the fan incoming from Shamrock Canyon (Fig.6). The Whittard Canyon drains most of the turbidity currents incoming from the marge.

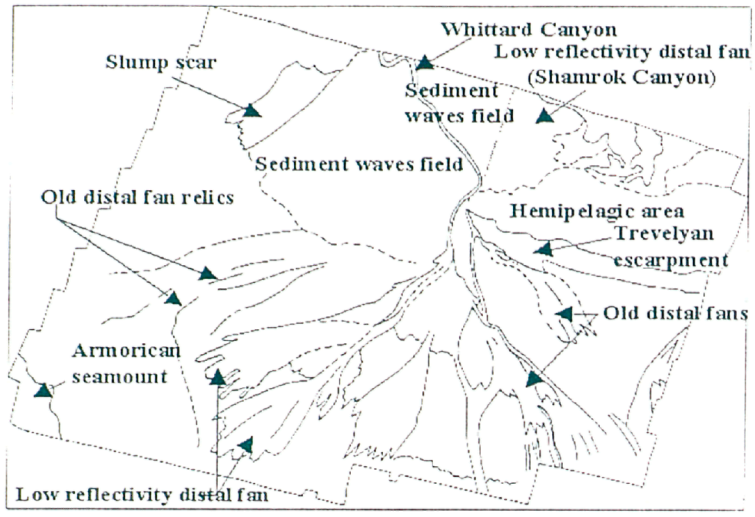


*Fig.6 - Main structure interpretation of the Celtic Fan sediment system*

The Celtic Fan *stricto sensu* features a few channels spread on a 140 degrees aperture, ended by distal lobes of large extent. Some of these channels are very impressive by their size and their well-marked morphology, with a distal part characterised by a very low reflectivity (white areas on Figure 1). We assume that those low reflectivity lobes correspond to the most recent depositional systems. Indeed, they appear to be the best delineated and, more important, they seem to be connected with the canyon ; while on the other hand, distal fans (East part of the imagery) are not connected and are more reflective.

The low reflectivity phenomena appears to be symptomatic of such a deposit model. We observed a similar case in the Ligurian Sea in the distal part of the Var lobe [6] Ground truth cruise ESSAM 2 on this low-reflectivity zone showed the presence of thick sand banks overlayed by only 10 to 20 centimetres of mud. Therefore the average BS (lateral value corrected of the Lambert's law for angle variation) should be at least - 30 dB/m²; hence the average measured value (-35 dB/m²) appears then to be quite too low for such a sandy environment. In the Celtic Fan, a Kullenberg core reports the presence of a one meter sand bank overlayed by 30 to 50 cm of surficial mud (estimated from the 3.5 kHz subbottom profiler) ; the measured BS (-37 dB/m²) is there even lower than in the Var fan. Studies are currently being conducted to link these low reflectivity facies with recent mass deposit consequenses. In particular, the settlement of mud layers underlying the new sand deposits may produce a weak water flow upwards. Therefore the water may be trapped by the actual surficial mud layer or may produce an excess pore pressure in the same surficial mud layer. Most certainly such phenomena will strongly affect the sound wave backscattering.

Fig.7 presents the results of the segmentation of the sonar image from fig.4. Five training zones were defined, corresponding to two facies from the low-reflectivity area, two other sandy facies from the rest of the fan, and one rock outcrops area. The final result offers quite a satisfactory partition of the zone into these five facies. Slight shortcomings may be observed along the specular tracks, as was already the case for the corrected image (fig.4), or in the N.E. zone, where the quality of the data is poorer due to bad weather conditions.

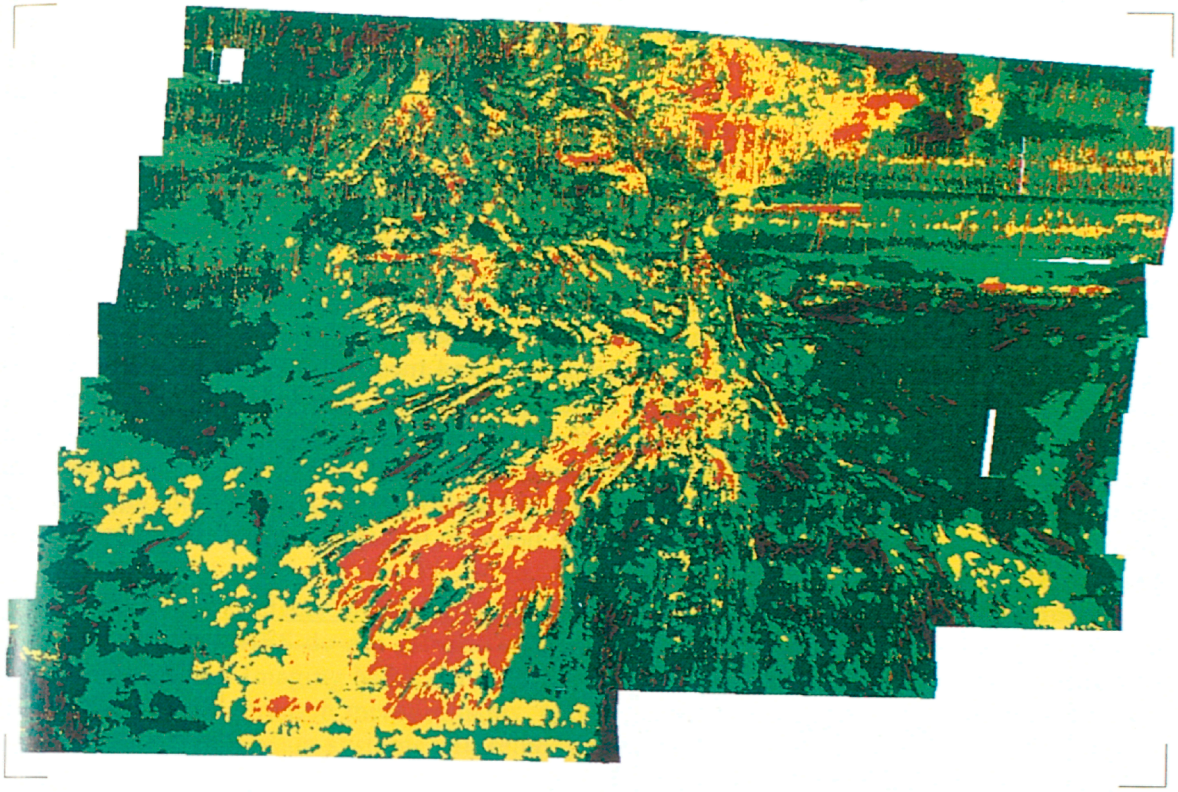

*Fig.7 - Segmentation of the Celtic Fan sonar image into five facies*

*4.2. Geoacoustic modeling*

The interpretation of the MBES images is based on the relations between average level of backscattered signal on one hand and geological structure of the seafloor on the other hand. A first approach of this problem is to associate low reflectivity levels with soft and flat seafloors and high reflectivity with hard and rough ones. But a lot of studied areas display critical or false examples of this reading [7]. Consequently, an empirical approach is prohibited in the view of seafloor characterisation and a good knowledge of the physical phenomenon of acoustical backscattering by the sea bottom is essential.

The BS classical model features two components: one for the rough water/sediment interface and one for the volumic inhomogeneities (see e.g. [8] or [9]). Practically, it is often difficult to separate the influences of these two contributions. Furthermore, most models are based on the assumption of a semi-infinite fluid seafloor. From a geologist's point of view, this hypothesis is very strong : on a decimetre scale, the seafloor is actually often stratified, with important impedance contrast between different layers. So, when the wavelength becomes decimetric (for cases of deep-sea water MBES), the penetration of the acoustical energy is no more negligible and the stratification of the seafloor must be taken into account.

We developed a model of acoustical backscattering by layered media based on the concept of "equivalent input backscattering strength" [10]. The seafloor modeled here is composed by a finite numbers of layers covering a basement (in the acoustical sense this

number is related to the effective penetration depth and not to the actual geological layering). Each layer contributes to the backscattered signal *via* a single backscattering strength, defined for a semi-infinite layer covered by water, and featuring two components (e.g. [8] for the interface contribution and a small perturbation model for the volume). The total backscattering strength of the structure is then the sum of all the individual layer contributions, modified by the layering and weighted by a transfer coefficient. There are three phenomena involved in this BS: a refraction effect due to change in sound speed from a layer to another ; a change in impedance contrast which implies a modification of the reflexion and transmission coefficients ; and a limitation of the layer volume. The transfer coefficient is computed by the way of classical transmission and reflexion coefficients in layered media [11]. This calculation can provide angular oscillations (due to interferences) which may be observed experimentally [12]. This BS model for layered media can fit experimental curves with a good agreement [10]. Especially, it can model a lot of geologist's hypothesis or observations, such as interferences, lowering of signal level with increasing of sediment layer thickness, etc... (see fig.8). On the other hand, this model features a high numbers of parameters (some of them being completly out of reach, e.g. the statistics of buried rough interfaces). So, it can provide a good accordance between theory and experiments for various geaoacoustic configurations.

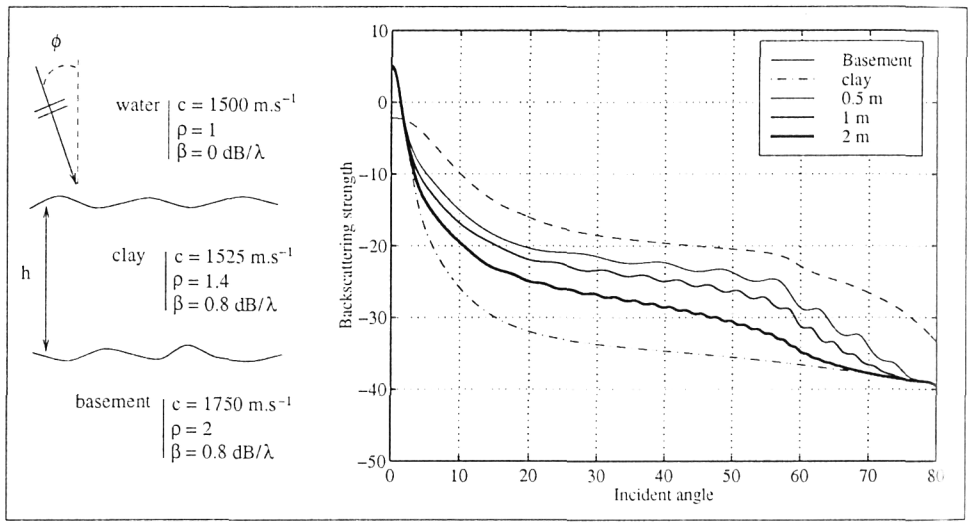


*Fig.8 - Example of modeling results for backscattering from a layered seabed: structure and parameters of the model (left), and computed BS vs angle (right) for basement alone, for water-sediment interface, and for various sediment layer thicknesses*

A way to improve this modeling is by a better knowledge of the geoacoustical parameters of the seafloor. This can be done from *in-situ* measurements [6] or by the use of geoacoustic models. One of these is the Biot theory [13] which describes the propagation of sound in porous media; it predicts speed and attenuation of three sound waves (two compressional and one shear) from a set of physical parameters; unfortunately these are quite numerous, and some of them are really difficult to estimate. We are currently trying to measure in laboratory some of these parameters for sandy sediments, in order to better characterise propagation of sound in this kind of seafloor.

# 5. CONCLUSIONS

Multibeam echosounders used nowadays prove to provide a very significant progress in the field of seafloor characterization, especially when used in conjunction with other seafloor survey systems such as sidescan sonars, sediment profilers and high resolution seismics. Their main potentiality lies of course in their ability to provide coherent bathymetry and imagery data on large zones, although they are usually less performant, on the second point, than side-scan sonars. Exploiting their data for sea floor characterisation implies, as it has been shown above, a series of indispensable processing that have to be rigorously conducted. Besides a correct application of the preliminary processing, a point of highest importance for a successful segmentation and interpretation of a MBES sonar image is the careful and relevant selection of the training zones, an operation that has to be conducted by a geology specialist. One cannot over-emphasize the importance of complementing, at this level of the processing, the geologist's expertize with (1) a thorough understanding of the MBES characteristics (and, as a corollary, the possible development of specific preprocessing algorithms) and (2) a sufficient mastering of the involved physics, namely basckscattering and propagation.

Although artefacts of bathymetric measurements are usually correctly addressed, we feel that today's MBES do not provide sufficient guaranties about the actual acoustical level measurements ; an imaging MBES should nowadays be considered as a scientific instrument for backscattering strength measurements, and developed in this respect. Confident that next generations of multibeam systems will remedy this, we had, in the meanwhile, to develop our own post-processing chains in order to compensate directivity effects and receiver processing gains.

A lot of work still remains to be done in the field of sea floor characterisation from MBES acoustical data. While direct modeling of sediment backscattering phenomena may be quite successful, the inverse problem of seafloor parameter estimation is made difficult by the non-unicity of relations between geological and acoustical features, leading to determination ambiguities. This problem is especially penalizing for low frequency MBES (around 10 kHz), whose poor resolution, on the other hand, precludes the exploitation of signal characteristics bound to the interface smaller features ; on the contrary MBES working above 100 kHz provide signals from the surficial interface, whoses amplitude statistics and spectra may be usefully exploited. Semi-automatized identification processings seem today possible for the latter. On the contrary the issues raised by deep-water low-frequency MBES are too numerous and do not allow such a potentiality ; the roles devoted, in this case, to multisensor data analysis and to geologist's expertise, in complement of the MBES data exploitation, are then prevalent. The use of acoustical devices is necessary for a good understanding of geological areas; but whatever the approach retained for applying it to seabed characterisation, it can not substitute for ground-truthing. The two approaches are indeed complementary and indissociable.

**Acknowledgements**

The authors wish to thank Gérard Auffret for the availability of the SEDIFAN data.

## REFERENCES

[1] Auffret G.A., et al. The Celtic deep sea fan : preliminary results on architectural organisation, historical development and recent activity. 2nd ENAM II Workshop, 30 october-2 november 1997, Kinsale Ireland. Abstract (1997)

[2] Lurton X., Augustin J.M., Dugelay S., Hellequin L., Voisset M., Shallow-water seafloor characterization for high-frequency multibeam echosounder: image segmentation using angular backscatter, in *High Frequency Shallow Water Acoustics* (Pace ed.), SACLANTCEN Conference Proceedings CP-45 (1997)

[3] Dugelay S., Lurton X., & Augustin J.M. A new method for seafloor characterization with multibeam echosounders: image segmentation using angular backscattering , 3rd European Conference on Underwater Acoustics, pp 439-444 (1996)

[4] Dugelay S. *Caractérisation des fonds marins à partir de données sondeur EM12*, Thèse de Doctorat de l'Université de Paris XI Orsay (1997)

[5] Jakeman and al. Non Gaussian models for the statistics of scattered waves, Advances in Physics, Vol 37, Number 5, pp 471-529. (1988)

[6] Unterseh S. et al. Acoustic data ground truthing through in-situ measurements of physical properties. ISOPE 98 (1998, in press).

[7] Gardner J.V. et al. Ground-truthing 6.5 kHz side scan sonographs: what are we really imaging ? J.Geophys.Res. 96 (B4) pp 5955-5974, (1991)

[8] Jackson D.R., Winnebrenner D.P. & Ishimaru A. Application of the composite roughness model to high frequency bottom backscattering. J. Acoust. Soc. Amer. 79 (5) pp 1410-1422, (1986)

[9] Ivakin A.N. & Lysanov Yu. Underwater sound scattering by volume inhomogeneities of a bottom medium bounded by a rough surface. Sov. Phys. Acoust. 27 (3) pp 212-215, (1981)

[10] Guillon L. & Lurton X. Backscattering by layered media: modeling and comparison with data. Proc.of the 16th International Congres of Acoustics, Seattle, USA, (1998, in press).

[11] Brekhovskikh L.M & Godin O.A. Acoustics of layered media. I : Plane and quasi-plane waves. Heidelberg, Springer-Verlag, (1991)

[12] Hugget et al. Interference fringes on GLORIA side-scan sonar images frome the Bering sea and their implications. Mar. Geophys. Res. , 14 , pp 47-63, (1992)

[13] Biot M.A. Theory of propagation of elastic waves in a fluid saturated porous solid. J. Acoust. Soc. Amer., 28 (2), pp 168-191, (1956)

# AUTOMATIC OUTLIERS ELIMINATION AND OPTIMAL MAPPING: A SOLUTION[1]

GAETANO CANEPA ODDBJØRN BERGEM

SACLANT Undersea Research Centre,
Viale S. Bartolomeo 400, I19138 La Spezia, Italy
email canepa@saclantc.nato.int

**Abstract**

During the last twenty years, many multibeam bathymetric sonars have been produced. The instrumentation is usually accompanied by a system to produce a seafloor map using the sonar data. There are also several public domain systems, which can be used to obtain a map from the data. The resulting gridded map must be filtered to reproduce the seafloor surface because of the effect of noise in the bathymetric data. The gridding and filtering algorithms introduce a source of error. Moreover, gridded maps may require significant storage space for a small amount of information. Until now, a systematic and efficient solution to the problem of identification and elimination of wrong data (outliers) has not been available. We present here an algorithm to fit bathymetric data and to automatically deal with outliers. The most important characteristics of the algorithm are: production of a triangulated map of uniform accuracy, irrespective of seafloor features, a map resolution which depends on the local data noise amplitude, automatic elimination of outliers, intrinsic modularity of the program that can be easily divided for a multiprocessor environment and low computing cost even on large data files. The algorithm was applied to synthetic data with and without outliers to demonstrate its behavior when parameters are changed. The algorithm has also been tested on real data. Some tests were also performed on the triangulation engine behavior, algorithm implementation speed and fitting errors.

# 1 Introduction

## 1.1 Background

As a consequence of increasing marine exploitation and exploration there is a need for accurate high resolution bathymetric data. To collect these data a number of sophisticated multibeam sonar has been produced for shallow and deep water (de Moustier 1988, Mitchell 1996). The data produced need to be corrected for systematic measurement errors and elaborated to produce an accurate Digital Terrain Model (DTM). The purpose of the algorithm presented here is to create an accurate map from multibeam bathymetric data. High-resolution bathymetric maps are important in a number of different applications (Vogt and Tucholke 1986):

- fish habitats identification (Lehodey and Grandperrin 1996).
- accurate geological map (e.g. for petroleum prospecting and study of morphology and morphological transformations of rifting or break-up of continental shelf Exon et al. 1996, Pratson and Edwards 1996).

[1]This work has been partially supported by EU, under the MAST-III initiative, project "ISACS", contract no. MAS3-CT95-0046.

- pipelaying operations (for petroleum, gas, *etc.*): charts for oil companies are typically produced at 1:2,500 scale with 1 m contour line interval (Midthassel et al. 1988).
- changes to harbour entrances, dock sites or dredged channels to effectively cope with large ship navigation (Burke et al. 1988).

## 1.2 Problem

Data for seabed mapping from multibeam echosounders consists of latitude, longitude and depth of a set of seafloor points. Even when acquired in near perfect conditions, the data are affected by nearly white noise due to uncertainty in the determination of the seafloor depth (Midthassel et al. 1988). A number of other systematic errors are added to the data points: roll, pitch, yaw and heave error, sound velocity variation in the water column, tide, GPS errors, *etc.* The latest multibeam sonar automatically compensates for these errors[2] (Bourillet et al. 1996, Miller et al. n.d.). Residual errors after compensation, considered as white noise, can be optimally treated using a Least Squares algorithm. Despite the considerable improvements in the performance of the new generation of multibeam echosounders, artifacts still occur in the bathymetry, due mainly to anomalous bottom detection.

Still concerned with the data characteristics, "one of the major problems which has to be addressed on implementing a swath sounding system is the managment of the prodigious amounts of data ensuing from the survey operations" (Midthassel et al. 1988). The last generation of multibeam sonar is able to acquire more than 1,000,000 depth measurements per hour. For example, the density of the data for a SIMRAD® EM3000 running at 10 knots at a depth of 10 m is around 25,000,000 points/km$^2$ and it can acquire more than 10,000,000 data points in one hour. With this amount of data even a low percentage of wrong data can take a very long time to be cleaned, even if an automatic outlier selection program with a highly interactive graphic user interface is used (Burke et al. 1988, Chayes 1991, Ware et al. 1992). An automatic outlier detection algorithm is necessary. Considering the volume of data, the production of a seafloor map must also be considered as a practical way of data reduction/compression, expecially if it contains other information (data standard deviation, data density, *etc*).

## 1.3 Available software

Available software mapping tools (for example the GMT-System package by Wessel and Smith (1995)) are only able to triangulate, contour and plot all data without fitting or (for example the MB-System package by Caress (1996)) to interpolate data on a regular grid basis and to filter the data from outliers (using a cleaning program followed by editing, `mbclean` and `mbedit`): anyway, the `mbclean` algorithm always needs an additional editing session. Other packages (such as the TRISMUS package by (Bourillet et al. 1996, Edy 1996)) apply the MB-System and GMT-System functionality to conventional gridded maps. TRISMUS contains an automatic filtering module to remove aberrant soundings (`BATHYMUL`, see Subsection 2.2). More information on software toolkits for mapping of scattered data can be found in (Mayer et al.

[2]The software MB-System also deals with this kind of errors (Caress 1996).

1997, Tyce et al. 1997). Gridding bathymetric data has a series of disadvantages. It introduces a low pass effect that can mask seafloor features. If the gridding is too sparse, the seafloor can be poorly defined while, if it is too dense, the map dimension can be too large for practical purposes. If a seafloor peak is not on a node of a regularly gridded map, its features are not well conserved and there is also the risk, if the grid is not dense enough, that the peak could disappear from the map. The best choice is a sparse grid where the seafloor is practically flat and a dense grid where it changes more dramatically. A substantial improvement can be obtained using a data driven triangulated map: it will always locate a node on or very near, to the seafloor peaks. There is no risk that the peak could disappear from the triangulated map[3].

# 2 Mapping multibeam bathymetric data

## 2.1 Problems of mapping

The creation of a DTM is the crucial phase of bathymetric data processing (Bourillet et al. 1996). Building a DTM starting from data points can be seen as a data interpolation or data fitting problem. When noise affects the data and when the density of data points is higher than the required map resolution, the map cannot be simply an interpolation of the data points: data fitting is required. Starting from an accurate DTM it is possible to produce a contour chart, a perspective view, a depth profile along a given path, differential and slope charts, volume calculation, *etc.*

When fitting a seafloor, as we saw in the preceding Section, the function $f$ is traditionally calculated on a uniform grid and interpolated between the grid's nodes. The calculation of the grid node depth is usually performed as a simple average (or weighted average) of the nearest data points. Claussen and Kruse (1988) and Mitchell (1996) use a more time consuming, but more accurate algorithm, based on the fitting of the nearest data points with a plane or a quadric surface.

A common situation after the map is produced using a common gridding technique is that the grid interval is so narrow that considerable noise is present on the gridded map and further filtering is necessary to obtain a correct DTM. The filtering phase must preserve the height and the dimensions of the sea details. Some of the algorithms presented in the literature do not give sufficient consideration to this important point. Common low-pass filter smooths well but does not preserve seafloor features.

## 2.2 Problems in the elimination of bad data

To obtain the best DTM, it is important to eliminate wrong data. The outliers elimination phase may be performed before or during the fitting phase. Two approaches exist in bathymetric data analysis: interactive outliers elimination by means of a computer aided graphics tool or software automatic elimination. Most commercial software uses a hybrid approach consisting of software detection of "possible outliers" followed by an interactive session to confirm the elimination (Ware et al. 1992, Caress 1996, Edy 1996). These "outlier elimination" sessions are tedious and time consuming given that 1% outliers on 1,000,000 points each acquisition hour, results in 10,000

[3]Another software package, Siscat, can be used to model data using maps that optimize storage space (SINTEF n.d.). However, it works on a pre-defined "correctly" gridded map or on scattered data that are supposed to be exact.

outliers per acquisition hour to be scanned. Caress (1996) affirmed that a "technician spends roughly four hours per day processing the data from the day before" and other "8 hours of effort per survey day were required to achieve the" final site map: the new multibeam sonar produces more data than the ones produced by the Caress instrumentation. Within the software for automatic outlier detection, different approaches exist: some of these are not able to find all the outliers (Caress 1996, Guenther and Green 1982, Grim 1988, Wells et al. 1989, Herlihy et al. 1992), others are too time consuming (Greenburg 1987) or need very high coverage to be accurate (Ware et al. 1990, Ware et al. 1992, SIMRAD 1992). An interesting algorithm is still far from practical application (Du 1995, Du et al. 1996, Du 1997). Finally, even commercial packages, such as NEPTUNE and TRISMUS, strongly suggest operator editing of outliers automatically flagged by their algorithm (SIMRAD 1992, Bourillet et al. 1996). It must be pointed out that some of the algorithms used to flag the outliers are questionable from a statistical point of view. A popular technique of outliers flagging consists, after a preliminary fitting surface has been found, of the calculation of the local standard deviation between data and surface and in the following outlier elimination phase based on the local standard deviation (Midthassel et al. 1988, SIMRAD 1992, Ware et al. 1992, Edy 1996). A further fitting phase, using the cleaned data, follows. This technique, as described by the authors, is also questionable from a statistical point of view (it is not *robust*).

An interesting problem concerning data noise is that when using different sonar systems or when the seafloor changes, the data noise variance changes and most of the outlier elimination algorithms we have cited depend on constants which are sensitive to noise level.

Some of the above methods perform filtering of the data file using only adiacent beams and soundings in the data file. The data file, however, is usually built using more than one track: each track is superimposed other tracks. Therefore, a percentage of the data points is in close proximity geographically but is not near in the data file. The methods just described do not use the information carried by these points.

## 2.3 Overview of the algorithm

The algorithm presented here is not completely innovative in the sense that it is composed of a series of steps, where each single step has already been used on seafloor fitting, outliers elimination or data reduction. The novelty of the algorithm consists in the conjunct use of these techniques in such a way that the calculations are performed using a computing time compatible with practical considerations. Moreover:

- The algorithm uses all the data points to eliminate outliers and prepare the map (not only the ones that are physically close in the data file)
- The algorithm attempts to address the problems of outlier elimination and storage space *versus* information optimization, which are still not optimally solved in the cited literature.

The characteristics of this algorithm are:

- a map which optimizes storage space;
- map resolution dependent on local data noise amplitude;
- robust treatment of outliers;
- interpolation of data produced by any echosounder;

- intrinsical modularity of the implementation software that can be easily divided for a multiprocessor environment;
- low computing cost even on large data files.

The fitting (mapping) algorithm described here is based on a triangulated grid which minimizes[4] the number of nodes necessary to describe the map and minimize the loss of information. The map produced is denser where the magnitude of the second derivatives of the seafloor are higher and the resolution depends on the noise level on the data. The algorithm enhances the accuracy of the seafloor map, calculating the map node depth, fitting the data points near the node using a quadric surface. At the same time, it produces a filtered DTM: the characteristics of which are such that they preserve the seafloor feature characteristics (depth, dimensions and position). The basic idea behind the outlier detection method described is that the outlier elimination phase is carried out during the mapping phase and consists of two distinct procedure: a first algorithm (*robust* but not accurate) eliminates far outliers and a second one (*quasi-robust* but accurate) removes the nearer outliers (Canepa and Bergem 1997).

The algorithm is fast and produces an already filtered map that can be easily gridded. Moreover, while the algorithm builds the map, it also eliminates outliers using all the data acquired from the site. The algorithm results shown in Section 3 illustrate the effectiveness of the triangulation procedure concerning data reduction.

To permit fast data fitting, a piecewise linear approximating surface is chosen for the algorithm: the simplest $C^0$ (continuous) function.

Two important points of tringulated surface fitting algorithms are the stopping criteria and the node choice of the fitting algorithm. Many criteria are available depending on the particular application. One of the criteria that fits well with the seafloor data mapping, depends on the local data noise (LDNC): the triangulation procedure will look for data points the distance of which from the map under construction, is higher than a certain number of times the local data noise. If the points are not outliers, they are chosen as map nodes. It is clear that most of the nodes considered will be outliers. This strategy is appropriated to the selection of points with the highest probability of being outliers. This criterion is also able to produce a map independently of data local noise. The triangulation produced using the LDNC is more dense where the second derivatives of the seafloor are high, that is where the surface "changes more." The triangulation will stop when all the data points that are not outliers are "near" to the constructed map.

The way in which a smoothing filter deals with seafloor features is an important characteristic to consider when a filter procedure for bathymetric data must be selected. For example, a moving average filter reduces the amplitude of a local maximum of the surface. This is also the case, for a gridding technique based on the average or the median of the points nearest to the grid node. Filtering techniques exist which are able to maintain such characteristics although losing some smoothing power. They are low-pass filters, well-adapted to data smoothing termed least-squares,filters (Press et al. 1992). For each point $p_i = (x_i, y_i, z_i)$, the least-square polynomial fit $P_{p_i,N_f}(x, y)$ to the $N_f$ points in the neighbourhood of $p_i$ is performed and the smooth value (SV) of the function $z_i^* = P_{p_i,N_f}(x_i, y_i)$ is taken as the value of the polynomial fit at $(x_i, y_i)$: $g_i = (x_i, y_i, z_i^*)$. Then, the filter is moved to the next

[4]If the node choice is data based.

point until all the smoothing function points are calculated. This kind of filtering can be performed using fast algorithms on gridded data, but it is very slow if they are not. As a consequence, it is not possible to filter all the bathymetric data using this powerful technique (Greenburg 1987). Our fitting algorithm automatically and efficiently performs a version of a least-squares filter.

## 2.4 Description of the bathymetric data fitting procedure

The bathymetric fitting procedure is a modified COMPRESS scheme applicable to noisy data (Dyn et al. 1990, Rippa 1992).

In simple terms, our algorithm starts from a first set of nodes which defines the map zones and calculates the SV of the seafloor surface at these points. The first triangulation is performed using the contour nodes and the SVes. The node with the maximum relative[5] error between the approximated map and the data set is calculated and if this error is higher than a certain constant, the point that generated the highest error is added to the set of map nodes after calculation of its SV. The algorithm stops when all the data points have a relative error from the map inside a given range. The mapping results are given as depth and local error at the node.

Global fitting of the seafloor surface can be very time consuming. For each step of the optimization, the error between the data points and the actual approximating surface must be computed. It is more efficient to divide the problem into a number of smaller problems in which the global solution can be efficiently found and then assemble the local solutions to generate a global one. This process is possible only if the local solutions are continuous when joined. In our case, considering that the approximating surface described here is based on triangulation, the local solution can be found on triangular sub-domains: the union of such sub-domains generates the global map.

## 2.5 Outlier elimination

A high level of outliers is a rule in bathymetric data: in such cases many authors prescribe that a better estimation of the surface location is obtained if an algorithm for outlier elimination is used (Launer and Wilkinson 1979, David 1979). Most methods for statistical outlier elimination are based on a *significance level*, the probability that good data could be discarded assuming that the data are distributed according to a given probability density function. For high levels of contamination (10 %), many authors in the book edited by Launer and Wilkinson (1979) prescribe the use of methods with a high probability threshold, in which case, the elimination of a small amount of good data permits a *robust* and *efficient* location of the surface.

The outlier elimination algorithm presented here is based on the application of two algorithms: a *robustness-inducing* algorithm and a *quasi*-robust algorithm. A *quasi*-robust algorithm is an algorithm that cannot be applied when outliers lie indiscriminately far from the real location. If outliers are reasonably near to the real location, a *quasi*-robust algorithm is able to estimate and identify the outliers. The presence of the *robustness-inducing* algorithm is clear: it is used to identify the presence of "far" outliers and of eventual seafloor discontinuities. In fact, the seafloor

[5]Relative to the local noise variance.

is one of the places, in nature, where a step can be encountered and a continuous fitting function cannot always be used: the presence of such discontinuities is taken into account in the *robustness-inducing* part of the outlier elimination algorithm.

The outlier elimination phase can be applied to the mapping algorithm without substantial changes.

The *quasi*-robust algorithm is based on a suggestion that can be found in the manual of the `loess` program (Cleveland et al. 1992): a program of local regression. It is based on an iteratively reweighted least-squares method ($W$-estimator) called iteratively Tukey's reweighted least-squares (Cleveland et al. 1992, Goodall 1983). It works on long-tailed distribution, but it has a high efficiency in the Gaussian case. It iteratively performs a surface fitting weighting of the data residuals: this algorithm is able to detect the presence of near outliers.

The iteratively Tukey's reweighted least-squares can have problems in presence of very far outliers. To avoid such problems, a *robustness-inducing* algorithm is applied before applying the $W$-estimator. The algorithm is applied during the $N_f$ fitting points selection phase. During that phase, a fitting of the surface is not available: as a consequence the points depth will not, in general, be Gaussian distributed. The idea is to use the *fourth-spread* range (based on an unknown Gaussian distribution, see Emerson (1983) for a description of the test), as a test to eliminate only the "far outliers": the complete elimination will be performed by the *quasi*-robust algorithm. Du suggests the use of an outlier elimination criterion based on the Uniform distribution[6] (Du 1995, Du et al. 1996). The use of the Gaussian distribution implies criteria that are more conservative with respect to those derived from the Uniform distribution.

Our algorithm, after producing a first approximation of the seafloor map, performs an outlier elimination step using the local standard deviation as a parameter for the elimination of the outliers that escaped the first scanning procedure (SIMRAD 1992, Midthassel et al. 1988, Edy 1996, Ware et al. 1992). A second mapping section is then performed. The improvement with respect to some of the cited algorithms is that the farthest outliers were already eliminated before proceeding with further elimination and the algorithm is, therefore, statistically *robust*.

# 3 Algorithm testing

The mapping procedure described in the preceding sections is tested here using both synthetic and real data. The values selected for the algorithm parameters during the test phase are a good balance of different exigencies.

A set of four standard functions was chosen to produce synthetic data in accor-

[6]He claims that a Uniform distribution is more appropriate to describe the statistic of the data if this is dominated by the seafloor variation: this hypothesis could be correct only if the considered points come form a large region that shows significant height variation.

dance with (Dyn et al. 1990).

$$f_1(x,y) = -\left(1-\frac{x}{2}\right)^6\left(1-\frac{y}{2}\right)^6 - 1000(1-x)^3x^3(1-y)^3y^3 - y^6\left(1-\frac{x}{2}\right)^6 - x^6\left(1-\frac{y}{2}\right)^6 \quad (1)$$

$$f_2(x,y) = \frac{\tanh(9y-9x)+1}{9} \quad (2)$$

$$f_3(x,y) = \exp\left(-\frac{81}{4}\left((x-0.5)^2+(y-0.5)^2\right)\right) \quad (3)$$

$$f_4(x,y) = \begin{cases} 1 & \text{if } y-\xi \geq \frac{1}{2} \\ 2(y-\xi) & \text{if } 0 \leq y-\xi \leq \frac{1}{2} \\ (\cos(4\pi r(\xi,y))+1)/2 & \text{if } r(\xi,y) \leq \frac{1}{4} \\ 0 & \text{otherwise} \end{cases} \quad (4)$$

where $r(\xi,y) = \left((\xi-\frac{3}{2})^2+(y-\frac{1}{2})^2\right)^{\frac{1}{2}}$, and $\xi = 2.1x - 0.1$.

To obtain data files comparable with those of a multibeam echosounder, the functions $f_i$ have been transformed to $F_i$: using this transformation "natural" variations of latitude and longitude result in "natural" variations of depth. The functions were sampled using random Uniform sampling: the resulting sample distribution is similar to the bathymetric data distribution, but the data are ordered differently. Figures 1.b, **d**, **f** are contour plots obtained using 10,000 random samples of $F_1$ to $F_3$.

Gaussian uncorrelated noise is added to all the synthetic data sets. To simulate different multibeam sonar, two values of noise variance are used: $\sigma_m = 0.5\,\text{m}$ and $\sigma_n = 0.05\,\text{m}$. Figure 2 shows an example of the effect of the noise on data sampled by the $F_4$ function.

Figure 3 shows (on the top) the results obtained from the algorithm when applied to the data in Fig. 2.**a**, in terms of reconstructed surface, triangulation, and statistics. Considering the high level of the noise, the surface is well reconstructed. In the table in Fig. 3, and in the following tables, the columns labelled $N_o$ and $N_n$ give, respectively, the number of outliers in the data set lying in the map and the number of nodes of the map. The column labeled $\sigma_F$ gives the value of the standard deviation of the noise added to the synthetic functions samples. When the algorithm is applied to a low noise data set (see Fig. 2.**b**) more points are necessary to obtain a result in which the map is sufficiently accurate to have a variance from the data of the same order of the variance of the noise on the data. Figure 3 shows (bottom) the results of the algorithm using 15 fitting points. It is noteworthy, in Fig. 3, that the mapping algorithm uses a high resolution where the surface second derivative is high, and a low resolution where it is zero. Similar results are obtained applying the algorithm to the other test functions.

An interesting test was applied to a synthetic data set of noise with constant variance $\sigma_m$ (i. e. constant depth). Table 1 reports the result of a single run of the algorithm in terms of error betweeen the reconstructed surface and the real one. It is clear that the error decreases when the number of fitting points increases (in the case of constant depth). When the number of fitting points is below or equal to 30 points, the error is high: this is a statistical limit for the algorithm. Two seafloor surfaces realized from data from the same site could therefore have a difference equal to twice the error reported in Table 1.

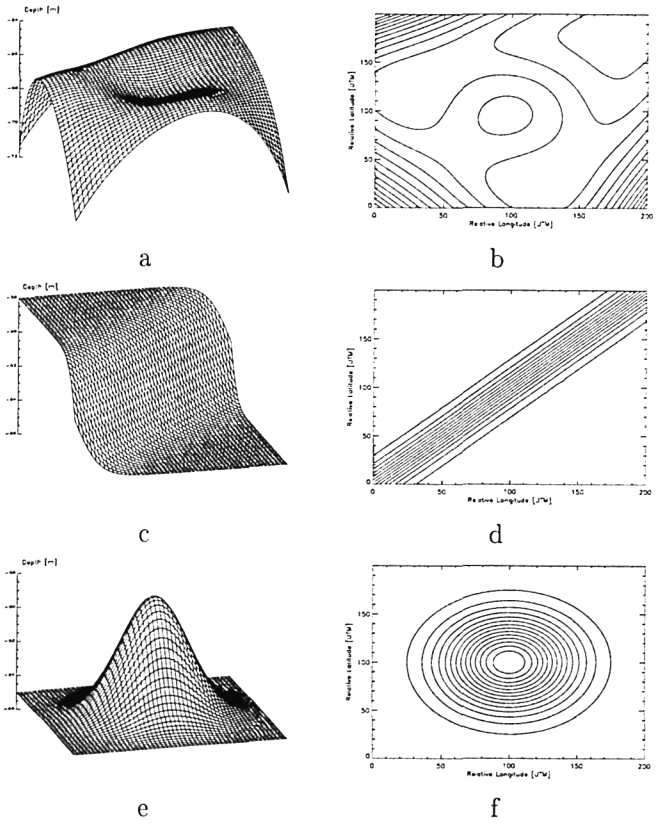


Figure 1: The first three synthetic test functions.

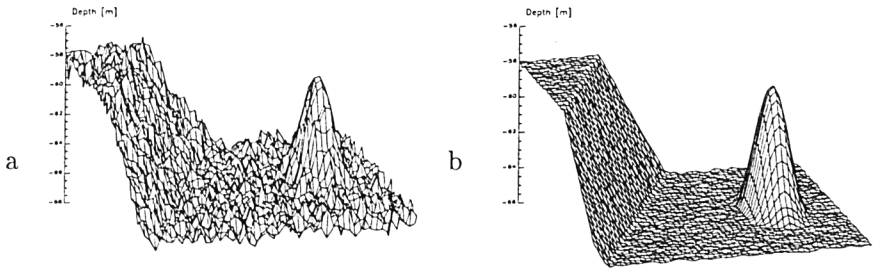


Figure 2: The effect of the noise added to the $F_4$ function: the variance of the noise applied to the data is, on the left, $\sigma_n$ and, on the right, $\sigma_m$.

| $N_f$ | 15 | 30 | 50 | 100 | 200 | 300 | 400 |
|---|---|---|---|---|---|---|---|
| $\lvert\varepsilon\rvert/\sigma_m$ | 2.00 | 1.22 | 0.96 | 0.66 | 0.20 | 0.18 | 0.17 |

Table 1: Relative error realized in the mapping of a constant depth synthetic seafloor data with a Gaussian noise of variance $\sigma_m$.

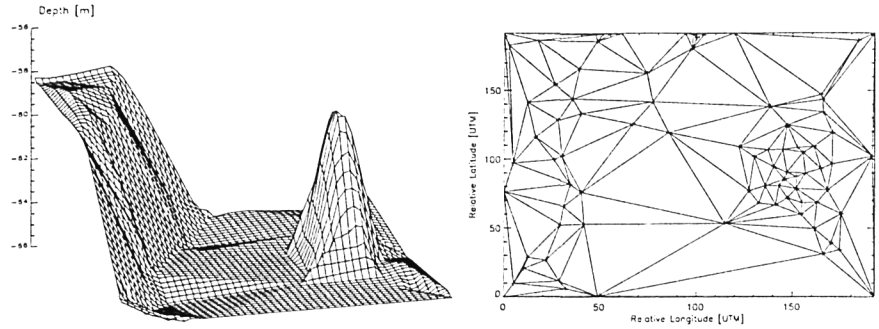


| $N_f$ | $\sigma_F$ [m] | $\sigma$ [m] | $\bar{\varepsilon}$ [m] | $\varepsilon$max [m] | $N_o$ | $N_n$ |
|---|---|---|---|---|---|---|
| 30 | .5 | .518 | .415 | 1.63 | 38 | 83 |

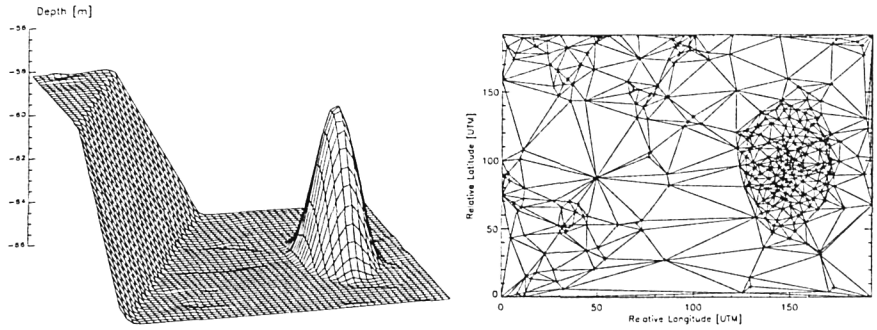


| $N_f$ | $\sigma_F$ [m] | $\sigma$ [m] | $\bar{\varepsilon}$ [m] | $\varepsilon$max [m] | $N_o$ | $N_n$ |
|---|---|---|---|---|---|---|
| 15 | .05 | .053 | .043 | .176 | 289 | 346 |

Figure 3: The results of the fitting algorithm applied to data characterized by a high (top) and low level of noise (bottom).

After the tests as global algorithm, other tests were performed on synthetic data using the algorithm on sub-maps. Two results on local application of the algorithm are shown in Fig. 4. The data sets consist of 120,000 points and the algorithm was applied using the selected parameters but dividing the problem into sub-maps with no more than 10,000 points each (16 maps in this case). The figures show that when the algorithm uses sub-maps it produces results very similar to the global application of the algorithm. The only difference is a small increase in the number of nodes and in the noise between the data and the reconstructed map.

To simulate real data, a synthetic data file with outliers was produced adding 5 % of data with a constant error from the synthetic surface ($\pm k\sigma$). With appropriate values for the algorithm parameters, when $k = 3$, 50 % of the outliers are identified; when $k = 5$, all the outliers are identified.

After the test on synthetic data some tests were performed on data collected at sea using an Atlas$^{TM}$ HYDROSWEEP MD© multibeam echosounder (STN ATLAS Elektronik GmbH, Bremen, Germany). Here only one of the test is shown on a shallow to deep water area in the Black Sea. Because the number of data points was high (about 350,000), the map was obtained by subdividing the problem into 59

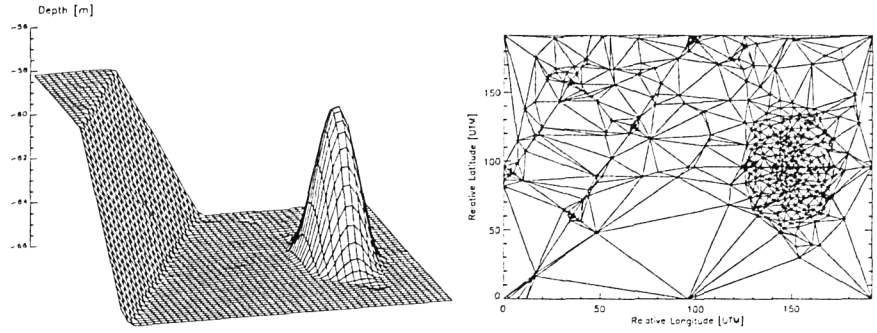


| $N_f$ | $\sigma_F$ [m] | $\sigma$ [m] | $\overline{\varepsilon}$ [m] | $\varepsilon$max [m] | $N_o$ | $N_n$ |
|---|---|---|---|---|---|---|
| 15 | .05 | .053 | .043 | .202 | 156 | 444 |

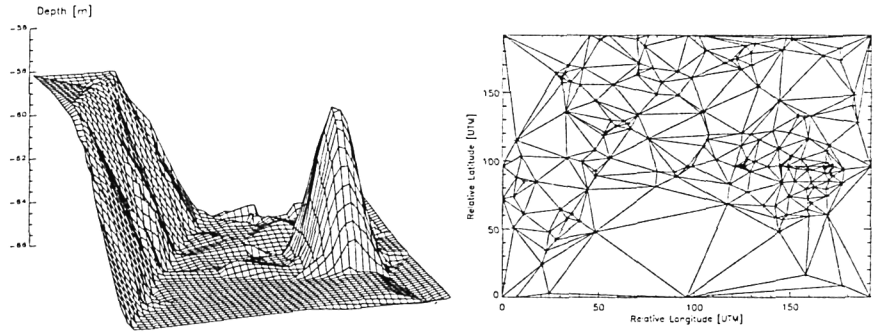


| $N_f$ | $\sigma_F$ [m] | $\sigma$ [m] | $\overline{\varepsilon}$ [m] | $\varepsilon$max [m] | $N_o$ | $N_n$ |
|---|---|---|---|---|---|---|
| 30 | 0.5 | .525 | .420 | 1.94 | 75 | 178 |

Figure 4: The results of multimap algorithm applied to synthetic data obtained from the $F_4$ function and characterized by a high level (top) and low level (bottom) of noise.

sub-maps. Figure 5 shows the seafloor surface obtained using $N_f = 150$: the number of nodes obtained using so many points is halved and the error is not increased with respect to the case of $N_f = 30$.

# 4 Conclusion

An algorithm to produce accurate maps from bathymetric data has been described. The main characteristics of the algorithm are:

- It produces a triangulated map of uniform accuracy irrespective of seafloor features
- The resolution of the map depends on local data noise amplitude
- Data outliers are automatically eliminated
- It is intrinsically modular (it can be easily divided for a multi-processor environment) and has low computing cost even on large data files (more than 1 million points)

The algorithm was applied to synthetic data to understand its behaviour when parameters are changed. In particular, data mapping with and without outliers has

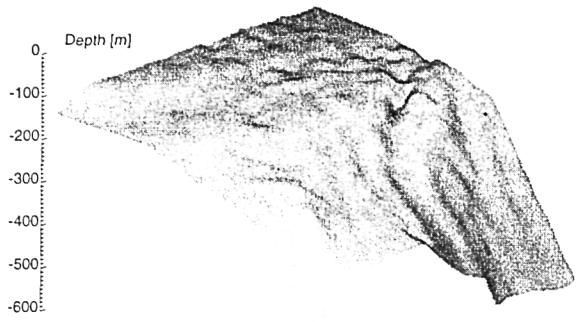


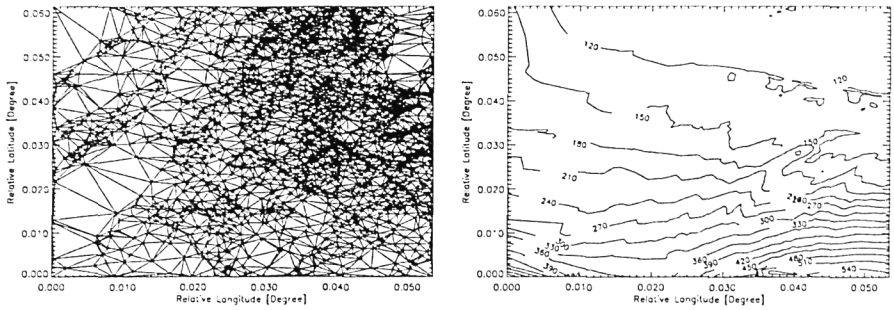


| $N_f$ | $\sigma$ [m] | $\bar{\varepsilon}$ [m] | $\varepsilon$max [m] | $N_o$ | $N_n$ | $N_o$% |
|---|---|---|---|---|---|---|
| 150 | 2.19 | 1.55 | 41.36 | 13585 | 2835 | 3.9 |

Figure 5: The results of the algorithm applied to a large data set.

been tested for both continuous and discontinuous synthetic seafloors. The algorithm has also been tested on real data. Some tests were performed on the triangulation engine behaviour, algorithm implementation speed, and fitting errors.

The algorithm can be used to reduce operator intervention during bathymetric data mapping. Raw bathymetric data are directly analyzed by the algorithm which automatically and robustly eliminates outliers and produces a map that can be finely tuned by the user (number of nodes, smoothing, level of data cleaning, etc.).

# References

Bourillet, J. F., Edy, C., Rambert, F., Satra, C. and Loubrieu, B. (1996), 'Swath mapping system processing: Bathymetry and cartography', *Marine Geophysical Researches* **18**, 487–506.

Burke, R. G., Forbes, S. and White, K. (1988), 'Processing 'large' data sets from 100% bottom coverage 'shallow' water sweep surveys – a new challenge for the canadian hydrographic service', *International Hydrographic Review* **LXV**(2), 75–89.

Canepa, G. and Bergem, O. (1997), An approach to robust map generation from multibeam bathymetric data, Technical Report SR-285, SACLANT Undersea Research Centre, La Spezia, Italy.

Caress, D. W. (1996), 'Improved processing of hydrosweep ds multibeam data on the r/v maurice ewing', *Marine Geophysical Researches* **18**, 631–650.

Chayes, D. N. (1991), Hydrosweep-ds on the r/v ewing, *in* 'Proceedings of the IEEE Conference OCEANS '91', Vol. 2, IEEE, New York, NY, USA, pp. 737–742.

Claussen, H. and Kruse, I. (1988), 'Application of the DTM-program TASH for bathymetric mapping', *International Hydrographic Review* **LXV**(2), 117–125.

Cleveland, W. S., Grosse, E. and Shyu, M. (1992), *A Package of C and Fortran Routines for Fitting Local Regression Models.* Available on the Internet at the `netlib` mathematics software library.

David, H. A. (1979), Robust estimation in the presence of outliers, *in* R. L. Launer and G. N. Wilkinson, eds, 'Robustness in Statistics', Academic Press, Inc., New York, pp. 61–74.

de Moustier, C. (1988), 'State of the art in swath bathymetry survey systems', *International Hydrographic Review* **LXV**(2), 25–54.

Du, Z. (1995), Uncertainty Handling in Multibeam Bathymetric Mapping, PhD thesis, The University of New Brunswick, Department of Geodesy and Geomatics Engineering, Fredicton, NB, Canada.

Du, Z. (1997). Personal comunication.

Du, Z., Wells, D. and Mayer, L. (1996), 'An approach to automatic detection of outliers in multibeam echo sounding data', *The Hydrographic Journal* **79**, 137–154.

Dyn, N., Levin, D. and Rippa, S. (1990), 'Data dependent triangulation for piecewise linear interpolation', *IMA J. of Numerical Analysis* **10**, 137–154.

Edy, C. (1996), *TRaitement Interactif des données de Sondeurs MUltifaiSceaux - TRISMUS.* Manuel de référence, Version 4.1.

Emerson, J. D. (1983), Boxplots and batch comparison, *in* D. C. Hoaglin, F. Mosteller and J. W. Tukey, eds, 'Understanding Robust and Exploratory Data Analysis', John Wiley & Sons, Inc, New York, chapter 3, pp. 58–96.

Exon, N. F., Royer, J. and Hill, P. J. (1996), 'Tasmante cruise: Swath-mapping and underway geophysics south and west of tasmania', *Marine Geophysical Researches* **18**, 275–287.

Goodall, C. (1983), M-estimators of location: An outline of the theory, *in* D. C. Hoaglin, F. Mosteller and J. W. Tukey, eds, 'Understanding Robust and Exploratory Data Analysis', John Wiley & Sons, Inc, New York, chapter 11, pp. 339–403.

Greenburg, A. R. (1987), Statistical filtering of bathymetric data, *in* 'Proc. of ASPRS-ACSM Fall Convention', Reno, Nevada.

Grim, P. J. (1988), The cop algorithm for selecting soundings within a pua, Technical Report Draft Report, National Oceanic and Atmospheric Administration, Department of Commerce, Rockville, MD.

Guenther, G. C. and Green, J. E. (1982), Improved depth selection in the bathymetric swath survey system (bs3) combined offline processing (cop) algorithm, Technical Report Technical Report OTES-10, National Oceanic and Atmospheric Administration, Department of Commerce, Rockville, MD.

Herlihy, D. R., Stepka, T. N. and Rulon, T. D. (1992), 'Filtering erroneous soundings from multibeam survey data', *International Hydrographic Review* **LXIX**(2), 67–76.

Launer, R. L. and Wilkinson, G. N., eds (1979), *Robustness in Statistics*, Academic Press, Inc., New York.

Lehodey, P. and Grandperrin, R. (1996), 'Swath mapping of the seafloor and its application to deep-bottom fisheries in new caledonia', *Marine Geophysical Researches* **18**, 449–458.

Mayer, L. A., Dijkstra, S., Clarke, J. H., Paton, M. and Ware, C. (1997), Interactive tools for the exploration and analysis of multibeam and other seafloor acoustic data, *in* N. G. Pace, E. Pouliquen, O. Bergem and A. P. Lyons, eds, 'High Frequency Acoustic in Shallow Water', NATO Undersea Research Centre, Viale San Bartolomeo 400, 19138 La Spezia, Italy, pp. 355–362.

Midthassel, A., Sølvberg, E. and Pøhner, F. (1988), 'Data management of swath sounding systems', *International Hydrographic Review* **LXV**(2), 91–115.

Miller, J. E., Clarke, J. E. H. and Patterson, J. (n.d.), 'How effectively have you covered your bottom?', *The Hydrographic Journal.* Appearing, see the WEB page `http://www.omg.unb.ca/ jhc/coverage_paper.html`.

Mitchell, N. C. (1996), 'Processing and analysis of simrad multibeam sonar data', *Marine Geophysical Researches* **18**, 729–739.

Pratson, L. F. and Edwards, M. H. (1996), 'Introduction to advance in seafloor mapping using sidescan sonar and multibeam bathymetry data', *Marine Geophysical Researches* **18**, 601–605.

Press, W. H., Teukolsky, S. A., Vetterling, W. T. and Flannery, B. P. (1992), *Numerical Recipes in C*, 2 edn, Cambridge University Press, Cambridge, UK.

Rippa, S. (1992), 'Adaptive approximation by piecewise linear polynomials on triangulation of subsets of scattered data', *SIAM J. Sci. Stat. Comput.* **13**(5), 1123–1141.

SIMRAD (1992), Simrad neptune postprocessing system, Technical report, SIMRAD Subsea A/S, Horten, Norway. Product Specifications.

SINTEF (n.d.). A description of Siscat© can be found at the Web site: `http://www.oslo.sintef.no/siscat`.

Tyce, R. C., Dzurenko, S. M., Cohen, P. A. and Caress, D. W. (1997), A pc/linux software toolkit for coastal swath mapping, *in* N. G. Pace, E. Pouliquen, O. Bergem and A. P. Lyons, eds, 'High Frequency Acoustic in Shallow Water', NATO Undersea Research Centre, Viale San Bartolomeo 400, 19138 La Spezia, Italy, pp. 579–586.

Vogt, P. R. and Tucholke, B. E. (1986), Imaging the ocean floor; history and state of the art, *in* G. S. Am., ed., 'The Western North Atlantic Region', Boulder, pp. 19–44. in the Collection, The Geology of North America.

Ware, C., Fellows, D. and Wells, D. (1990), Feasibility study on the use of algorithms for automatic error detection in data from the FCG smith, Technical report, Ocean Mapping Group, University of New Brunswick, Fredicton, NB, Canada. Contract Report.

Ware, C., Slipp, L., Wong, K. W., Nickerson, B., Wells, D., Lee, Y. C., Dodd, D. and Costello, G. (1992), 'A system for cleaning of high volume bathymetry', *International Hydrographic Review* **LXIX**(2), 77–94.

Wells, D., Nickerson, B. and Lee, Y. C. (1989), Error detection and correction in processing large bathymetric data sets, Technical report, Ocean Mapping Group, University of New Brunswick, Fredicton, NB, Canada. Contract Report.

Wessel, P. and Smith, W. H. F. (1995), 'New version of generic mapping tools released', *EOS Transaction* **76**, 329.

# SECTION III

## Processing and Interpretation

# Mapping of the benthic communities Common mussel and Neptune grass by use of hydroacoustic measurements

Per Settergren Sørensen and Kristian Nehring Madsen,
VKI - institute for the Water Environment, Denmark
and
Allan Aasbjerg Nielsen, Nette Schultz and Knut Conradsen,
Department of Mathematical Modelling (IMM), Technical University of Denmark,
and
Ola Oskarsson, Marin Mätteknik, Sweden.

Presented at the Third European Marine Science and Technology Conference, May 26th, 1998, Lisbon, Portugal.

## ABSTRACT

In this presentation a distinct activity of the BioSonar project is described, namely the classification of benthic patterns at the sea bottom by use echo sounder signals processed by the RoxAnn device. The field campaigns and gathering of the data material is described, as well as the results of the analyses conducted up to now. It is found that classification of the RoxAnn signals in feature space achieves a good separation on the $E_1$ signal (normally interpreted as roughness) of eelgrass, mussels and sand. The location and dispersion of data representing the different bottom types depends considerably on calibration and on variations in space and time, and cannot be considered stationary. Thus, it is recommended to classify data on the basis of a classification conducted for that particular survey from which the data originated, leaving the interpretation and comparison of data based on their absolute values out of consideration. It is stressed, that ground truthing is an indispensible requirement for ensuring the reliability of the derived sea bottom maps. It is recommended that distinct bottom type areas being exclusively covered by one sea bottom type, e.g. a mussel bed, be included in any survey to allow verification of results obtained from surveys of mixed areas.

## Introduction

In this presentation we will describe the findings that have emerged from one of the distinct activities in the BioSonar project, namely the issue of classification of bottom types using the echo sounding device RoxAnn. The general outline and an overall coverage of current results of the project has been described in (Conradsen *et al.*, 1998). The overall goals of the BioSonar project can be summarised as studies of

- Quantitative detection (ability to detect benthic communities, and to characterise their density with satisfactory precision)
- Reliability (reproducible or traceable, objective methods)
- Automation (computerisation of all possible work processes)
- Change detection (methods for monitoring changes in benthic communities).

Thus, it is an objective to assess the precision by quantitative methods and to automate the processes as far as possible. The aim is to attain a degree of automation where the overall processing is computerised, from the gathering of raw data through the preparation of the distribution maps to be inserted in GIS systems. Some of these processes are likely to require subjective decisions to be carried out during the use of computer programs, and might therefore not be fully objective or independent of the operator.

Here we will focus on the process of classifying a seabed, i.e. to provide a segmentation of a map into disjoint parts of different bottom types, with a particular view to identifying areas containing benthic communities like mussels and seagrasses. Focusing on classification of RoxAnn, we leave out many other subjects, such as the study of side scan sonar signals and the geostatistical study of spatial variability of the signals. Furthermore, the water depths surveyed lie within the range 5 - 10 metres, as we concentrate on data collected during surveys in Øresund between Denmark and Sweden, where eelgrass (*Zostera marina*) was measured as a nordic substitute for neptune grass (*Posidonia oceanica*).

## The device and the data material

For use in the project an echo sounder add-on device called RoxAnn and a side scan sonar add-on device called EOSCAN were selected. These are quite different hydroacoustic measurement devices, which give a good span of available technology and provide a basis for subsequent data fusion analyses.

The RoxAnn device, consisting of a head amplifier, a parallel receiver and a software package, records time-integrated parts of the first and the second backscattered echo from the sea floor, called $E_1$ and $E_2$, respectively. The existence of a relation between sea floor morphology and $E_1$ (sea floor roughness) and $E_2$ (sea floor hardness) is detailed on an empirical basis in Chivers, Emerson & Burns (1990) and Chivers & Burns (1992). A theoretical justification for the said interpretation of $E_1$ and $E_2$ is given by Heald & Pace (1996). In the BioSonar field campaigns an echo sounder frequency at 200 kHz was used.

The field campaigns in the Meditteranean and in Øresund have been carried out in the two consecutive years 1996 and 1997. The areas in Øresund were surveyed in late October in 1996 and 1997, and the Meditteranean areas were surveyed in November in 1996 and 1997, i.e. the change detection analyses will not be affected by elementary seasonal variations. The design of the field campaigns were based on three types of sea bed areas:

- Test areas, potentially containing mixed bottom types (two areas have been selected at sizes between 1 - 2 $km^2$)
- Bottom type areas (3 - 6 areas at a of size 100 x 100 metres)
- Footprint areas (one for each campaign having a size of 60 x 60 metres)

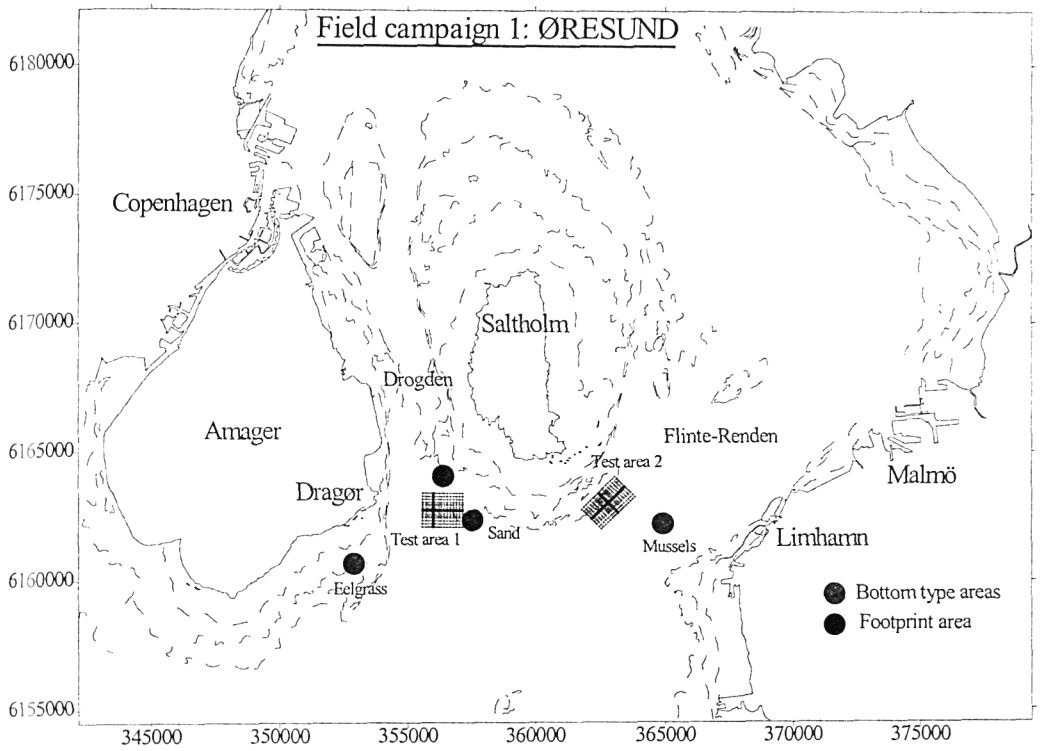


*Figure 1. Geographical map including test areas etc. in Øresund. Coordinates are UTM 33 Northings and Eastings.*

The purpose of the test areas was to collect mixed data representing real world cases. Thus, the intention was that the two test areas should be different e.g, one representing a density gradient of mussels and one centered on a mussel bed. In the Meditteranean one test area was an area of healthy neptune grass meadows (Cabo de Palos), and the other represented an area of degraded meadows (Mazarron). The purpose of the bottom type areas was to map practically uniform sea floor areas with solitary populations. The data from the so-called bottom type areas were used as references when the test areas are studied, and in preliminary studies of discriminating power of data. The footprint area measurements were introduced to assess repeatability and to assess drift from day to day, i.e. as a possible calibration means. The repeatability has been assessed for raw signals and for estimated areas.

In Øresund two test areas were applied, one located on the southern edge of Drogden and the other on the northwestern edge of Flinterenden. 3 bottom type areas were used in the Øresund, namely sand (100% coverage), a mussel bed (100% coverage), and solitary eelgrass (*Zostera marina*) meadow at approx. 100% coverage. These areas are depicted in Figure 1.

Ground truthing was prepared using video and still photos. Vertical video recordings were taken at fixed stations, primarily at intersection points in the transect grids. The video camera was mounted with a measuring tape. Still images were prepared for fixed stations by means

of a photo-sampler. The images cover approx. 2 $m^2$ of the sea bottom. A range of exogeneous and supplying variables were measured, including depth, temperature and salinity profiles, chlorophyll (when feasible), seston and transparency. Sea state was opted for, but the measurements were not implemented.

## Classification of the eelgrass, mussels and sand bottom types

Initial data analyses focused on the possibility to distinguish hydroacoustic measurements in feature space. The feature space is the 2D space consisting of (the logarithms of) $E_1$ and $E_2$, i.e. vectors

$$Y = (\log E_2, \log E_1)',$$

and is illustrated for the observations made in the bottom type areas in the 1996 field campaign in Øresund in Figure 2.

Bayesian discriminant analysis assuming Gaussian distributions of the bottom type observations were used to study the possibilities for segmentation of the sea floor in four distinct classes, being sand, mussel, eelgrass and other / reject class. The results yielded high resubstitution rates at 96% - 99% for the three bottom type classes, which establishes that the basic features of the observations can indeed be used to segment the sea floor in the said classes (Schultz *et al.*, in prep.).

Use of a non-parametric method called deformable templates, which it might be argued is more realistic, as it does not rely on assumptions of a certain shape of distribution of the observations in feature space, achieved similar high resubstitution rates, depicted in Table 1.

***Table 1.*** *Confusion matrix for classified RoxAnn data bottom type areas from the 1996 field campaign in Øresund, using Deformable Templates. The average accuracy rate is 96.9%.*

| | Classification classes | | | |
|---|---|---|---|---|
| True bottom type | Mussel | Zostera | Sand | Total |
| Mussel | 98.56% | 0.54% | 0.00% | 100% |
| Zostera | 1.25% | 96.84% | 0.51% | 100% |
| Sand | 2.89% | 0.83% | 95.39% | 100% |

Figure 2 shows a good separation of the eelgrass, mussels and sand bottom type data, they cluster in separate locations in feature space. The main direction of variation among clusters is just about vertical, and an analysis of variance accentuates $E_1$, roughness, as the variable to apply to separate the bottom type data, as the bottom type explains 82% of the variability of $E_1$. In comparison the bottom type codes obtained from ground truthing accounts for a mere 11% of the variability in the $E_2$, hardness, clearly rendering this variable inferior for

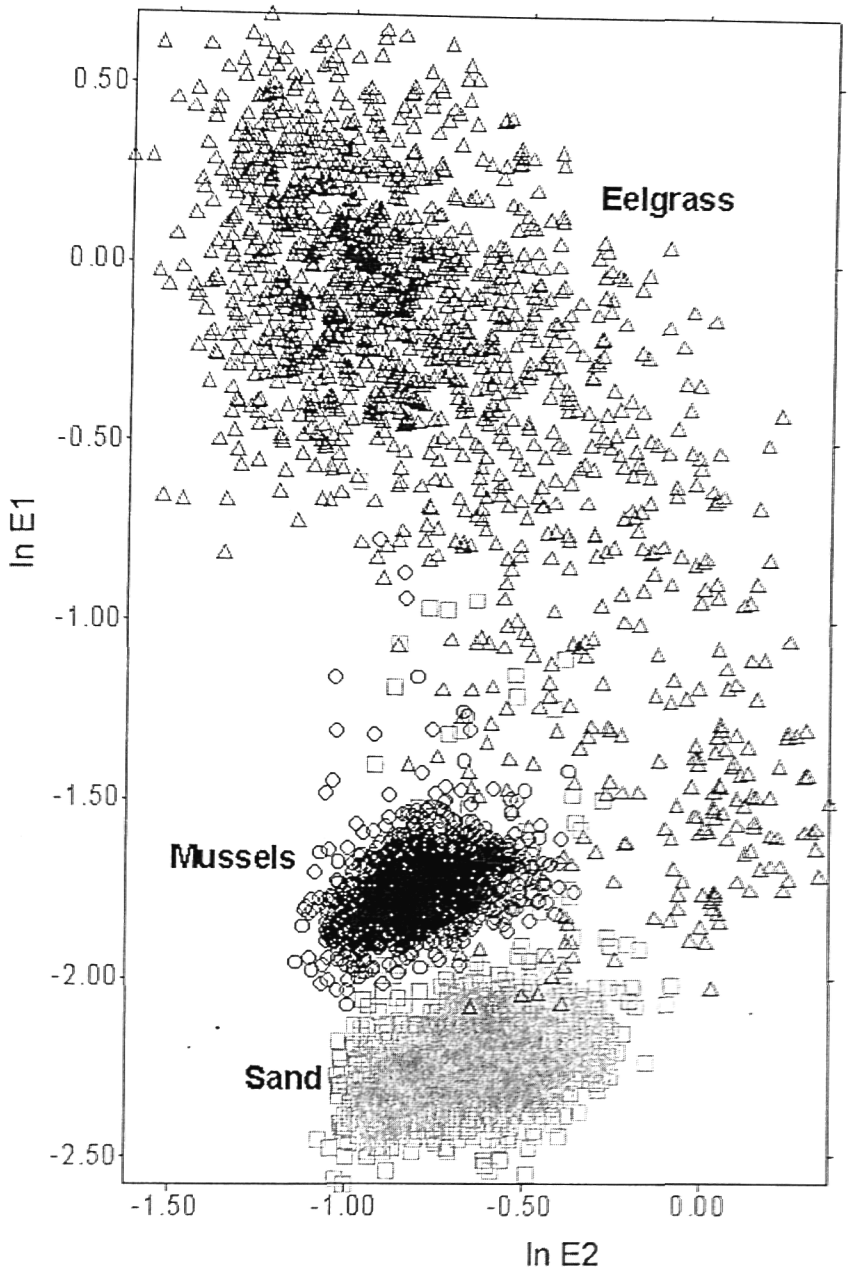


*Figure 2. The RoxAnn observations made in the bottom type areas sand, eelgrass and mussels in the 1996 field campaign in Øresund depicted in the logarithmic feature space.*

classification of bottom types. This result is sensible, as $E_1$ as a roughness measure is anticipated to be able to distinguish bottom types of sand, haivng a characteristic grain size at approx. 1 mm, mussel beds having grain sizes at approx. 5 cm, and eelgrass consisting of laminar segments varying in length from half a metre to several metres (Madsen, in prep.).

The classification results have been verified by the data from the survey of test area 2, which is just about entirely covered by mussels. The data from the mussel bottom type area and test area 2 are depicted in Figure 3. As can be seen, the observations from the two mussel bed locations overlap substantially.

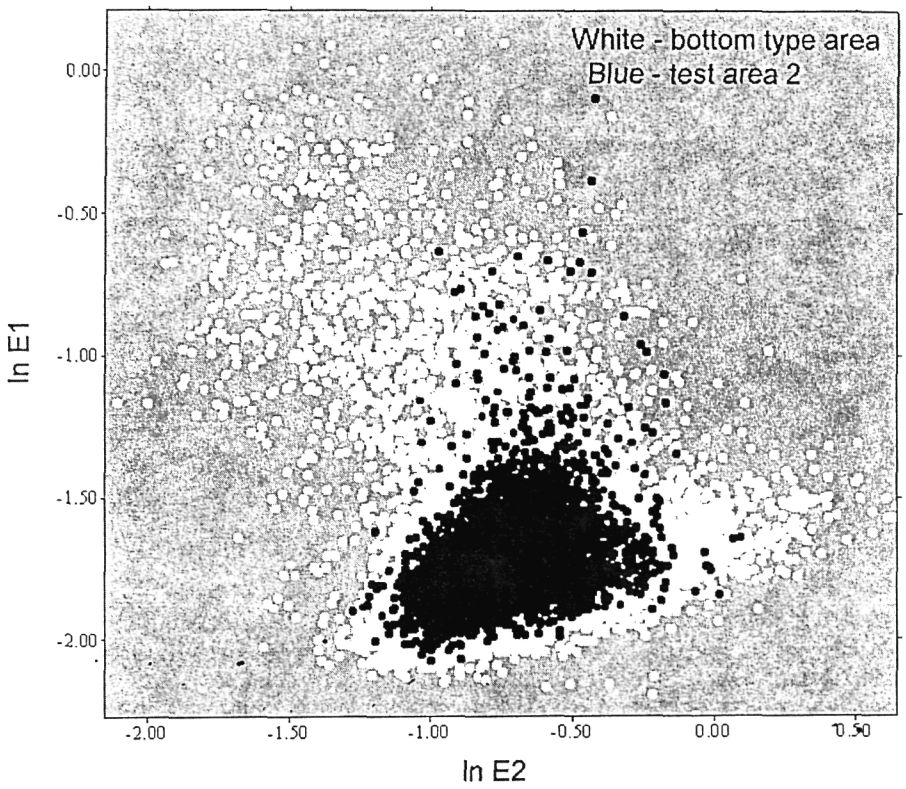


***Figure 3.*** *Overlap in 2D-feature space between mussel bottom type area and test area 2 in the 1996 field campaign in Øresund.*

## Variability and stationarity of $E_1$ and $E_2$

The influence of the exogeneous variables measured on $E_1$ and $E_2$ has been analysed. Concentrations of suspended matter were practically constant during the field campaigns, thus having no influence on the measurements (Madsen, in prep.). This was the case for salinity too. Among the exogeneous variables depth was singled out as a factor to be given

some attention. A series of analyses of variance, employing various models of the two factors bottom type and depth and their interaction, were conducted. The overall impression of the results is that, based on the datasets from the 1996 field campaign, the RoxAnn measurements and the water depth is not very strongly dependent, $E_2$ being slightly more dependent on depth than $E_1$ as expected (Schultz et al., in prep.).

Another important finding, which is only reported qualitatively at present, is that the RoxAnn recordings cannot be regarded stationary, neither in space, time nor for a fixed calibration. That is to say, that the variation from survey to survey is substantial and necessitates that the classifications of data in feature space be conducted on a survey to survey basis. Furthermore, the lack of stationarity of $E_1$ and $E_2$ is considered to render absolute values incomparable from survey to survey; thus, it is recommended to refrain from interpretation of absolute values of $E_1$ and $E_2$, and to use relative values only, i.e. relative to the current classification in feature space. Other studies support this finding, e.g. Gensane concluded that echo sounder signals backscattered by separate areas containing the same bottom type hardly can be regarded as stationary (Gensane, 1989).

## Ground truthing

The still photos and video recordings made in intersection grid points respectively along every 5$^{th}$ transect were used to check the classifications in feature space of the RoxAnn measurements. The inspection of ground truthing proved crucial to the success of data processing when it was found that a part of the eelgrass bottom type in Øresund actually consisted of sand beds, which is expected to resolve some obstacles in the classification analyses. Aerial flight photos available for the Eelgrass bottom type have been used for verification as well, with good results. Therefore, as a general finding, it is stressed, that ground truthing is considered an indispensible requirement for ensuring the reliability of the derived sea bottom maps (Madsen, in prep.). Figure 4 depicts a frame from a transect video in test area 1 in Øresund, an area containing a mix of mussel, sand and eelgrass at the sea bottom.

## Design of hydroacoustic surveys

The experience gathered in the BioSonar suggests that a two-step approach be applied for surveys of larger, unknown areas. The first step would consist of a survey traversing the area to be monitored at large, using a low to medium transect density; one of the subsequent uses of the collected data would be to identify or at least indicate subareas being entirely covered by one of the distinct bottom types anticipated to be present within the survey area. In the second step the bottom type subareas are monitored with a high sampling density, and the larger survey area is covered by a transect grid allowing high sampling densities in localised subregions containing interesting features, e.g. locations where the data from the first step


***Figure 4.*** *A frame from a ground truth video from a transect in test area 1.*

indicate a high degree of mixing of bottom types. This approach is suggested for preparation of baseline inventories of benthic communities, whereas a slightly different approach might be favorable where change detection is the primary aim.

For change detection a number of relatively small subareas of the survey area can be chosen, either at random or by use of some systematic scheme, and combined with a selection of distinct bottom type areas. These small subareas are then sampled at a very high sampling density - in the simplest design at two time points labelled "before" and "after" - and then analysed using a repeated measures design, where the statistics are compared on a subarea basis collecting the differences for every subarea in a collective change detection statistic (Sørensen, in prep.).

These design recommendations in both cases entail that subareas identified or indicated as containing one distinct bottom type are essential parts of any hydroacoustic survey aiming at mapping of benthic communities at larger scales.

## Possible ambiguity of the $E_1$ scale

The integrated part of the first backscatter, $E_1$, is usually interpreted as roughness. As mentioned this corresponds well with the good separation found along the $E_1$ axis of sand, mussels and eelgrass. Roughness can be thought of as a measure of the basic grain size of the sea bottom texture. For sand as a bottom type the typical grain size (of a sandparticle) is approx. 0.5-2 mm, the size of a mussel is 5-7 cm, and the typical grain size of eelgrass is 1 metres, say.

However, in the present case this interpretation of the success of the classification in feature space indicate the limitations of the approach too. Henceforth, if the interpretation is valid the roughness scale, $E_1$, will confuse benthic communities and patterns at the same characteristic scale or grain size, e.g. mud with sand, pebbles and stones with mussels and algae and other seaweeds with eelgrass. Therefore, it will in general not be valid to aim at the detailed mapping of a range of species having overlapping grain sizes using RoxAnn, except in cases not covered by our studies where $E_2$ might contain the sufficient supplementary information.

## Options for improvements and handling of obstacles

A number of problems related to RoxAnn were pointed out in this presentation, two of the most important being that only $E_1$ was found relevant for classification of the bottom types studied and the lack of stationarity of $E_1$ and $E_2$. One way of solving some of the problems would naturally be to acquire a more advanced hydroacoustic device. However, the lack of stationarity will probably be inherent for hydroacoustic measurements due to the vast amount of factors influencing the measurement process, wherefore it might be more promising to focus on the filtering of the measured signal.

An number of alternatives to $E_1$ and $E_2$ as aggregated values are reported in the literature, thus providing the potential for a feature space of a higher dimension. However, it could be advantageous to filter the unaggregated, raw signal, e.g. based on the frequency domain, similar to methods suggested for side scan sonar data (Pace & Dyer, 1979; Tamsett, 1993).

It might prove useful and yield more realistic results to include a sort of unmixing process (Bettle & Drake, 1993) to the resulting maps of the the bottom type classes within a surveyed area, thus allowing for spatial coordinates to be partially classified within several classes (Sørensen, in prep.).

Finally, it is emphasized that ground truthing from independent data souces is an indispensable requirement for hydroacoustic surveys to produce reliable results, and furthermore, that it is essential that the design of a survey contains a procedure whereby subareas containing distinct bottom types are identified and sampled to be used for classification purposes.

## Acknowledgements

We would like to acknowledge the kind support from the MAST office of the European Union for the BioSonar project, contract no. MAS3-CT95-0026. Furthermore, we would like to acknowledge the support from The Danish Øresund Consortium (Øresundskonsortiet A/S), for providing data for use in the initial phase of the project.

## References

Chivers, R.C., Emerson, N. and Burns, D.R. (1990): New Acoustic Processing for Underway Surveying. The Hydrographic Journal Vol 56, April 1990, pp. 9-17.

Chivers, R. & Burns, D. (1992): Acoustic surveying of the sea bed. Acoustics Bulletin, Vol. 17(1), pp. 5-9.

Conradsen, K. *et al.* (1998): Sonar Technology for Monitoring and Assessment of Benthic Communities (BioSonar). To be published in the 1998 MAST Conference Volume

Conradsen, K. (1984): En introduktion til statistik, 1a, 1b, 2a og 2b (In Danish). Institute of Mathematical Statistics and Operations Research, Technical University of Denmark, Lyngby.

Cressie, N.A.C (1991): Statistics for Spatial Data. John Wiley & Sons Inc., New York.

Gensane, M. (1989): A statistical study of acoustic signals backscattered from the sea bottom. IEEE Journal of Oceanic Engineering, Vol. 14/1, pp. 84-93.

Heald, G.J. & Pace, N.G. (1996): An analysis of the 1st and 2nd backscatter for seabed classification. Proceedings of the 3rd European Conference on Underwater Acoustics, 24-28. June 1996, Vol II, pp. 649-654.

Isaaks, E.H. & Srivastava, R.M. (1989): An Introduction to Applied Geostatistics. Oxford University Press, New York. 561 pp.

Madsen, K.N.: Discrimination of Blue Mussel (Mytilus edulis) by means of Underwater Acoustics. In preparation.

MAS3-CT95-0026 (1998): Scientific Report for Year 2 of the BioSonar Project. Report prepared by the BioSonar project partners to the MAST Office of the European Union.

MAS3-CT95-0026 (1997): Scientific Report for Year 1 of the BioSonar Project. Report prepared by the BioSonar project partners to the MAST Office of the European Union.

Pace, N.G. & Dyer,C.M. (1979): Machine classification of sedimentary sea bottoms. IEEE Transactions on Geoscience Electronics, Vol 17/3, pp. 52-56.

Schultz, N. *et al.*: Sea floor segmeantation using the RoxAnn echo sounder. In preparation.

Settle, J.J. & Drake, N.A. (1993): Linear mixing and the estimation of ground cover proportions. International Journal of Remote Sensing, vol. 14/6, pp. 1159-1177.

Sørensen, P.S.: Models of spatial patterns and their use in a geostatistical framework. In preparation.

Tamsett, D. (1993): Sea-bed characterisation and classification from the power spectra of side-scan sonar data. Marine Geophysical Researches, Vol. 15, pp. 43-64.

# RECENT SLOPE FAILURES AND MASS-MOVEMENTS IN THE NW MEDITERRANEAN SEA

S. Berné[1], M. Canals[2], B. Alonso[3], , B. Loubrieu[1], P. Cochonat[1] and the "BIG 95" and "CALMAR 97" shipboard parties

1: IFREMER Brest, DRO/GM, BP 70, 29280 Plouzané, France, sberne@ifremer.fr; ** 2: Universitat de Barcelona, GRC Geociències Marines, Facultat de Geologia, Zona Universitària de Pedralbes, E-08071 Barcelona, Spain. 3: Institut de Ciències del Mar, CSIC, Avgda. Joan de Borbó s/n, E-08039 Barcelona, Spain.**

## ABSTRACT

Two recent investigations in the Western Mediterranean Sea have evidenced recent slope failures and related deposits, thanks to the use of swath bathymetry and very high resolution seismic techniques. On the Ebro margin, swath bathymetry and bottom parametric seismic profiling reveal recent scars cutting across the upper continental slope, and related slided deposits on the lower slope and Valencia Channel. On the western Rhone margin, a large (>75 km3) debris flow has been identified. Its origin is both on the shelf break (with scarps more recent than ca. 22, 000 years BP cutting across Last Glacial Maximum Lowstand shoreline), and on the upper part of the western flank of the Rhone deep sea fan.

## INTRODUCTION

In the Western Mediterranean Sea, catastrophic events that cut telephone cables have been reported in modern times, e.g. the failure event off Nice in 1979 (Gennesseaux, et al., 1980; Malinverno, et al., 1988) or the large turbidity currents induced by the 1954 and 1980 earthquakes offshore El-Asnam (previously named Orleansville, Algeria) (El Robrini, et al., 1985). A few millennia old, major landslide-derived deposit, tens to hundred $km^3$ in volume, has been also reported on the western flank of the Rhone Deep-Sea Fan (Droz and Bellaiche, 1985; Méar, 1984; Torres, 1995). Recent investigations (respectively in 1995 and 1997), have mapped similar deposits on the Ebro and Rhone margins (**Figure 1**). Using various newly developped high and very high resolution geophysical techniques, these surveys have identified and mapped recent debris flows, in the Valencia Gulf (Canals and Alonso, 1996) and on the lower slope and rise of the Gulf of Lions-Rhone neofan transition zone (Loubrieu and Berné, 1998). In the Balearic abyssal plain, a megaturbidite has been mapped by Rothwell et al. ( et al., 1998). The emplacement of this bed is dated back to 22,000 calendar years, i.e. during Last Glacial Maximum.

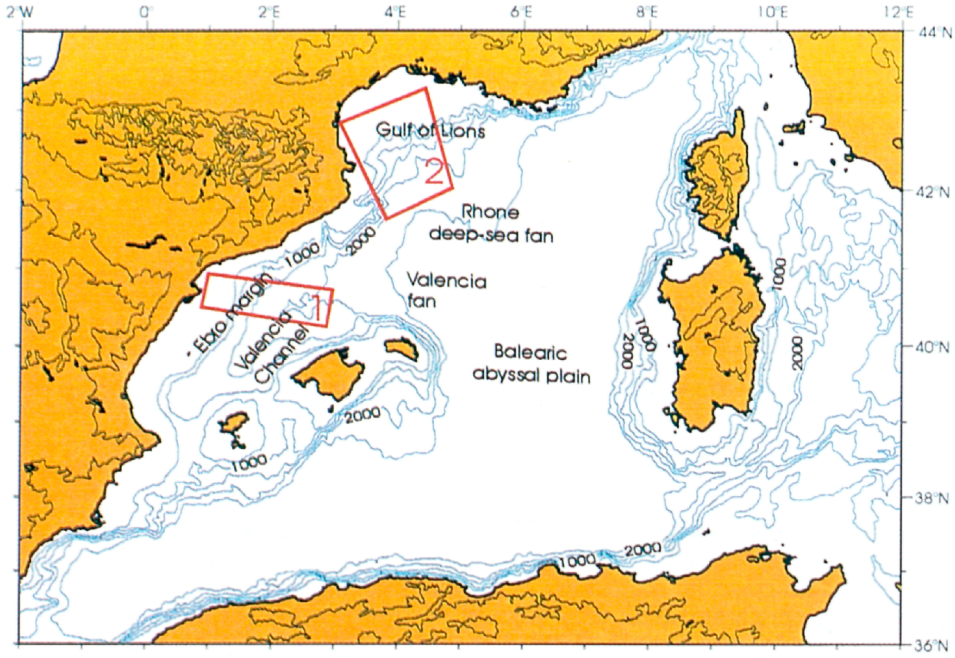


Figure 1: Position of the two studied areas in the Western Mediterranean Sea

## 1- THE EBRO MARGIN

The BIG'95 cruise of R/V Hesperides in 1995 allowed the mapping of a large slide scar and deposit, off the Ebro shelf (**Figure 2**). It extends from the prograding Ebro shelf break down to 1800 m water depth. A rough, distinct topography, very apparent on swath maps, characterises both the scar and the surface of the deposit, which forms a seismically transparent layer that buries the former sea-floor topography and partly fills the uppermost course of the Valencia mid-ocean type channel, opening between the Iberian and Balearic margins, in the Valencia Gulf. A horse tail structure appears on back scattering images, that corresponds to shallow, converging channels separated by segments with a blocky texture. Individual blocks have been measured to be as high as 35 m over the surrounding sea-floor. The mean thickness of the deposit is around 15 ms, with local maximum of 40 ms. The overall area affected by the slide covers about 1.300 $km^2$, with a maximum width of 30 km between 1400 and 1600 m water depth. Its volume has been estimated to be around 26 $km^3$.

### General setting

The North-Western Mediterranean Sea was the study area of the MAST II, Mediterranean Targeted Project I - EUROMARGE-NB Project, and is one of the key sectors being investigated into the Mediterranean Targeted Project II - MATER. Terrigenous, carbonate and mixed margin types coexist. These margins are incised by various kinds of submarine valleys, often forming

hierarchized patterns. Additionally, a noticeable mid-ocean valley type develops between the Iberian margin and the Balearic promontory, following a SW-NE direction : the Valencia Channel (Alonso et al., 1995). Submarine valleys can be either related to tectonic controls, like La Fonera and Blanes canyons, or to submarine sedimentary processes, like most of the canyons in the slopes of the Gulf of Lions and the Ebro margin. These two margins, dominated by the inputs of the Rhone and Ebro rivers, are clearly progradational. While the Rhône margin has been intensively studied during the last years with respect to the detailed morphosedimentary features and recent sedimentary processes (see the compilation in Torres, 1995), much less detailed work has been done till now in the Ebro margin.

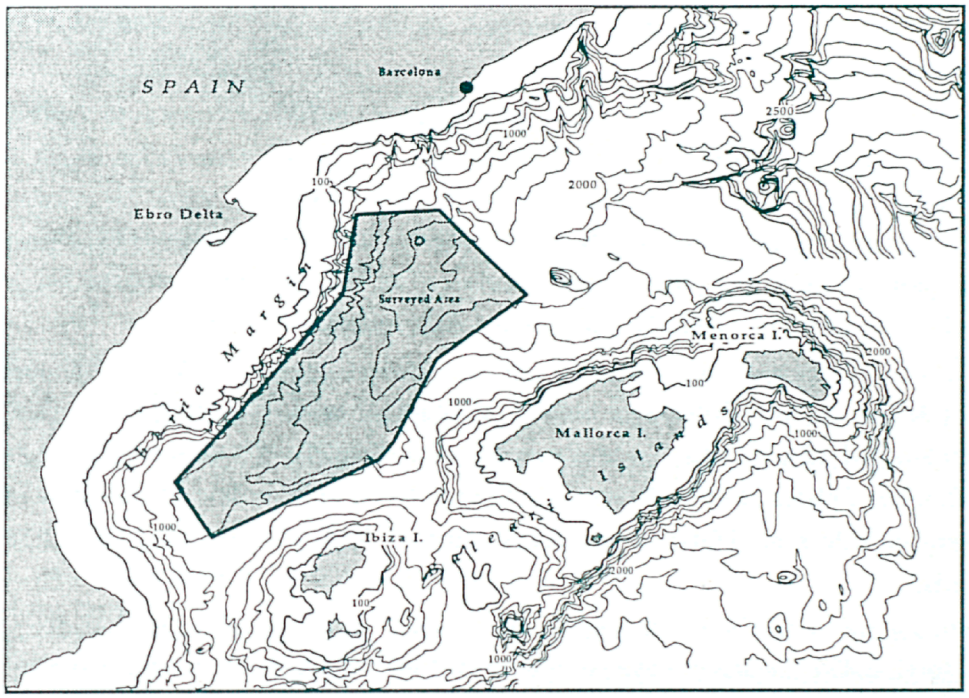


Figure 2: Position of the BIG 95 survey

The Ebro margin constitutes the western flank of the Valencia Valley, whose axis is entrenched by the above mentioned Valencia Channel. The eastern flank of the Valencia Valley is formed by the North Balearic margin.

The Balearic margin is defined by a steep continental slope and base-of slope, the absence of modern major tributaries, the carbonate nature of sediments and the lack of major river inputs. These features contrast with those of the Catalan, or Ebro continental margin, which is defined by a gentle slope, turbiditic channels cutting the slope and base-of-slope, and the terrigenous nature of

the sediments from the Ebro river. The progradational architecture of the Catalan margin is controlled by the influx of terrigenous sediments, amongst other parameters like sea level fluctuations (Field and Gardner, 1990).

In relation to the instability processes in the margins, previous works have reported significant slumps and slides in the slope of the Gulf of Lions (Canals, 1985), but only small sediment failures in restricted areas of the Catalan continental margin have been reported (Alonso et al., 1991; Field and Gardner, 1990) . These were identified by means of geophysical techniques of intermediate resolution. To this point, it is important to emphasise that at present the recent technological developments for high and ultra-high resolution sea-floor reconnaissance ( wath bathymetry, imagery and Bottom Parametric Source) allow sea floor investigations with unprecedented resolution.

**Data set**

This study is based on the combined analysis of different types of high and ultra-high resolution geophysical techniques obtained in the cruise BIG 95 made onboard BO Hesperides and covering the deep basin between the Catalan and the North Balearic margins.

The following tasks have been carried: a) acquisition of full coverage sea-floor mosaic with the multibeam EM-12S system, 2) simultaneous recording of very high resolution seismic profiles with the Benthec Subsea Bottom Parametric Source BPS, 3) recording of sea-floor images with the towed deep-sea side scan TOBI in key areas selected from the previously acquired EM-12S and BPS records.

In total, 2.472 linear km have been recorded with the EM-12 swath system, covering 1 2.357 $km^2$ of the sea-floor. These data have a volume of 2,5 Gb. Various shaded colour relief images and backscattering images, totalling 10 additional Mb, have been derived form the EM-12 data. The same amount of lineal km of BPS records has been acquired and recorded in 5 optical disks totalling about 300 Mb. The total length of TOBI profiles is 699 km, representing a coverage of 4.198 $km^2$.

**Results**

***Mass wasting features***

Morphology

The BIG 95 slide, off the Ebro shelf, fits into a geographical frame limited by the following coordinates: 39.5N to 40.3N, and 01.0E to 02.0E. It is to be noted that the following paragraphs are

dedicated to the description and interpretation of this huge slide although other and smaller ones have been also identified in the Ebro slope.

The BIG 95 slide general shape is rectangular (40 x 30 km), W-E oriented, with a horned termination at its shallowest part (head of slide), over the Ebro continental slope, and a long narrow arm, SW-NE oriented, following the axis of the Valencia Channel.

The surface covered by the central body of the slide is about 1300 $km^2$. The arm entering the Valencia Channel is 40 km long. The area where the slided mass is deposited goes from at least 1000 m down to 1800 m in the most distal part of the Valencia Channel. The maximum width of the slide, from 1400 to 1600 m depth, is about 30 km.

The sea-floor roughness is distinctive of the area where the slided mass is deposited, as seen in the detailed swath bathymetry chart. The top surface of the slided mass can be either blocky, mostly in the upper and intermediate part, or flat, mostly in the lower, distal part, before entering the incised axis of the Valencia Channel. Individual block heights can be up to 35 m, with 25 m height as average.

The headwall scar and upper reaches of the slide show complex interactions between mass wasting and slope channel dynamics. The southern limit of the uppermost part of the slided mass is formed by a channel that benches downslope and then disappears under the slide deposit.

Geometry

The lateral northern boundary of the slided mass is located at the lower reaches of the Ebro slope and masks the pre-existing topography. Locally the top of the slide deposit at its northern boundary presents convex morphologies. The southern boundary is always located at a lower bathymetric level and terminates against the base of the North Balearic slope.

The slided mass shows a basal irregular erosional surface below the upper and intermediate parts which becomes flat under the distal part. In a downslope direction, the basal surface of the slided mass evolves from concave, near the headwall scar, to irregular, in the intermediate part, and to smoothed, at the deepest distal part.

The slided mass clearly fills partly the incised Valencia Channel where it is apparent in the bathymetry. The obliteration of a former uppermost course of the Valencia Channel cannot, however, be excluded, although its eventual presence into the irregular basal area makes difficult its recognition.

The distribution of the thicknesses of the slided mass seems to be related with the two types of surficial roughness formerly mentioned (blocky and flat). In blocky areas, the thickness varies significantly from place to place, between 10 and 38 ms, thus paralleling the irregular, blocky top surface. It becomes more constant and smaller in the flat, deeper zones, from 10 to 20 ms. In the southernmost sector of the slided mass, thicknesses are always smaller than 10 ms. Along the NW-SE arm filling the Valencia Channel, there is an upper segment with 35 to 20 ms, and a lower segment with thicknesses less than 20 ms. The volume of the overall slide deposit has been estimated to be around 26 $km^3$.

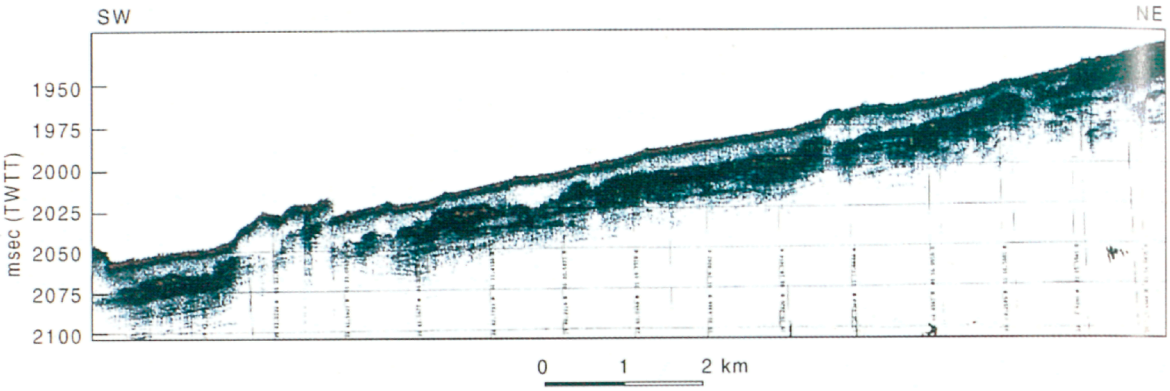


Figure 3: Bottom parametric Source profile cutting the western reaches of the BIG 95 slide. The upper unit, corresponding to the slided mass, has a transparent character which is attributed to the destruction of the initial internal structure. Also note the erosional nature of the bottom of the slided mass.

Seismic facies

The seismic facies of the whole BIG 95 slided mass in the BPS records is transparent. This facies allows to differentiate undoubtedly the sediment body over and against its lower and lateral boundaries, which are characterised by stratified facies (Figures 3 and 4).

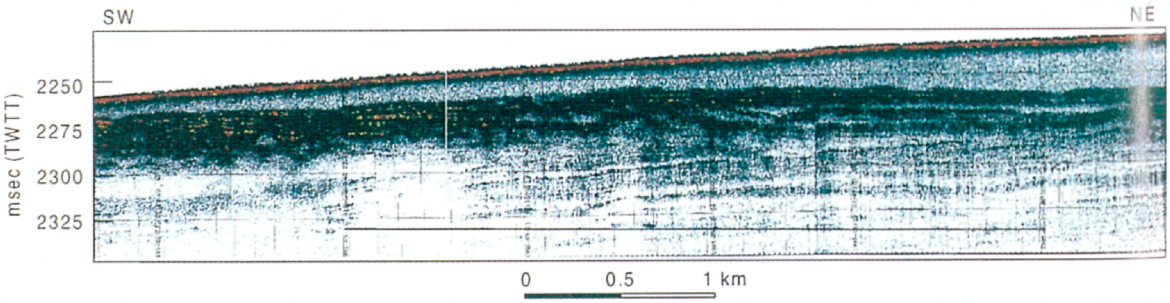


Figure 4: Bottom parametric Source profile cutting the western reaches of the BIG 95 slide

Recent sedimentary processes

One of the diagnostic features of the slided mass is the presence of abundant, sub parallel flow lines on the backscattering imagery. These flow lines spread from the headwall area, reach their maximum development coinciding with the widest area of the slided deposit, and finally converge towards the uppermost incised course of the Valencia Channel.

Downslope, the flow lines initially follow a NW-SE direction to sharply change to a SW-NE direction, later followed by the partly filled upper course of the Valencia Channel.

As revealed by the merging of deep tow side scan and sea-floor backscattering data, these flow lines correspond to slightly sinuous channels between the blocks featuring the blocky terrain described above. These slide channels are not connected with slope turbidite channels. Nor the slide channels, nor the blocks are obliterated by later deposits. These characteristics, together with the fresh appearance of the morphological elements (slide scar, top surface of the slided deposit) linked with the slide demonstrate that it is the latest major sedimentary event in the area.

*Slope channel systems*

Morpho-sedimentary features

The merging of swath bathymetry and deep tow side scan data allows to identify the morphological features of the various slope channels in the Ebro margin, from 600 to 1800 m of water depth. The different morphological elements reveal the recent processes affecting the evolution of the slope channel systems and, hence, of the overall slope.

According to the size of the many slope channels identified, five of them are of major significance. These have been named 1 to 5, from south to north. The channels cross the continental slope and fed the base-of-slope environments, where they form channel-levee complexes. The path of the channel segments goes from straight to sinuous to meandering. The length of the channels is up to 50 km, with their amplitude ranging from 0.3 to 1.5 km. Their entrenchment into the slope sediments varies from place to place, locally reaching up to 90 m. Asymmetry of the channels walls is the rule. The cross profile of the slope channels evolves from V shapes in the upper course to U shapes in the lower course.

Channel 1, in the southern part of the study area, becomes progressively narrower and less entrenched, finally disappearing on the base-of-slope. By the contrary, those in the northern half of

the Ebro slope (channels 2 to 5) tribute into the SW-NE Valencia Channel. The two groups of channels are separated by the area occupied by the BIG 95 slide deposit.

The detailed analysis of the morphology of the channels reveals that different types of **erosive-depositional processes** have been active in recent times. These are:

- *Misfit channels:* a misfit channel is one whose meanders do not fit the size of the main channel into which it is presently flowing. That is, the meanders of the present inner channel are smaller in amplitude and more intricate than the bends in the major channel walls. Misfit inner courses reveal thalweg erosion and, possibly, reduction in the volumes of sediment flowing along a former main channel. They can also develop because of the softness of the sediments filling the main channel after a major transport and deposition event.

- *Incised meanders:* they form when the winding channel of a stream is cut deeply into the surface. Incision occurs when there is a change in the environment causing renewing of downcutting. Erosion concentrates in the concave part of a meander, while in the convex side deposition or non-erosion prevails. Eventually, hanging abandoned meanders, or ox-bows, can result from meandering incision, as well as lateral terraces. Some channel walls show extremely tight curvatures, with cuspidate forms and curvatures forming semicircular wall scars. Small gullies locally develop upwall.

- *Captures:* retrogressive erosion of the head of and existing channel can led to the capture of a second channel, thus drastically modifying the downslope transport pattern. This process has been observed in channel 5, where upslope retrogressive erosion from a branch connected to the Valencia Channel has caused the capture of a former channel which did not reach the Valencia Channel before the capture occurred.

- *Hanging valleys:* they develop when the base level of the recipient channel is deepened because of axial erosion. Then, former tributary valleys become hanging valleys, separated by a morphological step from the main valley they open to. This has been observed in channel 4, separated by a100 m high step from their merging with the Valencia Channel, as well as in other minor channels.

- *Avulsions:* channels in channel-levee complexes are flanked by lateral levees. The occasional break of a levee can give place to the formation of a new channel and to the abandonment of the pre-existing one. Avulsion processes have been also observed in the slope channels of the study area.
- *Braided patterns:* meandering starts with local bank erosion and then deposition, and perhaps braiding begins in the same way. However, the obvious origin seems to be the appearance of a mid-

channel bar. This bar grows downstream and may even be built up vertically. Downcurrent transportation shadows then aid in trapping finer material. Progressive changes take place linked to current deflection against the sidewalls of the channel, causing erosion and formation of new bars. A braided stream is characterised by the general instability of the bars and channel ways and by caving of the channel walls. Braided patterns are well developed in the upper course of the Valencia Channel, between 1700 and 2000 m of water depth, where it has an amplitude of about 2 km.

## 2- The western Rhone margin

In November 1997, a complete swath mapping (Simrad EM 12D) of the Western Gulf of Lions slope and rise (water depths comprised between 150 and 2200 m) was carried out by "L'Atalante" together with sub-bottom and seismic profiling, and piston coring. This cruise named "CALMAR" (CAtalano-Languedocian MARgin) is part of a larger project dedicated to the integrated study of sedimentary processes and sequences in the Gulf of Lions. One particularity of this project is to examine the entire margin, from the coast line to the deep sea (**Figure 5**). A first requisite was the availability of a digital terrain model (DTM) covering the entire study area. For the areas deeper than 150m, three swath bathymetry surveys, including the 1997 "CALMAR" cruise, were utilised. In total, more than 40 days with "Jean Charcot" and "L'Atalante" were necessary for the complete coverage of an area more than 100 000 $km^2$ in surface. The shelf (water depth 0-150m) is relatively well developed in the Gulf of Lions, by comparison with the adjacent Provencal and Catalan margin. A complete coverage with swath bathymetry would require more than 400 days of ship time. Thus, the strategy was to compile sounding charts of the French Hydrographic Service at scales of 1/10,000 and 1/20,000. After manual interpretation, these maps were digitised and DTMs were produced at various scales (nominal grids of 50 m x 50 m). Some areas of specific interest were surveyed with a shallow water SIMRAD EM950 swath bathymetry system installed on the R/V "L'Europe", utilised simultaneously with a high frequency side scan sonar and a high resolution seismic source.

One of the objective of the project, to be achieved in 1999, is to obtain a set of detailed morpho-bathymetric maps (1/20,000 to 1/100,000) and DTMs, covering water depths comprised between 1 and 2200m. Several products may be derived from these data, including 3D views, slope or "roughness" maps, of particular interest for determining recent sediment processes and pathways. Some results of this "integrated" study of the continental margin, mainly based on the "CALMAR" and adjacent data, are presented hereafter. It must be emphasised that the data base, here employed for the study of sedimentary processes, may have several other uses for physical oceanography, management of sea resources and Geographic Information Systems.

### The shelf break

On the shelf, the new data reveals sediment bulges connecting present (highstand) outlets of several streams to some of the canyons cutting across the shelf edge. This is the case, in particular, for the Petit-Rhône, Herault, Aude and Lacaze-Duthiers canyons. These sediment bulges are interpreted as remnants of depocenters associated with streams flowing from the Alps, the Massif Central and the Pyrénées (Rhône, Herault, Aude, Agly, respectively). As the post-glacial

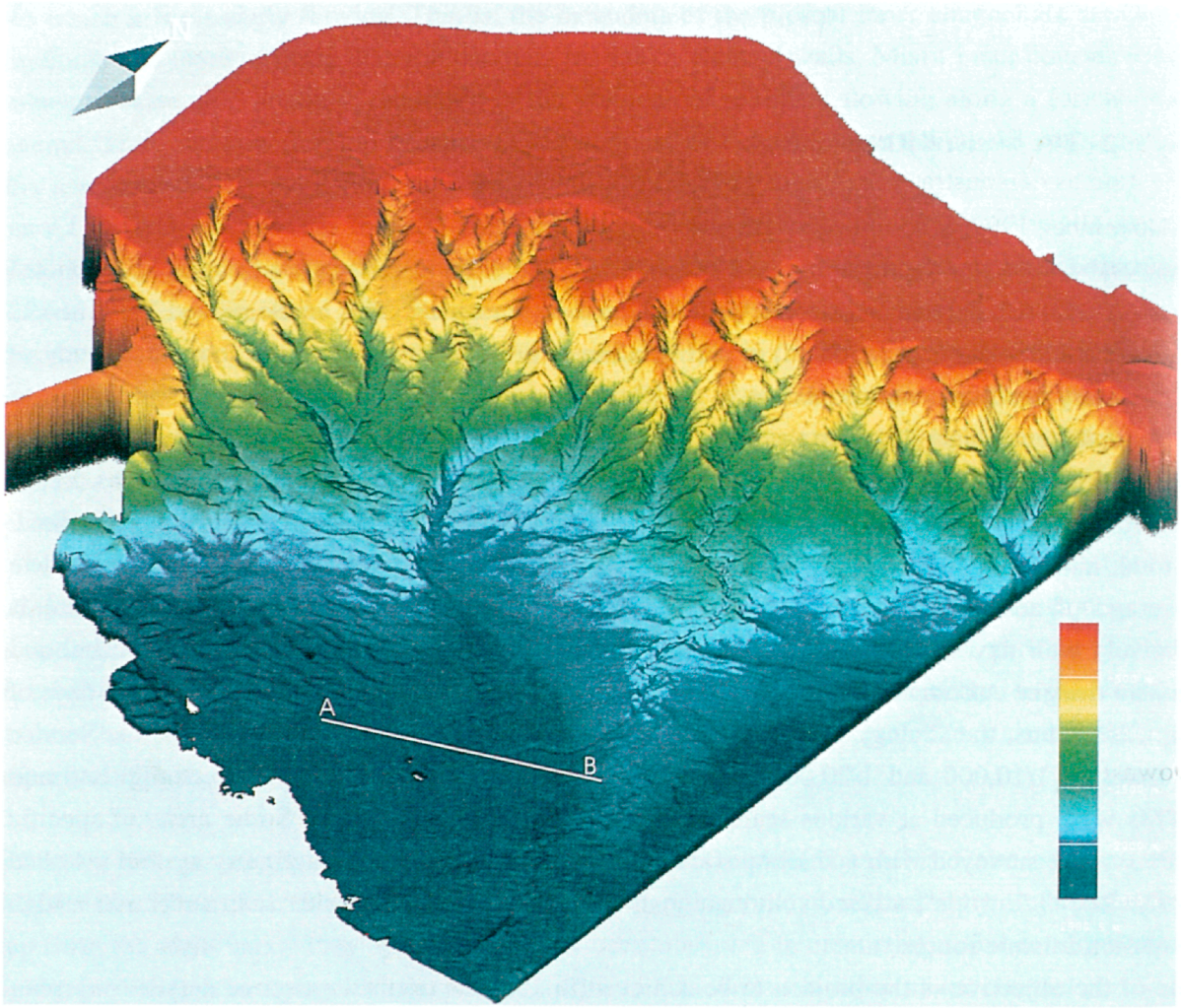


Figure 5: 3D view of the western Rhone shelf, slope and rise. Note the shape of the sedimentary ridge to the SW, and the Rhone deep sea fan to the SE. The avulsion of the Rhone deep sea fan channel is clearly visible. AB gives the position of Figure 6.

transgression proceeded, these streams retrograded, depositing sediments which were eventually reworked into transgressive deposits whose position roughly indicates the retreat path of streams during the sea-level rise. The retreat path of the Rhone is particularly well preserved, and demonstrates that, during the last lowstand and transgressive period, this stream had tributaries flowing toward the Petit Rhone canyon and also the Marti canyon, and possibly the Herault canyon. The course of these paleo-rivers is well evidenced on gradient maps, were some sinuous slope anomalies indicate the position of preserved meandering channels clearly visible on high resolution side scan sonar images.

**Canyons**

Canyons are Plio-Quaternary features, some of them having recently migrated in a SW direction as demonstrated by 3D mapping and seismic strike sections showing the shifting of buried High Amplitude Reflections (HAR) in this direction. However, some canyons, especially the Lacaze-Duthiers Canyon, are established within larger depressions corresponding to canyons incised during the Messinian lowstand(s). A striking feature is the presence of minor channels within the main course of several canyons, these channels being generally connected to upper-slope scars . Some of these scars truncate lowstand shorelines which have been dated to the Last Glacial Maximum (Berné, et al., 1998; Rabineau, et al., 1998). As a result, the minor courses of the canyons must have been created -or rejuvenated- more recently than 22, 000 y. B.P. The Sète Canyon appears as a major feature, capturing Cap de Creus, Lacaze Duthiers, Pruvôt, Aude, Hérault and Marti canyons.

**The Pyreneo-languedocian sedimentary ridge**

Downslope, immediately SW of the main canyon system drained by the Sète canyon, a large sediment body has been mapped. Firstly noticed by Got and Stanley (1974), it was named Pyrenean Canyons Deep Sedimentary Body (PCDSB) by Canals (1985), Canals and Got (1986) and Alonso et al. (1991). Our detailed investigation reveals that it is more than 0.8s twt in thickness. Its internal structure exhibits lobate morphologies suggesting channel/levee systems, with High Amplitude Reflections (HAR). It is covered with sediment waves spaced 2.5 km apart, with their lee side facing upslope. We interpret it as a sedimentary ridge similar to the Var sedimentary ridge (Gennesseaux and Rehault, 1977) .

**Large debris flow**

Swath bathymetry, acoustic images and sub-bottom profiling allow the identification of a large debris flow on the lower slope and continental rise of the study area. On sub-bottom profiles, this

unit is characterised by a relatively transparent facies (**Figure 6**) similar to that of the BIG 95 debris flow, very distinct from the well-stratified acoustic facies of the Pyreneo-languedocian sedimentary ridge or of the Rhône deep sea fan. The corresponding Simrad EM 12D data has low backscattered image, as observed on other debris flows to the west of Corsica and on the Celtic Sea fan (Unterseh, et al., in press). This debris flow extends beyond the southern limit of the surveyed area, namely N41°30' (Figure 7). It has an average thickness of about 30 ms and an average width of 25 km. Therefore, the volume of the mapped portion of this debris flow is more than 75 $km^3$. Some faint internal reflections suggest that this unit could be the result of several mass-wasting episodes. Two indirect ways allow to propose a time interval for the deposition of this sedimentary unit: (a) the debris flow is overlained by the Rhône neofan, which is supposed to be Holocene in age (Méar, 1984; Torres, et al., 1997); (b) slump scars along the shelf break, directly connected to the debris flow through incised channels (see above), cut across "shelf-perched lowstand wedges" dated from the Last Glacial Maximum (Berné, et al., 1998). This allows to propose a time interval of about 20,000-10,000 y. B.P. for the deposition of the debris flow.

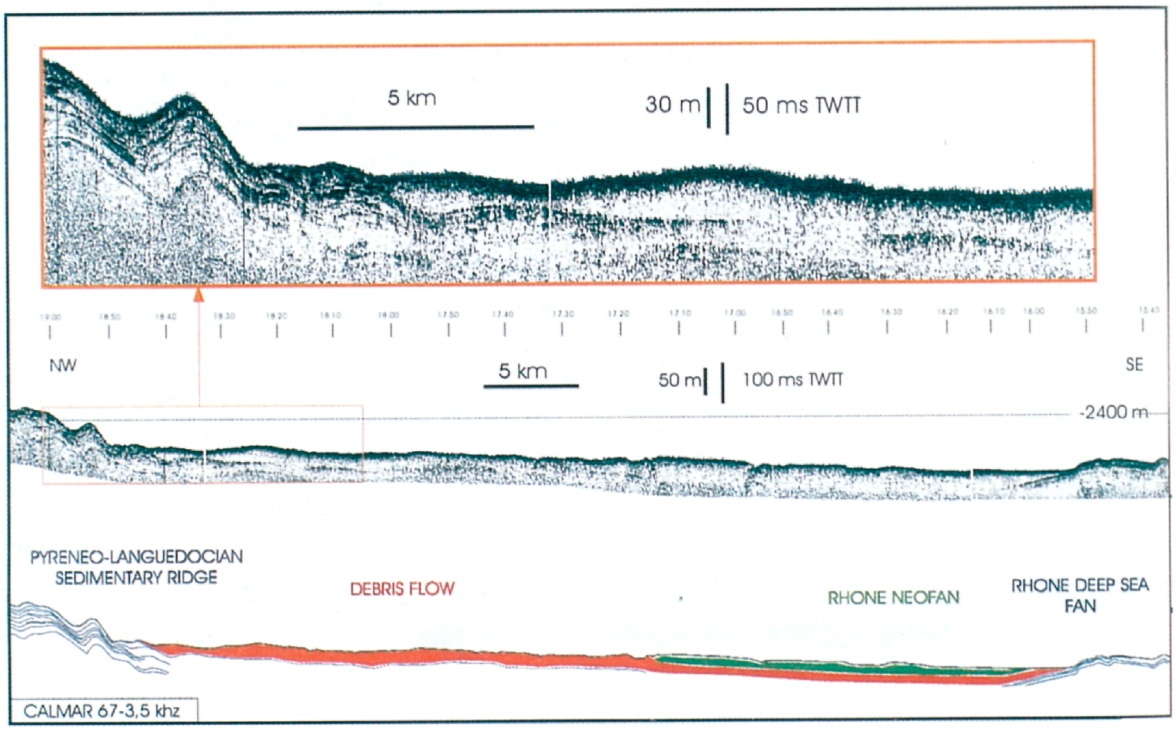


Figure 6: Mud penetrator profile across the continental rise in the CALMAR area (position in figure 5). Note the similarity between the transparent acoustic facies in the BIG 95 and CALMAR areas.

## Erosion of the shelf and slope as a source for deep sea sediments

It has been shown that direct connection of the streams to the canyons existed during the last lowstand. This provides an important source of material, including sand, for the recent deposits identified on the rise and in the basin. Furthermore, relict beach rocks dredged during "CALMAR" form topographic highs more than 20 m above the surrounding continental shelf. Because the sediment underlying the beach rocks has been deposited during Last Glacial Maximum, it can be inferred that large scale erosion of lowstand shorelines took place more recently than 20,000 y. B.P., very probably during the deglacial transgression. This provides an additional source of sediment, including sand, which was partly recycled into transgressive shelf sand bodies and partly transferred to the basin.

In addition to the large amount of sediment transferred from shelf erosion and fluvial output, a very large slump affecting the upper part of the western flank of the Rhône deep sea fan appears as another major source of sediment. The interpretation of swath bathymetry, backscattered images and sub-bottom profiles clearly shows that the large debris flow originates both from the Sète canyon (which represent the main "conduit" for sediment transfer in the Western Gulf of Lions) and from this slump scar.

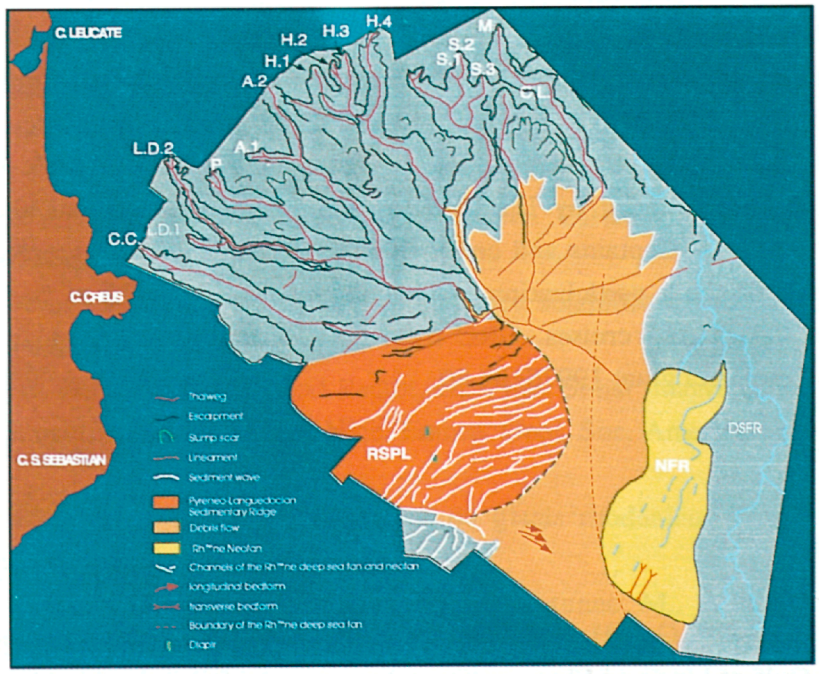


Fig. 7: Morpho-sedimentary interpretation of the CALMAR area based on the use of swath bathymetry and seismic data. CC: Cap Creus canyon; LD: Lacaze-Duthiers canyon; A: Aude canyon; H: Herault canyon; S: Sète canyon; M: Marti canyon; CL: Catherine Laurence canyon. RSPL: Pyreno-languedocian sedimentary ridge; NFR: Rhone neofan; DSFR: Rhone deep-sea fan

## SYNTHESIS AND CONCLUSIONS

There is no doubt that both debris flows from the Valencia Gulf and Gulf of Lions represent the most recent large sedimentary events in these two areas.

An important aspect in future studies will be to establish the exact timing (and possible synchronism) and origin of these sedimentary events, in relation with tectonic activity (seismicity and/or salt tectonism), changes in sea-level (and their effects on slope stability), hydrodynamical regime, physical properties of sediments and position of depo-centers. Regonial mapping would also be important for establishing possible geometrical and genetical relations with sedimentary events along the margin and the megaturbidite identified in the Balearic plain (Rothwell et al., 1998).

Beside the classical ways for dating marine sediments, the analysis of very well preserved outer shelf depositional sequences could be a way for determining the post-glacial history of slope mass-wasting in these two areas of the North-Western Mediterranean Sea. This will require high resolution (100-300m) drillings in areas of the outer shelf/upper slope, seaward of the lowest lowstand shorelines in interfluves not affected by slope failure.

## ACKNOWLEDGEMENTS

The study of the Ebro margin was partly funded by the European Community MAST 2 programme (EUROMARGE-NB project, MAS2-CT93-0053). GRC from the University of Barcelona is also funded by Generalitat de Catalunya grant 1997SGR-80. The CALMAR investigation has been funded by IFREMER, with financial and technical support from ELF Exploration Production. Captains and crews of R/Vs "L'Atalante", "Hesperides" and "L'Europe" are thanked for their active participation, as well as the scientific teams of the "BIG 95", "BASAR 1 and 2" and "CALMAR" cruises. GRC from the University of Barcelona is also funded by Generalitat de Catalunya grant 1997SGR-80.

## REFERENCES

Alonso, B., Canals, M., Got, H. and Maldonado, A., 1991. Sea valleys and related depositional systems in the Gulf of Lion and Ebro continental margin, AAPG Bull., 75, 1195-1214.

Berné, S., Lericolais, G., Marsset, T., Bourillet, J.F. and de Batist, M., 1998. Erosional shelf sand ridges and lowstand shorefaces: examples from tide and wave dominated environments of France. J. Sed. Research, 68, 540-555.

Canals, M., 1985. Estructura sedimentaria y evolución morfológica del talud y el glacis continentales del Golfo de León: fenómenos de desestabilización de la coberta sedimentaria plio-cuaternaria. University of Barcelona.

Canals, M. and Alonso, B., 1996. The BIG 95 mass wasting deposit and the slope channel systems in the Catalan Ebro margin. In: M. Canals, J.L. Casamor, I. Cacho, A.M. Calafat and A. Monaco, (Ed.), Euromarge-NB Final report, MAST III programme, Univ. Barcelona, 2, Barcelona, pp. 107-135.

Canals, M. and Got, H. (1986).- La morphologie de la pente continentale du Golfe du Lion: Une résultante structuro-sédimentaire; Vie Milieu, 36 (3): 153-163.

Droz, L. and Bellaiche, G., 1985. Rhône deep-sea fan: morphostructure and growth pattern. AAPG Bull., 69, 460-479.

El Robrini, M., Gennesseaux, M. and Mauffret, A., 1985. Consequences of the El Asnam earthquakes: turbidity currents and slumps on the Algeria margin (Western Mediterranean). Geo-Mar. Lett., 5, 171-176.

Field, M.E. and Gardner, J.V., 1990. Plio-Quaternary growth of the Rio Ebro margin, northeast Spain. A prograding-slope model. Geol. Soc. Amer. Bull., 102, 721-733.

Gennesseaux, M., Mauffret, A. and Pautot, G., 1980. Les glissements sous-marins de la pente continentale niçoise et la rupture des cables en mer Ligure (Méditerranée occidentale). C.R. Acad. Sci. Paris, 290, 959-962.

Gennesseaux, M. and Rehault, J.-P., 1977. La ride sédimentaire du Var: implications tectoniques et phénomènes sédimentaires liés aux marges continentales. Rapp. Comm. Internat. Medit., 24, 261.

Got, H. and Stanley, D.J., 1974. Sedimentation in two Catalonian canyons, northwestern Mediterranean. Mar. Geol., 16, 91-100.

Loubrieu, B. and Berné, S., 1998. CALMAR: preliminary scientific report. IFREMER internal report DRO/GM 98-01, Brest, 52p.

Malinverno, A., Ryan, B.F., Auffret, G. and Pautot, G., 1988. Sonar images of the path of recent failure events on the continental margin off Nice, France. Geol. Soc. America Special Paper, 229, 59-75.

Méar, Y., 1984. Séquences et unités sédimentaires du glacis rhodanien, thèse de 3ème cycle. Université de Perpignan, 223 p.

Rabineau, M., Berné, S., Le Drezen, E., Lericoalis, G. and Rotunno, M., 1998. 3D architecture of lowstand and transgressive Quaternary sand bodies on the outer shelf of the Gulf of Lions, France. Marine and Petroleum Geology, in press,

Rothwell, R.G., Thomson, J. and Kähler, G., 1998. Low-sea-level emplacement of a very large Late Pleistocene "megaturbidite" in the western Mediterranean Sea. Nature, 392, 377-380.

Torres, J., 1995. Analyse détaillée du transfert de sédiment du continent vers le bassin: le Quaternaire terminal au large du delta du Rhône (Méditerranée nord-occidentale). Unpublished PhD thesis, Bretagne occidentale.

Torres, J., Droz, M., Savoye, B., Terentieva, E., Cochonat, P., Kenyon, N.H. and Canals, M., 1997. Deep-sea avulsion and morphosedimentary evolution of the Rhône Fan Valley and Neofan during the Late Quaternary (northwestern Mediterranean Sea). Sedimentology, 44, 457-477.

Unterseh, S., Cochonat, P., Voisset, M., Ollier, G. and Harmegnies, F., 1998. Acoustic data ground truthing through in situ measurements of physical properties. In 8th International Offshore and Polar Engineering Conference Proceedings, ISOPE 98, Montreal, Vol. 3, 686-692..

# GAS HYDRATES AND SLOPE INSTABILITIES ON THE EUROPEAN NORTH ATLANTIC MARGIN (ENAM) AS INDICATED BY SEA FLOOR MAPPING AND DRILLING

J. Mienert[1], H.-P. Sejrup[2], H. Haflidason[2], T. Vorren[3], Jan-Sverre Laberg[3], A. Elverhoi[4a], C. B. Harbitz[4b], P. Bryn[5] and ENAM Partners

[1]GEOMAR Research Center, Wischhofstr.1-3, D-24148 Kiel
[2]University of Bergen, Department of Geology, Allegt. 41, N-5007 Bergen
[3]University of Tromsø, Institute of Biology and Geology, N-9037 Tromsø
[4a]University of Oslo, Department of Geology, Box 1047 Blindern, N-0316 Oslo
[4b]University of Oslo, P.O. Box 3930, Ullevaal Hageby, N-0806 Oslo
[5]Norsk Hydro AS, U&P Division, Postboks 200, N-1321 Stabekk

## SUMMARY

The European North Atlantic Margin (ENAM II) studies are to provide geophysical and geological observations on sediment instability, gas hydrates and major mass wasting events occurring on the continental slope from the Celtic Margin to the Norwegian Margin. Over 10,000 km$^2$ side scan sonar coverage and high frequency seismic profiles were obtained in selected areas. The determination of the timing, causes and flow processes of mass wasting events associated with gas hydrates and margin instability will provide detailed knowledge about the spatial and temporal variability of marine systems from the shelf edge to the slope, which clearly also has relevance for the offshore industry in designing platforms and infrastructures. The target areas presented are at the Traenadjupet and Storegga Slides on the passive Mid Norwegian Margin. This appears to be a natural laboratory for the interaction between gas hydrates and slope instabilities, where the slides or potential hazards have been investigated using single and multi-channel seismics, Ocean Bottom Hydrophone seismics, TOBI high-resolution side scan sonar, and finally, drilling. It turns out that the hydrate zone is a complex, multiphase system with fluid transport, where one often observes up to 100 m high and several up to 1000 m wide mud volcanoes and pockmarks at the sea floor. The developments of such zones with time still needs clarification. We know that the stability of gas hydrates is mainly controlled by the temperature regime of the oceans and by pressure conditions on the seabed. They are directly linked to global change climate processes and thus to temperature and sea level changes. Seismic data show that large slides on the Norwegian continental margin seem to be associated with gas hydrate reflectors. We cannot exclude that any major modification of the ocean's dynamic thermal structure in a warming world might cause outbursts of vast amounts of methane from the seabed reservoir and cause an increase in mass wasting activity. The morpholgical character of the Storegga Slide, for example, and the preservation of structures may lead to the conclusion that the present slide scarp and the features down slope cannot be 25,000 yrs old as previuosly thought. The present slide zones and the associated seismically-bedded areas indicate instead a much younger instability than previously thought. Modelling of hydrate formation and dissociation processes during climate changes (warming and cooling) and combining laboratory and field results may shed light on

the still not well understood sea floor dynamics in hydrated regions where careful drilling campaigns are needed.

## INTRODUCTION

Submarine gas hydrates appear to be common in northern European continental margin sediments because seismic reflection data and sampling have documented their existence (Andreassen & Hansen, 1995; Mienert & Posewang, 1997; Vogt et al., 1997, Mienert & Bryn, 1997; Posewang & Mienert, in press). Quantitative information about the distribution and concentration of gas hydrates in Norwegian margin sediments, however, is still poorly constrained. They are mainly inferred from seismic reflection surveys (e.g. Andreassen & Hansen, 1995; Posewang & Mienert, in press). Even though large research efforts have been devoted to deciphering the sedimentary processes moulding the margins (e.g. Dowdeswell et al., 1996), the timing, causes and flow behaviour of these large-scale events in relationship to gas hydrates are still largely unknown (Mienert et al., 1998). Physical properties of sediments prone to sliding and slumping are also poorly known, as are the timing and amplitudes of the destabilisation of gas hydrates. These changes must be understood in order to generate reliable models for large-scale sedimentary processes, in particular, mass wasting events. In the future this will require major research programmes and efforts to develop new technologies in close co operation with industry.

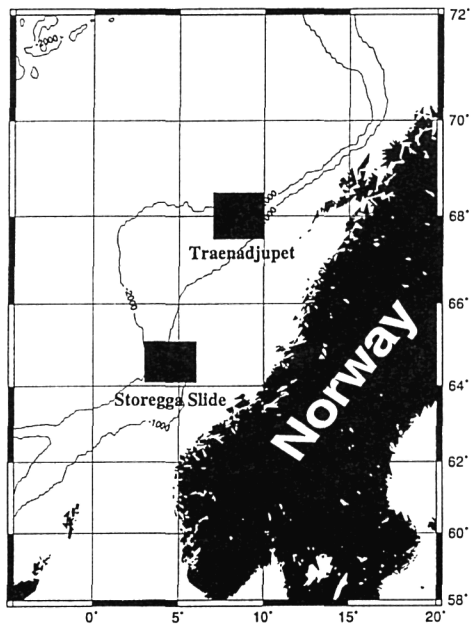


**Figure 1:** The Norwegian continental margin showing the location of the Storegga and the Trænadjupet Slides.

RESULTS

At the Mid Norwegian Margin, two major sediment slides - Storegga and Traenadjupet - caused large scale down slope transport of sediments during Quaternary times (Figure 1). The Trænadjupet Slide has affected an area of about 15,700 km$^2$, of which the slide scar area comprises 8,170 km$^2$ (Figure 2) (Laberg & Vorren, in prep). The Trænadjupet Slide involves sediments of late Cenozoic age and has a total volume of 760 km$^3$. The slope gradient within the slide scar is approx. 1.2° and sediments have moved up to 200 km from the present shelf break into the Lofoten Basin. The headwall of the slide scar is 150 m high and 120 km long (Figure 3). An up to 100 m high escarpment has been found further downslope. This may imply that sediments at different stratigraphic levels were affected by the failure or that several episodes of sediment failure have occurred within this area. Relatively little sediments have been deposited within the slide scar after the failure(s) occurred. The area where slide sediments accumulated is characterised by a hummocky topography indicating that the sediment failure(s) has affected both unconsolidated and more consolidated sediments, i.e. smaller and larger blocks floating in an unconsolidated matrix (Figure 4). The distal slide accumulation is draped by 1 - 2 m of hemipelagic sediments. The Trænadjupet Slide is probably relatively young (late Pleistocene - Holocene ?) because: i) the slide scar forms a prominent relief within the present sea floor , and ii) the slide-affected area is draped by a relatively thin layer of hemipelagic sediments. The existence of gas hydrates has been suggested on the base of bottom simulating reflectors observed in reflection seismic profiles and in (HF-OBH) high-frequency ocean bottom seismic data. The decomposition of these gas hydrates and the emergence of mud diapirs at the headwall of the slide may have triggered the slide event.

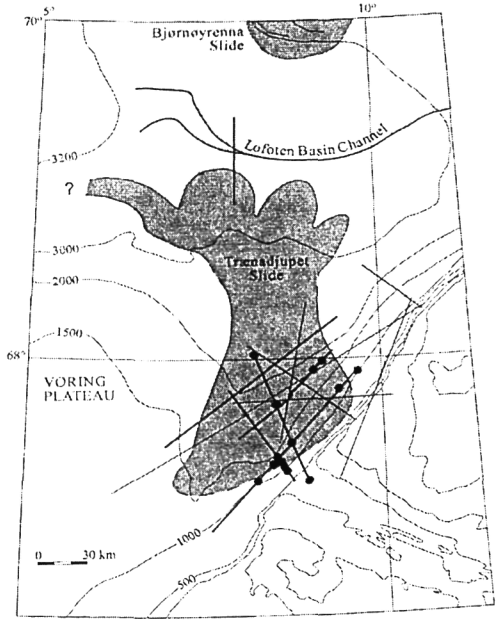


**Figure 2:** Area on the Mid Norwegian Margin continental slope where the Trænadjupet Slide events eroded the sea floor. The seismic profiles are indicated by solid lines and the core stations by solid circles.

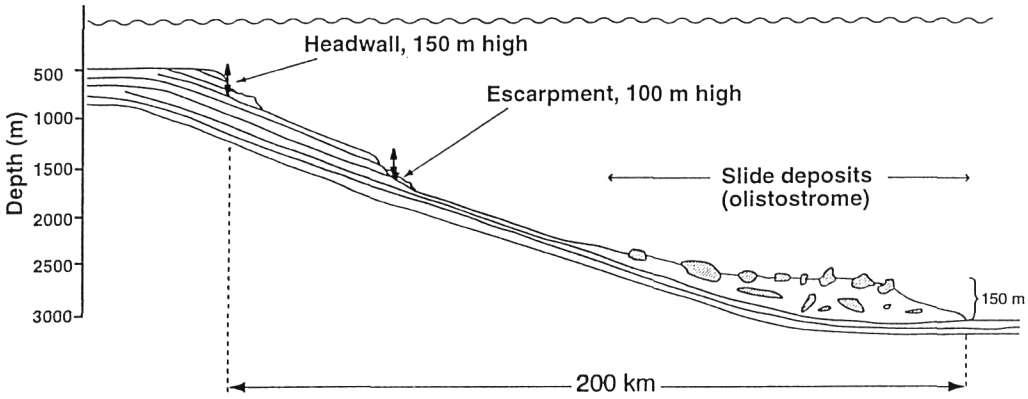


**Figure 3:** Cross-section of the Trænadjupet Slide showing the head walls.

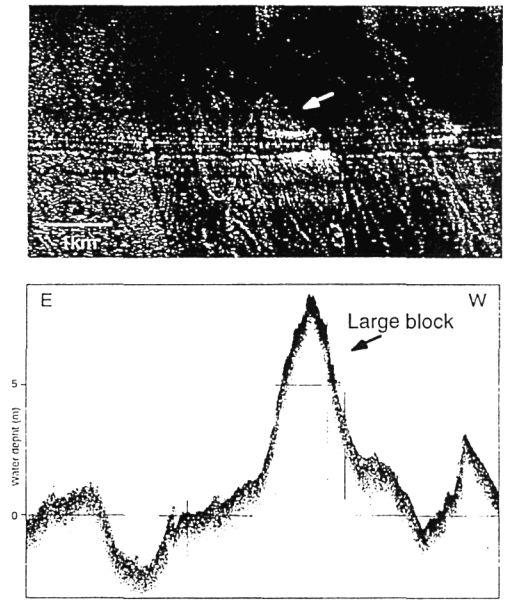


**Figure 4:** Large, up to 100 m high sediment block floating in an unconsolidated matrix shown in (top) the side-scan sonar and (bottom) the sediment profiler record.

At the Storegga Slide region, geophysical studies of gas hydrates at a drill site location (Mienert & Bryn, 1997) show an unusual acoustic pattern of bottom simulating reflectors (BSR). A classical BSR indicates the lower boundary of hydrate occurences (BSR 1) which is

detectable by means of seismic methods if an interface between hydrated sediments and free gas bearing layers gives rise to a sufficient (negative) impedance contrast (Figures 5 and 6). ENAM ocean bottom hydrophone (HF-OBH) and acoustic profiling seismic data, which are from the area NW of the drill site, show two BSRs, the deeper one indicating the base and the shallower one, the top of the hydrate zone (Posewang & Mienert, subm.) (Figures 5 and 6). Using average compressional wave velocities the deeper BSR (BSR 1) is placed at approx. 285 mbsf, which corresponds well to the theoretical base of the hydrate stability zone (HSZ) (Posewang & Mienert, subm.). The calculated geothermal gradient using the phase diagram is approx. 50°C/km, which is in agreement with the measured temperature gradient of 50°C/km in the bore hole (pers. comm. Norsk Hydro) where the strong BSR occurs at about 270 mbsf. The BSRs show a patchy distribution and lateral consistency, and moreover are not continously traceable such as internal lithological reflections. At the present research is concentrating on the environmental P-T conditions which may have changed the hydrate stability zone.

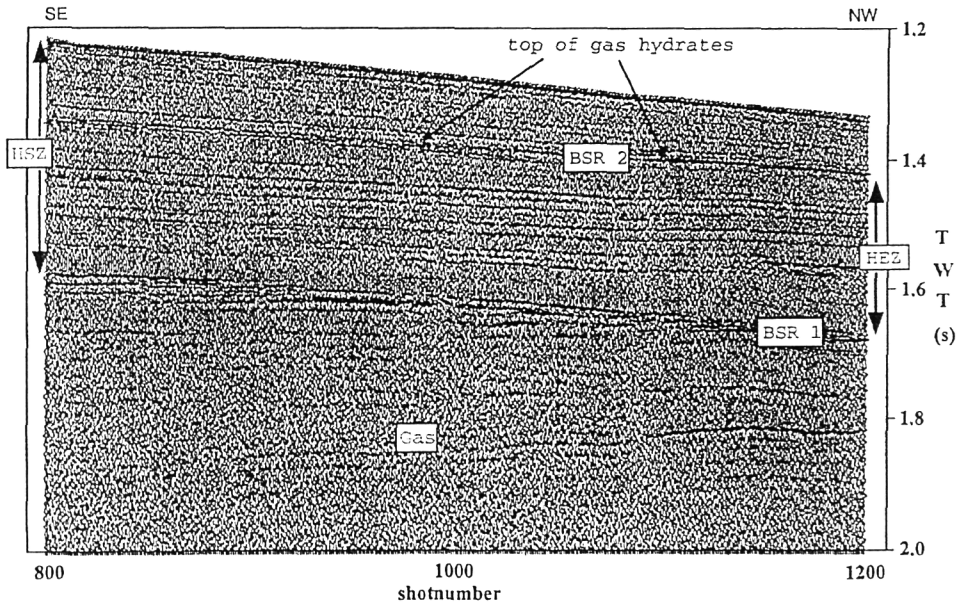


**Figure 5:** Section of a seismic reflection profile based on a 2-liter airgun and a 6-channel streamer. Anomalously high amplitudes of cross horizons and a phase reversal are typical indicators for the existence of free gas below BSR 1. The top of the gas hydrates is called BSR 2. The zone between BSR 1 and BSR 2 is called the hydrate existence zone (HEZ), in contrast to the hydrate stability zone (HSZ).

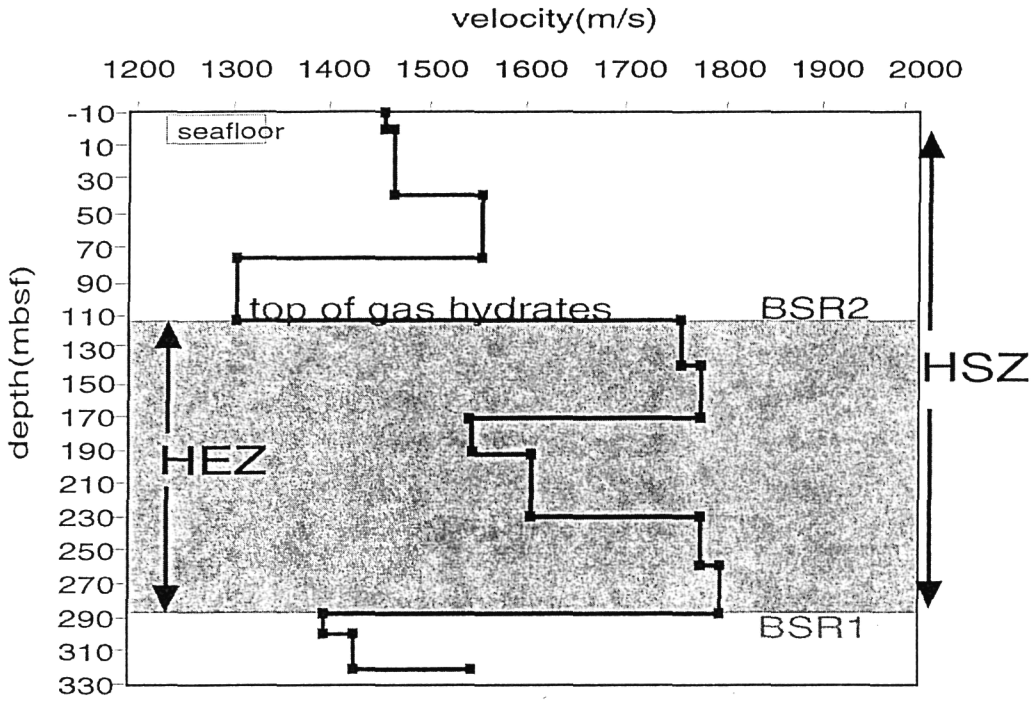


**Figure 6:** High-frequency ocean bottom hydrophone (HF-OBH) data shows a low and high velocity zone in the velocity-depth model, which provide evidence for a zone of free gas and a storey-like appearance of gas hydrates.

Modelling of the HSZ development for the time period from the Last Glacial Maximum (LGM) to the present indicates that the HSZ decreased between 120 and 40 metres depending on water depth. At about 1000 m water depth, the HSZ decreased by about 80 metres. Since changes in the HSZ are apparently long-term processes, we are still far away from understanding the sea floor reactions and developments involved in such a scenario. This is particularly true for the case where the BSR is extending directly into the glide plane of the Storegga Slide (Figures 7 and 8) (Mienert et al., 1998). The identification of pockmarks and mud volcanoes on the continental slope (Vogt et al., 1997; Mienert et al., 1998) and craters on the shelf (Solheim and Elverhoi, 1993) point towards ongoing or past gas/fluid escape processes (Mienert and Posewang, in press).

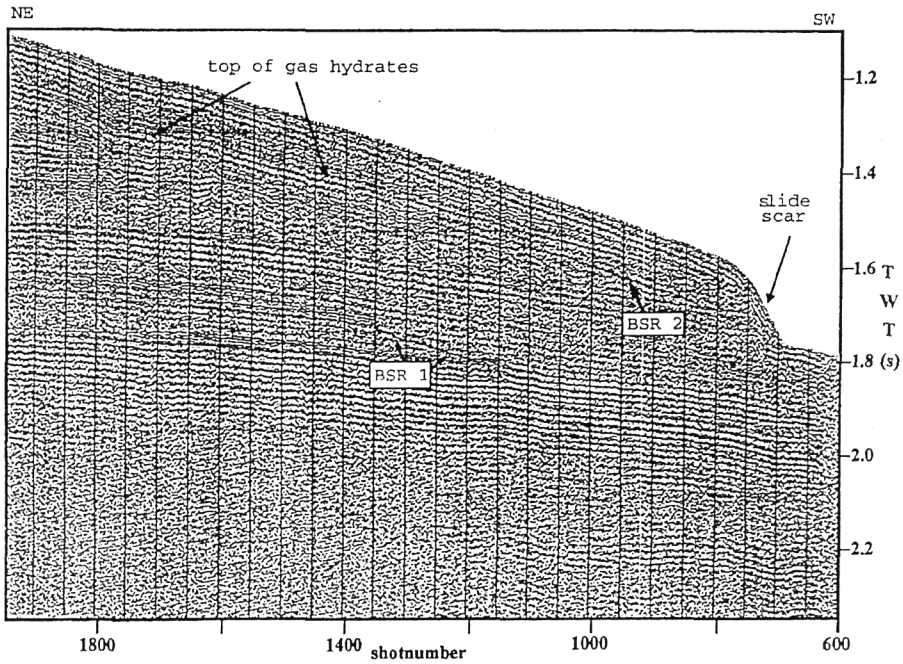


**Figure 7:** Section of a seismic reflection profile based on a 2-liter airgun. The shallow BSR (BSR 2) occurs at the same depth as the glide plane of Storegga at approximately 75 m depth below the sea floor.

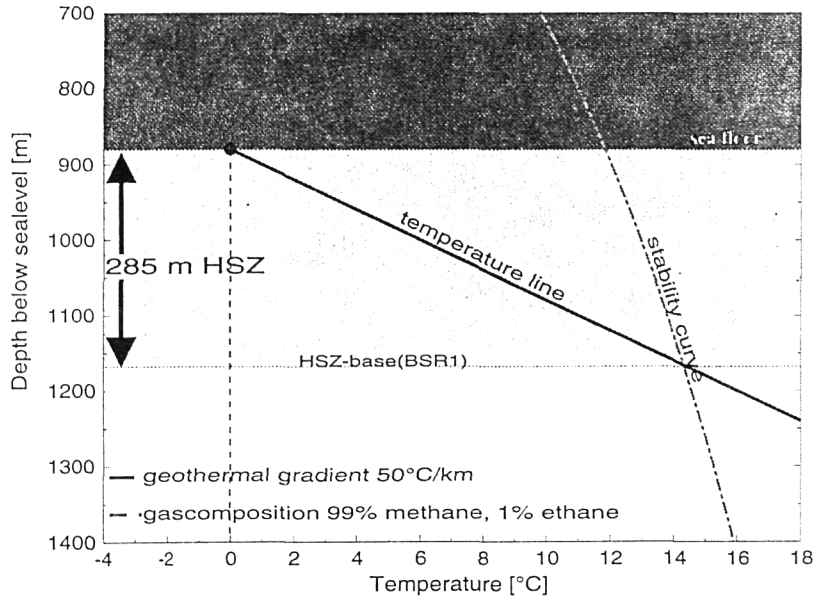


**Figure 8:** P-T diagram calculated with the equiphase hydrate program (DBRR, 1995). The temperature line crosses the stability curve at a depth of 285 m below the sea floor indicating the HSZ base at BSR 1.

## ACKNOWLEDGEMENT

The contributions from ENAM partners are greatly acknowledged. This work is funded by the European Commission under contract MAS3-CT95-0003.

## REFERENCES

Andreassen, K. and Hansen, T. (1995). Inferred gas hydrates offshore Norway and Svalbard. Norsk Geologisk Tidsskrift 45 : 10-34.

Dowdeswell, J.A., Kenyon, N.H., Elverhoi, A., Laberg, J.S., Hollender, F.-J., Mienert, J. and Siegert, M.J. (1996). Large-scale sedimentation on the glacier-influenced Polar North Atlantic margins: Long-range side-scan sonar evidence. Geophys. Research Letters, 23: 3535-3538.

Laberg, J.S. and Vorren T. (in prep.). The Trænadjupet slide events.

Mienert, J. and Bryn, P. (1997). Gas Hydrate Drilling conducted on the European Margin. EOS, Transactions, American Geophysical Union, 78; 49:567-571.

Mienert, J. and Posewang, J. (1997). High-frequency geophysical signatures of gas hydrates and free gas along the north-eastern Atlantic Margin: possible hydrate bound margin instabilities and possible release of methane from oceanosphere to atmosphere. AGU spring meeting, Baltimore, MD, Eos, 29 April: 189

Mienert, J. Posewang, J. Baumann, M. (1998). Gas hydrates along the north-eastern Atlantic margin: Possible hydrate-bound margin instabilities and possible release of methane. In: Henriet, J.P. and Mienert, J. (eds) Gas Hydrates: Relevance to world margin stability and climatic change. Geological Society, London, Special Publication.

Mienert, J. and Posewang, J. (in press). Evidence of shallow- and deep-water gas hydrate destabilizations in North Atlantic polar continental margin sediments. Geo-Mar. Letters.

Posewang, J. and Mienert, J. (in press). High-resolution seismic studies of gas hydrates west of Svalbard. Geo-Mar. Letters.

Posewang, J. and Mienert, J. (subm.). The enigma of double BSRs: Indicators for changes in the hydrate stability field. Geo-Mar. Letters.

Solheim, A. and Elverhøi, A. (1993). A pockmark field in the central Barents Sea; Geo-Mar. Letters 13:, 235-243.

Vogt, P., Cherkashev, G., Ginsburg, G., Ivanov, G., Crane, K., Egorov, A., Lein, A., Pimenov, N. and Sundvor, E. (1997). Haakon Mosby Mud Volcano: A warm methane seep with seafloor hydrates and chemosyntheses-based ecosystem in Late Quaternary slide valley, Bear island fan, Barents Sea Passive Margin. AGU 1997 spring meeting, Baltimore, Eos, 187, 1997.

Vogt, P., Cherkashev, G., Ginsburg, G., Ivanov, G., Milkov, A., Crane, K., Lein, A., Sundvor, E., Pimenov, N. and Egorov, A. (1997). Haakon Mosby Mud Volcano provides unusual example of venting. EOS, Transactions, American Geophysical Union, 78, 48:

European Commission

**Report of the seafloor characterisation session of the third European marine science and techno conference**

*Edited by Gilles Ollier, Pierre Cochonat and Luiz Mendes Victor*

Luxembourg: Office for Official Publications of the European Communities

1999 — 134 pp. – 17.6 x 25 cm

ISBN 92-828-5060-9

Price (excluding VAT) in Luxembourg: EUR 10

# Venta • Salg • Verkauf • Πωλήσεις • Sales • Vente • Vendita • Verkoop • Venda • Myynti • Försäljning

## BELGIQUE/BELGIË

**Jean De Lannoy**
Avenue du Roi 202/Koningslaan 202
B-1190 Bruxelles/Brussel
Tél. (32-2) 538 43 08
Fax (32-2) 538 08 41
E-mail: jean.de.lannoy@infoboard.be
URL: http://www.jean-de-lannoy.be

**La librairie européenne/De Europese Boekhandel**
Rue de la Loi 244/Wetstraat 244
B-1040 Bruxelles/Brussel
Tél. (32-2) 295 26 39
Fax (32-2) 735 08 60
E-mail: mail@libeurop.be
URL: http://www.libeurop.be

**Moniteur belge/Belgisch Staatsblad**
Rue de Louvain 40-42/Leuvenseweg 40-42
B-1000 Bruxelles/Brussel
Tél. (32-2) 552 22 11
Fax (32-2) 511 01 84

## DANMARK

**J. H. Schultz Information A/S**
Herstedvang 10-12
DK-2620 Albertslund
Tlf. (45) 43 63 23 00
Fax (45) 43 63 19 69
E-mail: schultz@schultz.dk
URL: http://www.schultz.dk

## DEUTSCHLAND

**Bundesanzeiger Verlag GmbH**
Vertriebsabteilung
Amsterdamer Straße 192
D-50735 Köln
Tel. (49-221) 97 66 80
Fax (49-221) 97 66 82 78
E-Mail: vertrieb@bundesanzeiger.de
URL: http://www.bundesanzeiger.de

## ΕΛΛΑΔΑ/GREECE

**G. C. Eleftheroudakis SA**
International Bookstore
Panepistimiou 17
GR-10564 Athina
Tel. (30-1) 331 41 80/1/2/3/4/5
Fax (30-1) 323 98 21
E-mail: elebooks@netor.gr

## ESPAÑA

**Boletín Oficial del Estado**
Trafalgar, 27
E-28071 Madrid
Tel. (34) 915 38 21 11 (Libros),
913 84 17 15 (Suscrip.)
Fax (34) 915 38 21 21 (Libros),
913 84 17 14 (Suscrip.)
E-mail: clientes@com.boe.es
URL: http://www.boe.es

**Mundi Prensa Libros, SA**
Castelló, 37
E-28001 Madrid
Tel. (34) 914 36 37 00
Fax (34) 915 75 39 98
E-mail: libreria@mundiprensa.es
URL: http://www.mundiprensa.com

## FRANCE

**Journal officiel**
Service des publications des CE
26, rue Desaix
F-75727 Paris Cedex 15
Tél. (33) 140 58 77 31
Fax (33) 140 58 77 00

## IRELAND

**Government Supplies Agency**
Publications Section
4-5 Harcourt Road
Dublin 2
Tel. (353-1) 661 31 11
Fax (353-1) 475 27 60
E-mail: opw@iol.ie

## ITALIA

**Licosa SpA**
Via Duca di Calabria, 1/1
Casella postale 552
I-50125 Firenze
Tel. (39-55) 064 54 15
Fax (39-55) 064 12 57
E-mail: licosa@ftbcc.it
URL: http://www.ftbcc.it/licosa

## LUXEMBOURG

**Messageries du livre SARL**
5, rue Raiffeisen
L-2411 Luxembourg
Tél. (352) 40 10 20
Fax (352) 49 06 61
E-mail: mdl@pt.lu
URL: http://www.mdl.lu

Abonnements:

**Messageries Paul Kraus**
11, rue Christophe Plantin
L-2339 Luxembourg
Tél. (352) 49 98 88-8
Fax (352) 49 98 88-444
E-mail: mpk@pt.lu
URL: http://www.mpk.lu

## NEDERLAND

**SDU Servicecentrum Uitgevers**
Christoffel Plantijnstraat 2
Postbus 20014
2500 EA Den Haag
Tel. (31-70) 378 98 80
Fax (31-70) 378 97 83
E-mail: sdu@sdu.nl
URL: http://www.sdu.nl

## ÖSTERREICH

**Manz'sche Verlags- und Universitätsbuchhandlung GmbH**
Kohlmarkt 16
A-1014 Wien
Tel. (43-1) 53 16 11 00
Fax (43-1) 53 16 11 67
E-Mail: bestellen@manz.co.at
URL: http://www.austria.EU.net:81/manz

## PORTUGAL

**Distribuidora de Livros Bertrand Ld.ª**
Grupo Bertrand, SA
Rua das Terras dos Vales, 4-A
Apartado 60037
P-2700 Amadora
Tel. (351-1) 495 90 50
Fax (351-1) 496 02 55

**Imprensa Nacional-Casa da Moeda, EP**
Rua Marquês Sá da Bandeira, 16-A
P-1050 Lisboa Codex
Tel. (351-1) 353 03 99
Fax (351-1) 353 02 94
E-mail: del.incm@mail.telepac.pt
URL: http://www.incm.pt

## SUOMI/FINLAND

**Akateeminen Kirjakauppa/Akademiska Bokhandeln**
Keskuskatu 1/Centralgatan 1
PL/PB 128
FIN-00101 Helsinki/Helsingfors
P./tfn (358-9) 121 44 18
F./fax (358-9) 121 44 35
Sähköposti: akatilaus@akateeminen.com
URL: http://www.akateeminen.com

## SVERIGE

**BTJ AB**
Traktorvägen 11
S-221 82 Lund
Tfn (46-46) 18 00 00
Fax (46-46) 30 79 47
E-post: btjeu-pub@btj.se
URL: http://www.btj.se

## UNITED KINGDOM

**The Stationery Office Ltd**
International Sales Agency
51 Nine Elms Lane
London SW8 5DR
Tel. (44-171) 873 90 90
Fax (44-171) 873 84 63
E-mail: ipa.enquiries@theso.co.uk
URL: http://www.theso.co.uk

## ÍSLAND

**Bokabud Larusar Blöndal**
Skólavördustig, 2
IS-101 Reykjavik
Tel. (354) 551 56 50
Fax (354) 552 55 60

## NORGE

**Swets Norge AS**
Ostenjoveien 18
Boks 6512 Etterstad
N-0606 Oslo
Tel. (47-22) 97 45 00
Fax (47-22) 97 45 45

## SCHWEIZ/SUISSE/SVIZZERA

**Euro Info Center Schweiz**
c/o OSEC
Stampfenbachstraße 85
PF 492
CH-8035 Zürich
Tel. (41-1) 365 53 15
Fax (41-1) 365 54 11
E-mail: eics@osec.ch
URL: http://www.osec.ch/eics

## BĂLGARIJA

**Europress Euromedia Ltd**
59, blvd Vitosha
BG-1000 Sofia
Tel. (359-2) 980 37 66
Fax (359-2) 980 42 30
E-mail: Milena@mbox.cit.bg

## ČESKÁ REPUBLIKA

**ÚSIS**
NIS-prodejna
Havelkova 22
CZ-130 00 Praha 3
Tel. (420-2) 24 23 14 86
Fax (420-2) 24 23 11 14
E-mail: nkposp@dec.nis.cz
URL: http://usiscr.cz

## CYPRUS

**Cyprus Chamber of Commerce and Industry**
PO Box 1455
CY-1509 Nicosia
Tel. (357-2) 66 95 00
Fax (357-2) 66 10 44
E-mail: info@ccci.org.cy

## EESTI

**Eesti Kaubandus-Tööstuskoda (Estonian Chamber of Commerce and Industry)**
Toom-Kooli 17
EE-0001 Tallinn
Tel. (372) 646 02 44
Fax (372) 646 02 45
E-mail: einfo@koda.ee
URL: http://www.koda.ee

## HRVATSKA

**Mediatrade Ltd**
Pavla Hatza 1
HR-10000 Zagreb
Tel. (385-1) 43 03 92
Fax (385-1) 43 03 92

## MAGYARORSZÁG

**Euro Info Service**
Európa Ház
Margitsziget
PO Box 475
H-1396 Budapest 62
Tel. (36-1) 350 80 25
Fax (36-1) 350 90 32
E-mail: euroinfo@mail.matav.hu
URL: http://www.euroinfo.hu/index.htm

## MALTA

**Miller Distributors Ltd**
Malta International Airport
PO Box 25
Luqa LQA 05
Tel. (356) 66 44 88
Fax (356) 67 67 99
E-mail: gwirth@usa.net

## POLSKA

**Ars Polona**
Krakowskie Przedmiescie 7
Skr. pocztowa 1001
PL-00-950 Warszawa
Tel. (48-22) 826 12 01
Fax (48-22) 826 62 40
E-mail: ars_pol@bevy.hsn.com.pl

## ROMÂNIA

**Euromedia**
Str. G-ral Berthelot Nr 41
RO-70749 Bucuresti
Tel. (40-1) 315 44 03
Fax (40-1) 315 44 03

## RUSSIA

**CCEC**
60-letiya Oktyabrya Av. 9
117312 Moscow
Tel. (7-095) 135 52 27
Fax (7-095) 135 52 27

## SLOVAKIA

**Centrum VTI SR**
Nám. Slobody, 19
SK-81223 Bratislava
Tel. (421-7) 531 83 64
Fax (421-7) 531 83 64
E-mail: europ@tbb1.sltk.stuba.sk
URL: http://www.sltk.stuba.sk

## SLOVENIA

**Gospodarski Vestnik**
Dunajska cesta 5
SLO-1000 Ljubljana
Tel. (386) 611 33 03 54
Fax (386) 611 33 91 28
E-mail: europ@gvestnik.si
URL: http://www.gvestnik.si

## TÜRKIYE

**Dünya Infotel AS**
100, Yil Mahallessi 34440
TR-80050 Bagcilar-Istanbul
Tel. (90-212) 629 46 89
Fax (90-212) 629 46 27
E-mail: infotel@dunya-gazete.com.tr

## AUSTRALIA

**Hunter Publications**
PO Box 404
3067 Abbotsford, Victoria
Tel. (61-3) 94 17 53 61
Fax (61-3) 94 19 71 54
E-mail: jpdavies@ozemail.com.au

## CANADA

**Les éditions La Liberté Inc.**
3020, chemin Sainte-Foy
G1X 3V Sainte-Foy, Québec
Tel. (1-418) 658 37 63
Fax (1-800) 567 54 49
E-mail: liberte@mediom.qc.ca

**Renouf Publishing Co. Ltd**
5369 Chemin Canotek Road Unit 1
K1J 9J3 Ottawa, Ontario
Tel. (1-613) 745 26 65
Fax (1-613) 745 76 60
E-mail: order.dept@renoufbooks.com
URL: http://www.renoufbooks.com

## EGYPT

**The Middle East Observer**
41 Sherif Street
Cairo
Tel. (20-2) 393 97 32
Fax (20-2) 393 97 32
E-mail: order_book@meobserver.com.eg
URL: www.meobserver.com.eg

## INDIA

**EBIC India**
3rd Floor, Y. B. Chavan Centre
Gen. J. Bhosale Marg.
400 021 Mumbai
Tel. (91-22) 282 60 64
Fax (91-22) 285 45 64
E-mail: ebic@giasbm01.vsnl.net.in
URL: http://www.ebicindia.com

## ISRAEL

**ROY International**
41, Mishmar Hayarden Street
PO Box 13056
61130 Tel Aviv
Tel. (972-3) 649 94 69
Fax (972-3) 648 60 39
E-mail: royil@netvision.net.il

Sub-agent for the Palestinian Authority:

**Index Information Services**
PO Box 19502
Jerusalem
Tel. (972-2) 627 16 34
Fax (972-2) 627 12 19

## JAPAN

**PSI-Japan**
Asahi Sanbancho Plaza #206
7-1 Sanbancho, Chiyoda-ku
Tokyo 102
Tel. (81-3) 32 34 69 21
Fax (81-3) 32 34 69 15
E-mail: books@psi-japan.co.jp
URL: http://www.psi-japan.com

## MALAYSIA

**EBIC Malaysia**
Level 7, Wisma Hong Leong
18 Jalan Perak
50450 Kuala Lumpur
Tel. (60-3) 262 62 98
Fax (60-3) 262 61 98
E-mail: ebic-kl@mol.net.my

## PHILIPPINES

**EBIC Philippines**
19th Floor, PS Bank Tower
Sen. Gil J. Puyat Ave. cor. Tindalo St.
Makati City
Metro Manilla
Tel. (63-2) 759 66 80
Fax (63-2) 759 66 90
E-mail: eccpcom@globe.com.ph
URL: http://www.eccp.com

## SOUTH KOREA

**Information Centre for Europe (ICE)**
204 Woo Sol Parktel
395-185 Seogyo Dong, Mapo Ku
121-210 Seoul
Tel. (82-2) 322 53 03
Fax (82-2) 322 53 14
E-mail: euroinfo@shinbiro.com

## THAILAND

**EBIC Thailand**
29 Vanissa Building, 8th Floor
Soi Chidlom
Ploenchit
10330 Bangkok
Tel. (66-2) 655 06 27
Fax (66-2) 655 06 28
E-mail: ebicbkk@ksc15.th.com
URL: http:/www.ebicbkk.org

## UNITED STATES OF AMERICA

**Bernan Associates**
4611-F Assembly Drive
Lanham MD20706
Tel. (1-800) 274 44 47 (toll free telephone)
Fax (1-800) 865 34 50 (toll free fax)
E-mail: query@bernan.com
URL: http://www.bernan.com

## ANDERE LÄNDER/OTHER COUNTRIES/ AUTRES PAYS

**Bitte wenden Sie sich an ein Büro Ihrer Wahl / Please contact the sales office of your choice / Veuillez vous adresser au bureau de vente de votre choix**

## NOTICE TO THE READER

*Information on European Commission publications in the areas of research and innovation can be obtained from:*

**RTD info**

The European Commission's free magazine on European research, with the focus on project results and policy issues, issued every three months in English, French and German.
For more information and subscriptions, contact:
DG XII Communication Unit, rue de la Loi/Wetstraat 200, B-1049 Brussels
Fax (32-2) 29-58220; e-mail: info@dg12.cec.be

14 15 CG-15-98-099-EN-C

Price (excluding VAT) in Luxembourg: EUR 10

OFFICE FOR OFFICIAL PUBLICATIONS
OF THE EUROPEAN COMMUNITIES

L-2985 Luxembourg

ISBN 92-828-5060-9